MULTIPLE-BEAM SPECTROSCOPY

Contents

MULTIPLE-BEAM SPECTROSCOPY

Peter S. Rostler

ABSTRACT

This report describes a new spectroscopic technique which provides spatially localized information about fine scale fluctuations in the density of light sources within a self-luminous plasma. In conventional spectroscopic methods, only the frequency spectrum of the light is measured. Yet light is characterized by phase as well as frequency. If a source is observed from several directions (through several beams), one can measure the correlations in phase between light emitted in different directions. With an incoherent source, two-beam correlations can only be due to common sources, i.e., to light emitted from within that small region which is observed through both beams. Thus the result of a correlation measurement is not an average along a line of sight; it is a local measurement.

It is shown that the light accepted by a two-beam system can be described in terms of spatial Fourier transforms of the field. The mutual coherence between light of wave number $|\underline{k}_A| = |\underline{k}_B|$ emitted in directions $\hat{k}_A$ and $\hat{k}_B$ is then shown to be proportional to the $\underline{k}_\Delta = \underline{k}_B - \underline{k}_A$ Fourier component of the light source distribution. This result is similar to what is found in an analysis of laser-light scattering. Thus the type of information given by a scattering experiment can also be obtained from spectroscopic measurements upon the light emitted by the plasma itself. Multiple-beam spectroscopy and laser-light scattering differ, however,

both in applications and in basic principles, as is explained in a detailed comparison of the two methods.

A two-beam spectrometer is only the simplest of many possible instruments of this type. For applications one needs to employ a more efficient system--one which presents a much larger solid angle of acceptance. It is shown how this can be conveniently done with polarizing optics, using birefringent optical components to manipulate two sets of beams, whose mutual coherence can then be deduced from polarization measurements. A general mathematical description of such systems is developed, and several examples are examined in detail.

An estimate is given of the noise level expected in the output of a multiple-beam spectrometer. The effect of photon noise is analyzed and a criterion obtained for the amount of light required for acceptable photon statistics.

The results of an experimental study of spectrometers of this type are presented. Several multiple-beam spectroscopic systems were assembled and tested with light from a small gas laser. The polarization fringe patterns obtained agree with those predicted by the theory.

The final system studied was then used to observe fluctuations in a laboratory plasma. The plasma was produced in helium by an electron beam, the fluctuations were imposed upon it with a probe, and a selected wavelength and frequency component of the disturbance in the plasma was observed through measurements of fluctuations in the distributions of the sources of the strongest

neutral helium emission line. The plasma phenomena observed were not extensively explored, but the results obtained show that a multiple-beam spectrometer can actually be used for plasma diagnostics.

The theory developed to describe these measurements is then extended to some other cases. These include the use of higher order optical correlation measurements to detect higher order correlations in the source, the use of several optical frequencies to observe high-frequency phenomena within a plasma, and the use of a broad portion of the optical spectrum to make one observation more efficiently.

I. INTRODUCTION

A. Optical Diagnostic Techniques

Optical diagnostic techniques are used in nearly every field of physics. Progress made in recent years in optics[1,2] has led to the use of improved optical methods in many areas of research. The purpose of this investigation was to explore the possibility of extending the optical methods which are used in experimental plasma physics.

In plasma physics, much effort has been invested in the development of diagnostic techniques.[3] Plasma diagnostics is particularly difficult because the phenomena of interest occur during short times and because a high-temperature plasma is easily perturbed by almost any instrument. A probe is required which can respond quickly--at high frequencies--but which will not disturb the plasma under study. Both of these requirements suggest the use of optical methods.

Several optical diagnostic techniques are used in plasma physics. The variety of existing methods calls for a discussion of the general problem of an interacting system of optical radiation and plasma. Such an analysis suggests that other useful optical techniques could be developed. One possibility, "multiple-beam spectroscopy", is discussed in this report.

The basis of this approach[4] is the measurement of the coherence, or correlation in phase, between various components of the light emitted by a plasma. Analysis shows that such a measurement should provide information about local values of the fluctua-

tions or correlations in the distribution of light sources within a plasma. To explore the practicality of using this technique for diagnostics, a model optical system was constructed and used to observe imposed fluctuations in the density of a helium plasma produced by an electron beam.

Before explaining these ideas further, it is useful to review the basic principles and limitations of some standard optical plasma diagnostic techniques. This is done next and then the concept of the present study is presented in the second chapter.

Note added in proof: All assembled, the report is longer than anticipated. A few comments on its structure may be helpful. The central portion of the text is Sect. IIA. Chapter I is just preliminary to IIA, and later sections all stem from that basic argument. In particular, Sect. IIB (with Appendix C), Sect. IIC, Chapter III, and Chapter V are four completely separate discussions, all of which directly follow Sect. IIA.

The experimental work is described in Chapter IV. This should be understandable if one has read IIA and then Appendices C and D.

B. Plasma Spectroscopy

Any optical diagnostic technique involves an interacting system of radiation and plasma (actually, any extended source of light would suffice for this analysis). (See Fig. I-1.) The plasma is assumed to be bounded, but many optical wavelengths

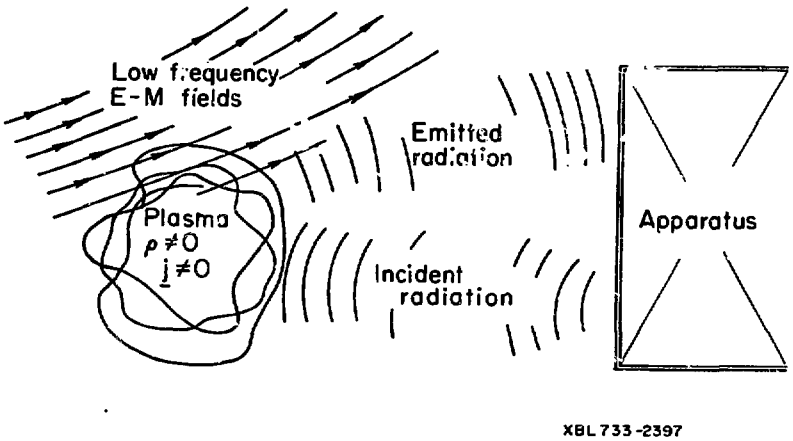

Fig. I-1. The general type of system considered.

$$\nabla^2 \underline{E} - \frac{1}{c^2} \frac{\partial^2 \underline{E}}{\partial t^2} = 4\pi \left(\nabla \rho + \frac{1}{c^2} \frac{\partial \underline{J}}{\partial t} \right) \qquad (I.4)$$

and $\underline{B}$ obeys a similar equation. Thus, for the fields themselves, one has again a set of equations of the form of (I.3).

In a system like that of Fig. I-1, the source density, $s(\underline{r},t)$ is nonzero only within the plasma, but $\xi(\underline{r},t)$ extends beyond the source. This, of course permits optical diagnostics: The optical frequency components of $\xi(\underline{r},t)$ (which may include incident, as well as emitted or scattered light) are observed--outside the plasma. This provides, according to Eq. (I.3), some degree of information about the optical frequency components of $s(\underline{r},t)$. And $s(\underline{r},t)$ depends upon various properties of the plasma. In general, $s(\underline{r},t)$ depends also upon the fields, including those of light waves. This effect of the light must be considered, for example, to explain scattering and to compute the index of refraction of the plasma.

In some situations, however, the effect of the light may be neglected. The optical radiation may then be considered separately, using Eq. (I.3) with a specified $s(\underline{r},t)$. This may be done if the light is emitted in collisions or atomic transitions and propagates unaffected by the plasma. We consider first such an $s(\underline{r},t)$, a transparent extended source, with $n = 1$ (n is the index of refraction).

There are, then, three elements: The plasma, the optical radiation, and the apparatus of measurement. To explain a particular observation, one can calculate the effects of various

plasma phenomena. But to determine what apparatus to use it is necessary to first consider carefully the nature of the optical radiation. What types of information are contained in the light from such a source? And what types of observation might one make?

To measure the optical radiation one can simply photograph the plasma.[6] But photographs alone can only begin to describe plasma phenomena and a measure of the total intensity gives only a small part of the information in the emitted light.

Much more information is contained in the spectrum of the light.[7] The light from a plasma consists of line radiation from atoms and ions and continuum radiation due mainly to bremsstrahlung and cyclotron emission.[8] With a spectrometer (Fig. I-2) one can compare the intensities of various portions of the spectrum and measure the shapes and locations of spectral lines. Since several mechanisms, including the Doppler effect and the Stark effect, can broaden spectral lines, several plasma parameters may be determined spectroscopically.

The accuracy of a spectroscopic measurement is limited by the intensity of the available light. This, of course, is true of any optical technique. In addition to this, a spectrometer like that shown in Fig. I-2 has two inherent limitations not necessarily shared by other optical diagnostic apparatus.

First of all, the various components of the light are emitted from small discrete sources--atoms, ions, electrons, colliding particles, etc. Such light contains information about the source and its immediate vicinity--the velocity of the source, the local

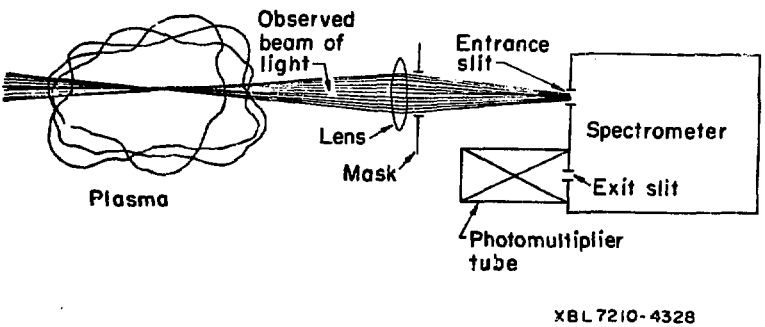

Fig. 1-2. Conventional spectroscopic apparatus.

electric field, etc. From the spectrum, which is merely the superposition of such contributions, one can determine "single point" plasma parameters such as particle densities and temperatures, and field strengths and frequencies. Plasma dynamics, however, is dominated by collective effects due to long range forces by which particles some distance apart may interact. Within the confines of the observed beam,[9] it is impossible to measure with an apparatus like that in Fig. I-2 such "plasma" properties as the wavelengths and frequencies of density fluctuations, or shielding distances, or correlation lengths.

The second limitation is the lack of depth perception. A spectrometer like that in Fig. I-2 accepts light from sources within an observed beam. A typical focused beam is shown in Fig. I-3. For sources not too near the focus and well within the beam, the optical system accepts any light emitted along a ray which when traced back goes through the focal spot. Such rays are spread over an angle $b \approx \delta/x$, that is, a solid angle $\sim b^2 \approx \delta^2/x^2$ (δ = focal spot size; x = distance to focus). The radius of the observed region is $r \approx \frac{1}{2} ax$ (a = angular spread of the beam). So, the amount of light received from some element along the line of sight (see Fig. I-3) is

$$\text{Intensity} = \begin{pmatrix}\text{brightness}\\ \text{of source}\end{pmatrix}\begin{pmatrix}\text{volume}\\ \text{of region}\end{pmatrix}\begin{pmatrix}\text{solid angle}\\ \text{subtended}\end{pmatrix}$$

$$= \begin{pmatrix}\text{brightness}\\ \text{of source}\end{pmatrix} \pi \left(\frac{ax}{2}\right)^2 \Delta x \left(\frac{\delta}{x}\right)^2$$

$$= \begin{pmatrix}\text{brightness}\\ \text{of source}\end{pmatrix} \frac{\pi}{4} a^2 \delta^2 \Delta x$$

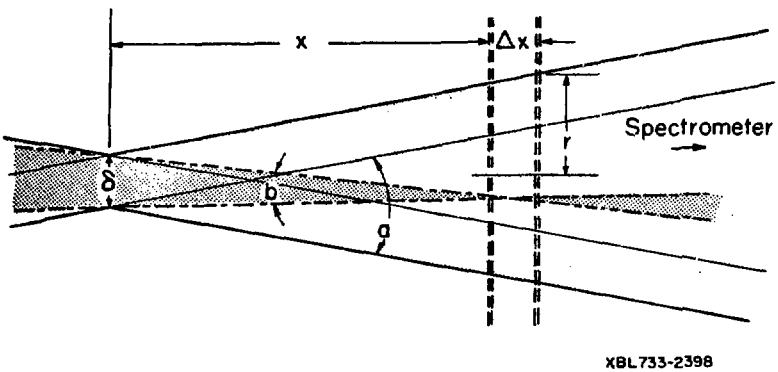

Fig. I-3. A typical observation region (single focused beam). δ is the width of the focus, a is the angle of acceptance at the focus, b is the angular width of the focus as seen from a point a distance x away from the focus.

--independent of x, except through the brightness of the source. So, at least according to this simple, approximate analysis, there is no spatial resolution at all in the axial direction.

This conclusion is valid within geometrical optics. The intensity of optical radiation (the energy per unit solid angle crossing unit area in unit time, i.e., the energy flux per solid angle) is not changed by an optical system free of losses and aberrations.[10] This is just the result, familiar in photometry and photography, that the apparent brightness of a source depends upon its actual brightness, but not upon its distance from the observer.

However expressed, invariance of intensity means that any measured optical spectrum is an unweighted average of spectra of light emitted all along the line of sight.[11] If the source is nonuniform, different regions with different emission spectra contribute to every observation. Some type of "unfolding" is required. For this one must record spectra of light emitted along many different lines of sight. An additional assumption, such as cylindrical symmetry of the plasma, is generally also invoked to simplify the analysis.

Nevertheless, plasma spectroscopy has been found extremely useful. An optical spectrum contains a large amount of information. Interpretation of various spectral features can become quite complicated and present understanding is based on work by many investigators.

Explanation of the optics of the spectrometer, on the other

hand, is quite straightforward when an idealized instrument, free of lens aberrations, misalignments, etc., is used as a model. The apparatus depicted in Fig. I-2 measures the intensity of various frequency components of the light in some bundle of rays. The frequency (more precisely, the wavelength) is selected by the spectrometer (slits, mirror and diffraction grating) and the intensity is measured with a photomultiplier tube.

A light wave, even in a simple scalar model, is characterized by intensity, frequency, and phase. The spectrometer makes use of phase information to define the incident beam. Different spectrometers select different spectral features, but all conventional instruments make similar use of the phase of the incident light: A lens or set of lenses and a pinhole or slit are used to select a bundle of rays--a result which can be described by geometrical optics.

C. The Use of Coherent Light: Interferometry and Light Scattering Measurements

There are optical diagnostic methods which do make different use of phase information. Within the last decade, optical interferometry and light scattering measurements have both become widely used in plasma physics. These techniques differ from spectroscopy in that light from an external source is used and in that the light interacts with the plasma [affects $s(\underline{r},t)$].

In spectroscopy, the intensity of the light used is the sum of the intensities of components from different sources. In interferometry and in scattering, the observed intensity of the

light depends also upon the relative phases of various components. This is true because this light is coherent. It originates from a common source and its coherence length exceeds any differences in optical path.

Optical interferometry is useful in studies of dense plasmas such as theta pinches. In such an observation, interference is used to measure the phase of light which has traversed a plasma. This phase depends upon the path of the light and upon the plasma index of refraction, which, in most experiments, is determined mainly by the electron density. This effect is analyzed in the review by Jahoda and Sawyer[12] who show that, at a given optical frequency, the expected phase shift is proportional to the integral of the electron density along the path of the light--again, a nonlocal measurement of a single point parameter. For ruby laser light, an integrated density of $3.2 \times 10^{17}/cm^2$ is needed to change the optical path length by one wavelength. For plasmas much smaller or less dense than this, zero phase shift is a good approximation unless phase is measured very precisely or light crosses the plasma many times.

The present analysis assumes throughout that the index of refraction of any plasma considered is equal to unity. This assumption is made to simplify the analysis, but it is not necessarily a general limitation since in many cases some variation in n would be inconsequential.

Many interferometric techniques, including some which can be used to measure very small phase shifts, have been developed.

These methods are well summarized in several reviews.[12,13]

A different type of information is provided by studies of the scattering of electromagnetic radiation by a plasma. This technique was first used in radar backscattering studies of the ionosphere.[14] Thereafter, theoretical analyses by several authors[15] explained such scattering in terms of predicted fluctuations in the plasma electron density. Laser light scattering has since been used to study a variety of laboratory plasmas.[16] Because an analysis of this type of measurement is similar to less familiar problems considered in later chapters, a brief discussion of this by now well-known technique appears indicated in this place.

The apparatus for a typical scattering measurement is shown in Fig. I-4. The basic procedure is simple: A laser illuminates the plasma and the light scattered into some observed beam is spectrally analyzed. The measured spectrum is found to differ from that of the incident laser light because components of the scattered light are shifted in frequency by amounts comparable to various characteristic frequencies of the plasma. To understand the scattered spectrum--indeed, to understand why scattering occurs at all--one must consider the combined effect of scattering by many plasma particles.

The observed scattering occurs within the intersection of the incident and observed beams. In this region the incident light may be represented as a linearly polarized monochromatic plane wave:[17]

$$\underline{E}_i(\underline{r},t) = \underline{E}_0 \cos(\underline{k}_i \cdot \underline{r} - |\underline{k}_i|ct). \qquad (I.5)$$

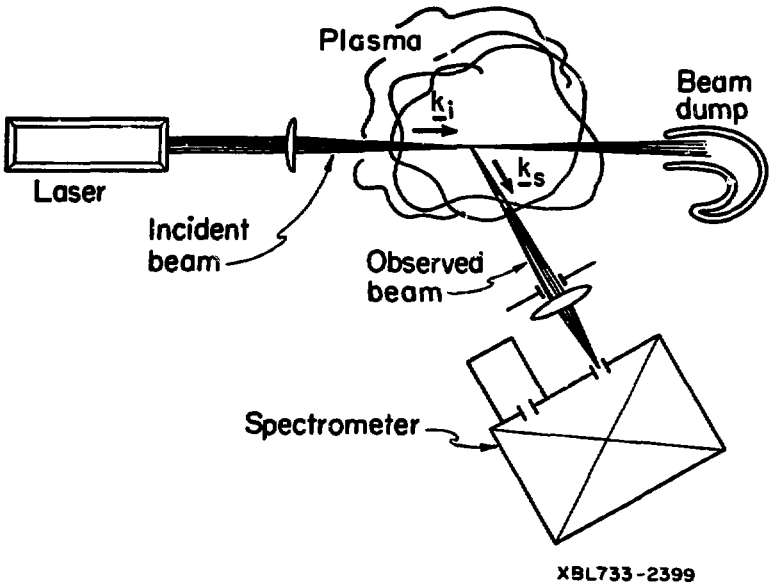

Fig. I-4a. Typical laser light scattering apparatus. $\underline{k}_i$ = wave vector of the incident light, $\underline{k}_s$ = wave vector of the observed scattered light.

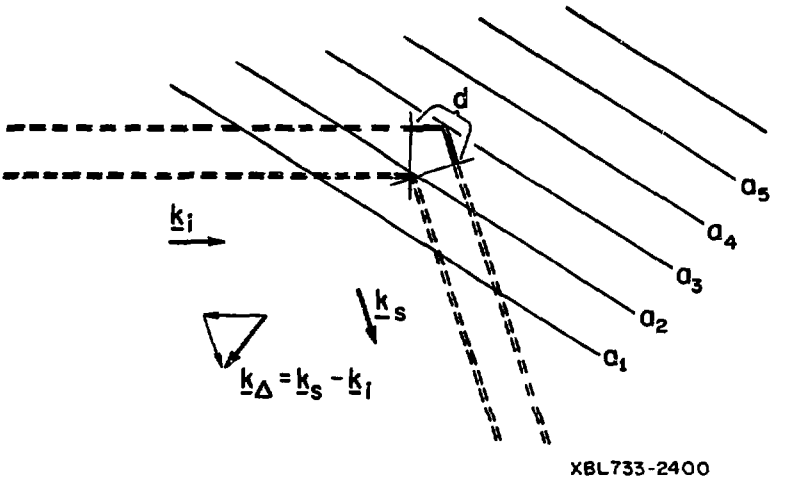

Fig. I-4b. Detail of the scattering region. a_1, a_2, a_3, ... are the maxima of a wave of wave vector $\underline{k}_\Delta$. d is a difference in path of one optical wavelength.

Each charged particle is accelerated by this field, $\underline{a} = \frac{e}{m}\underline{E}_i$ and emits a scattered wave, $\underline{E}_s$. The total scattered wave is the superposition of such contributions.[18]

For nonrelativistic motion, the radiation electric field of an accelerated point charge is:[19]

$$\underline{E}_s(\underline{r},t) = \frac{e}{c^2}\frac{1}{|\underline{r}-\underline{r}'|}\cdot\left[\hat{n}\times(\hat{n}\times\underline{a}')\right]\Big|_{ret}$$

$$\hat{n} \equiv \frac{\underline{r}-\underline{r}'}{|\underline{r}-\underline{r}'|}\ .$$

$\underline{r}'$ and $\underline{a}'$ are the position and acceleration of the particle at the retarded time

$$t' = t - \frac{1}{c}|\underline{r}-\underline{r}'|.$$

Since the acceleration, and hence the scattering, is inversely proportional to particle mass, appreciable scattering is produced only by plasma electrons. If these are described by an electron density $n_e(\underline{r},t)$, then from a volume d^3r' around a point $\underline{r}'$ is emitted a scattered wave,

$$\underline{E}_s(\underline{r},t;\underline{r}') = \frac{e^2}{mc^2}\frac{1}{|\underline{r}-\underline{r}'|}\,n_e(\underline{r}',t')\cdot\left\{\hat{n}\times\left[\hat{n}\times\underline{E}_i(\underline{r}',t')\right]\right\}\ .$$

And the total scattered wave is the superposition,

$$\underline{E}_s(\underline{r},t) = \int_{\substack{\text{scattering}\\ \text{volume}}} d^3r'\ \underline{E}_s(\underline{r},t;\underline{r}').$$

This wave is analyzed by a spectrometer which transmits only the $\underline{k}_s$ component (see Appendix E.1),

$$\underline{E}_s(\underline{k}_s,t) \equiv \int d^3r\, e^{-i\underline{k}_s\cdot\underline{r}}\,\underline{E}_s(\underline{r},t)$$

$$= \frac{e^2}{mc^2}\int d^3r\, e^{-i\underline{k}_s\cdot\underline{r}} \int d^3r'\, n_e\left(\underline{r}', t - \frac{|\underline{r}-\underline{r}'|}{c}\right)$$

$$\cdot \left[\hat{n}\times(\hat{n}\times\underline{E}_0)\right]\frac{1}{|\underline{r}-\underline{r}'|}$$

$$\cdot \cos\left[\underline{k}_i\cdot\underline{r}' - \omega_i\left(t - \frac{|\underline{r}-\underline{r}'|}{c}\right)\right] \qquad (I.6)$$

($\omega_i \equiv |\underline{k}_i|c$). This expression reduces to (see Appendix B for details),

$$\underline{E}_s(\underline{k}_s,t) \underset{t\to\infty}{\to} \frac{-i\pi}{|\underline{k}_s|}\left(\frac{e^2}{mc}\right)\underline{E}_0^{\perp}$$

$$\cdot\Big\{e^{-i\omega_s t}\left[n_e(\underline{k}_s - \underline{k}_i,\ \omega_s - \omega_i) + n_e(\underline{k}_s + \underline{k}_i,\ \omega_s + \omega_i)\right]$$

$$+ e^{-i(-\omega_s)t}\left[n_e(\underline{k}_s - \underline{k}_i,\ -\omega_s - \omega_i) + n_e(\underline{k}_s + \underline{k}_i,\ \omega_i - \omega_s)\right]\Big\} \qquad (I.7)$$

($\omega_s \equiv |\underline{k}_s|c$). Here $\underline{E}_0^{\perp} \equiv (I - \hat{k}_s\hat{k}_s)\underline{E}_0$ is the component of $\underline{E}_0$ which is normal to $\underline{k}_s$ and

$$n_e(\underline{k},\omega) \equiv \int\int d^3r\, dt\, e^{-i(\underline{k}\cdot\underline{r}-\omega t)} n_e(\underline{r},t) \qquad (I.8)$$

is the Fourier transform of the electron density.

If we retain only positive frequency components of $\underline{E}_s$ (see Appendix E.1) and neglect the high-frequency ($\omega = \omega_s + \omega_i$) com-

ponents of n_e, Eq. (I.7) reduces to

$$\underline{E}_s^{(+)}(\underline{k}_s,t) \underset{t\to\infty}{\to} \frac{-i\pi}{|\underline{k}_s|}\left(\frac{e^2}{mc}\right)\underline{E}_0^{\perp} e^{-i\omega_s t} n_e(\underline{k}_\Delta,\omega_\Delta). \qquad (I.9)$$

Here,

$$\underline{k}_\Delta \equiv \underline{k}_s - \underline{k}_i$$
$$\omega_\Delta \equiv \omega_s - \omega_i.$$

This analysis neglects the width, Δk, of the spectrometer instrument function. With equal precision, the long time limit may be replaced by equality after $t \sim \tau = (c\Delta k)^{-1}$, the corresponding correlation time. This retains a slow time dependence in n_e:

$$\underline{E}_s^{(+)}(\underline{k}_s,t) \simeq \frac{-i\pi}{|\underline{k}_s|}\left(\frac{e^2}{mc}\right)\underline{E}_0^{\perp} e^{-i\omega_s t} n_e(\underline{k}_\Delta,\omega_\Delta;t). \qquad (I.10)$$

We thus introduce a time-dependent spectrum. This operation is considered more carefully in Appendix E.3. The measured light intensity, which depends upon $\underline{E}^{(+)}(\underline{k}_s,t)$ (see Appendix E.1-3) exhibits only this slow time dependence:

$$I(\hat{k}_s,|\underline{k}_s|;t) = \left(\frac{|\underline{k}_s|}{4\pi^2}\right)^2 |\underline{E}^{(+)}(\hat{k}_s,|\underline{k}_s|,t)|^2$$

$$= \frac{1}{16\pi^2}\left(\frac{e^2}{mc}\right)^2 |\underline{E}_0|^2 |n_e(\underline{k}_\Delta,\omega_\Delta;t)|^2. \qquad (I.11)$$

The observed scattering is thus due to one Fourier component, the $(\underline{k}_\Delta,\omega_\Delta)$ component, of the electron density. A single electron would produce a scattered wave, but when many electrons are present,

only fluctuations in their density will cause scattering. This can be simply explained. All light scattered by electrons located in a plane normal to $\underline{k}_\Delta$ will have the same phase. Contributions from scatterers separated by $2\pi\hat{k}_\Delta|\underline{k}_\Delta|^{-1}$ will differ in phase by n cycles. If n is an integer, there will be constructive interference; if n is half integral, the contributions will cancel. If the electron distribution is uniform, there will be complete cancellation. But any fluctuations $n_e(\underline{k}_\Delta,\omega_\Delta)$ will produce very strong scattering. [The scattered intensity is proportional to the square of $|n_e(\underline{k}_\Delta,\omega_\Delta)|$.]

A plasma wave can produce such fluctuations. Indeed, a description of scattering may be included in a more general analysis of three-wave interactions. In this context the resonance conditions $\underline{k}_\Delta = \underline{k}_s - \underline{k}_i$, $\omega_\Delta = \omega_s - \omega_i$ are seen as statements of the conservation of momentum and energy.[20] An analysis of scattering as a three-wave process may include the effect of the interaction upon n_e and perhaps also upon $\underline{E}_i$. These effects have been neglected here.

In conventional notation, the result of Eq. (I.11) is often expressed in terms of frequency,

$$I(\hat{k}_s,|\underline{k}_s|;t)d^2\hat{k}_s d|\underline{k}_s| = I(\hat{k}_s,|\underline{k}_s|;t)d^2\hat{k}_s \frac{d\omega_s}{c}$$

$$= \frac{c}{16\pi^2}\left(\frac{e^2}{mc^2}\right)^2 |\underline{E}_0^{\perp}|^2 |n_e(\underline{k}_\Delta,\omega_\Delta;t)|^2 d^2\hat{k}_s d\omega_s$$

$$= I_0 n_{e0}\sigma_T S(\underline{k}_\Delta,\omega_\Delta)d^2\hat{k}_s d\omega \qquad (I.12)$$

where

$$I_0 = \frac{c}{4\pi} 2|\underline{E}_1^{(+)}(\underline{r},t)|^2 = \frac{c}{4\pi} 2\left|\frac{\underline{E}_0}{2}\right|^2 = \frac{c}{8\pi}|\underline{E}_0|^2,$$

n_{e0} is the mean electron density,

$$\sigma_T = \left(\frac{e^2}{mc^2}\right)^2 \frac{|\underline{E}_0^{\perp}|^2}{|\underline{E}_0|^2}$$

is the differential Thompson scattering cross section, and

$$S(\underline{k}_\Delta,\omega_\Delta) = \frac{1}{2\pi n_{e0}}|n_e(\underline{k}_\Delta,\omega_\Delta;t)|^2$$

is called the "dynamic form factor."

In a scattering experiment, one records a spectrum of the light scattered into some direction $\hat{k}_s$. The relative variation in optical wavelength is usually negligible, so the scattering is all due to fluctuations of one wavelength, $2\pi|\underline{k}_\Delta|^{-1}$. This is customarily related to the plasma Debye length λ_D by a "scattering parameter",

$$\alpha \equiv \frac{1}{|\underline{k}_\Delta|\lambda_D}. \tag{I.13}$$

The spectrum of scattered light then provides a frequency spectrum of the $\underline{k}_\Delta$ component of n_e. By the Wiener-Khintchine theorem,[21]

$$\frac{1}{2\pi}|n_e(\underline{k}_\Delta,\omega)|^2 = \int d\tau e^{i\omega\tau}\,\overline{n_e^*(\underline{k}_\Delta,t)n_e(\underline{k}_\Delta,t+\tau)}, \tag{I.14}$$

this is equivalent to a measure of the time correlation function,

$$C_{n_e(\underline{k}_\Delta)}(\tau) \equiv \overline{n_e^*(\underline{k}_\Delta, t) n_e(\underline{k}_\Delta, t+\tau)}. \qquad \text{(I.15)}$$

A complete knowledge of $n_e(\underline{k},\omega)$ would also provide the complete spatial correlation function, but this would require many observations. A single measurement provides partial--yet extremely useful--information about spatial correlations.

Scattering measurements are very useful precisely because they are not subject to either of the previously noted limitations of spectroscopy. A spectrum of scattered light is not an average along a line of sight. The observed scattering occurs entirely within the intersection of the incident and observed beams. This well localized scattering volume may be selected at will. And the measured correlation function is not a single-point parameter. The interference between light scattered from different points provides information about fine-scale fluctuations within a plasma.

With Eq. (I.11) one can deduce, from an optical measurement, a spectrum of electron density fluctuations. This result may then be compared with calculations of predicted spectra. Considerable effort has been invested in this type of study. The measured spectrum is found to depend strongly upon α, the scattering parameter. For $\alpha \ll 1$, the observed fluctuations are those of a random distribution. In this regime the frequency spectrum is determined by the electron velocity distribution.[22] If $\alpha > 1$, electron-ion correlations permit observation of ion motions as well.[23]

Calculations of predicted fluctuation spectra differ in method and in assumptions, but the relation of such results to any scattering measurement depends upon optical considerations which are common to all such experiments. In this report we consider further this first part of the problem--the relation between a distributed source such as a plasma and the associated optical radiation. It will be seen that various aspects of the foregoing analysis are not unique to scattering.

D. Information in the Emitted Light

Consider further the general system of Fig. I-1 . The simplest such situation is, again, a self-luminous plasma. In the optical problem, the source distribution $s(\underline{r},t)$ is then determined by the various plasma processes. We assume for now that the plasma is an incoherent source. If one range of frequencies is considered, there is no correlation between the phases of $s(\underline{r},\omega)$ at different points.

The resulting radiation, however, is not completely incoherent. Components of the light at different points are due to common sources and therefore the light $\xi(\underline{r},t)$ observed at widely separated points may well be correlated in its phase. If the correlations are considered, an analysis of the radiation from a luminous plasma is far from trivial. And such an analysis presents the possibility of developing useful optical diagnostic techniques.

The basis of "multiple-beam spectroscopy" is the fact that information about the local values of fluctuations and correla-

tions in plasma particle densities is in fact present in the light emitted by the plasma itself. The above noted limitations of spectroscopy are not limitations on the information contained in the emitted light. They are limitations of the type of apparatus represented in Fig. I-2. To make a different type of measurement, one must make different use of the phase of the light.

Although these conclusions can be justified by a general analysis, they were first obtained by consideration of particular optical systems. This approach has been retained in the explanation which follows. We first describe a simple two-beam spectrometer and then consider the possibilities and the difficulties suggested by the new arrangement.

The development of "multiple-beam spectroscopy" was based upon experience with a scattering experiment and this is reflected in the following explanation. Laser light scattering methods are familiar to plasma physicists, but a scattering measurement is not the only optical technique which uses phase information in a way which cannot be explained by geometrical optics. In particular, the invention of the laser has also led to the practical development of optical holography.[24-26] A "hologram" is a recorded set of interference fringes which can be used to produce a three-dimensional image of a stationary object. In a conventional holographic process, interference with the light in a reference beam is used to produce a record of the amplitude and phase of the light reflected by a coherently illuminated object. An explanation of this procedure bears considerable similarity to an analysis

of laser light scattering.

More recently, the possibility of making holograms of self luminous objects, or of incoherently illuminated objects, has also been explored.[27-31] This work is of interest in connection with the present study. The relation between holography and optical plasma diagnostics is examined in Appendix A of this discussion.

In the next chapter, multiple-beam spectroscopy is explained in terms of classical optics. Some consequences of the discreteness of light quanta are discussed in Chapter III.

II. THE USE OF PHASE INFORMATION

A. A Two-Beam Spectrometer

1. Light from an Incoherent Source: The Sum of Many Interference Patterns

Every optical phase measurement requires a comparison between different components or beams of light. In interferometry, a recorded pattern of interference fringes reveals the difference in phase between transmitted light and light in a reference beam. In a scattering process, the interference between light scattered by different electrons depends upon the coherence imposed by the light in the incident beam.

A self-luminous plasma provides no incident or reference beam, but since a plasma radiates in all directions, the emitted light may be considered to consist of many beams. Light from different points within a plasma is, in general, not coherent, but light emitted in different directions from one region should have some coherence. Thus, if a volume of plasma were observed from several directions at once, both phase and frequency measurements could be made.

Most simply, one could define two distinct "observed beams"--A and B--as shown in Fig. II-1. Beyond a spectral analysis, or any other measurement on either beam alone, there is then a further possibility: to compare the light in the two beams.

This suggests at once that a local spectroscopic measurement might be possible. The two observed beams can be defined to intersect in only a small, well localized, common source volume. Then

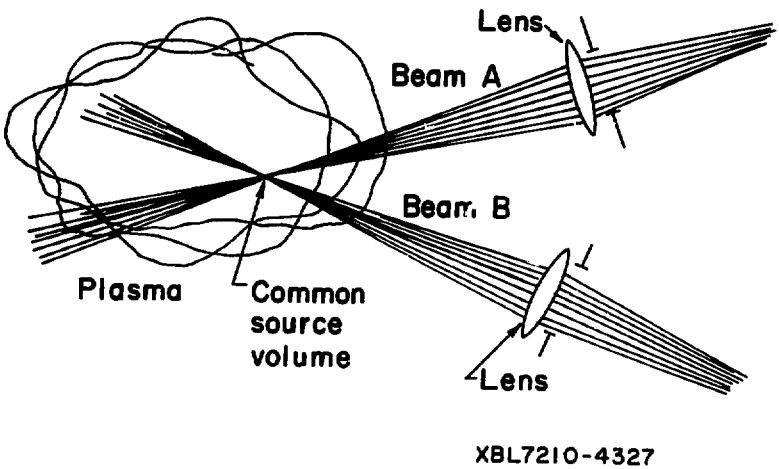

Fig. II-1. A two-beam observation.

if any component of the light can be identified as common to both beams, the location of the source is known at once. In human vision, for example, depth perception is provided by the recognition of two images of a single object. This procedure would be difficult to duplicate with scientific apparatus, but in observations of a plasma, the very incoherence of the source provides another way in which a common optical component might be recognized. We have noted already that light from a common source is (or may be) coherent. If it is assumed that light from different sources in a plasma is completely incoherent, then any correlations in phase between the light in beams A and B must be due to common sources. Any measured mutual coherence between components of the light in different beams must give local information about the common region where the two beams intersect.

To measure the mutual coherence between beams A and B, one can combine them and observe any two-beam interference which results. A simple optical system with which this could be done is shown in Fig. II-2. Here a set of masks and lenses is used to define two narrow beams which intersect in a common source volume. The light in each beam goes through a filter (that is, through some spectroscopic apparatus, the same for each). We suppose that the observed light contains a spectral line of width $\Delta\omega$, that the filter transmits only this line, and that the coherence length, $c/\Delta\omega$, of this transmitted light, exceeds any differences in the lengths of optical paths through the system.

Beams A and B are focused at a common point on a screen. The

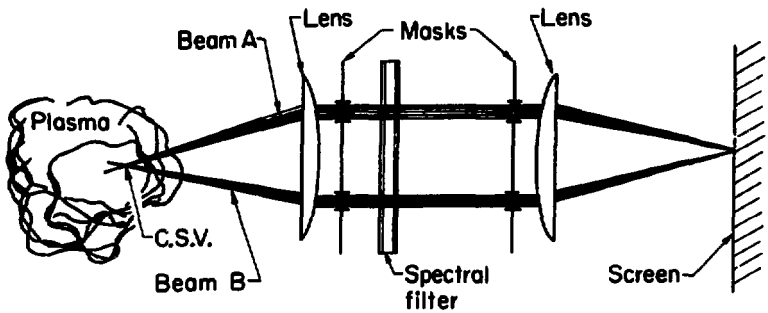

Fig. II-2. A two-beam spectrometer. c.s.v. = common source volume.

illumination of the screen then depends upon the mutual coherence of the light in the two beams. If the light were all due to a single point source which was observed through only one of the beams, then a single aperture diffraction pattern would appear on the screen, as shown in Fig. II-3a. The width of the illuminated area would be determined by the angle ϕ subtended at the screen by a single beam.

If, however, the light were due to an isotropic point source which was observed through both beams, the result would be quite different. In this case, a two-beam interference pattern would appear on the screen, as shown in Fig. II-3b. The spacing of the fringes of this pattern would depend upon the angle θ between the two component beams. Since $\theta \gg \phi$, the angle subtended by a single beam, the fringe spacing would be much less than the size of the whole pattern and many fringes would be seen.

If several separate incoherent sources were observed at once, the resulting pattern of illumination would be simply the superposition of the light intensity distributions due to each of the sources alone, as shown in Fig. II-3c. Two sources, one observed through each beam, would not together produce a two-beam interference pattern. Interference requires mutual coherence which, under our assumptions, could be provided only by a common source.

These conclusions are based upon quite elementary optics, but the essential difference between the effects of sources which are observed through one beam and the effects of sources which are observed through both beams presents a practical useful possibility.

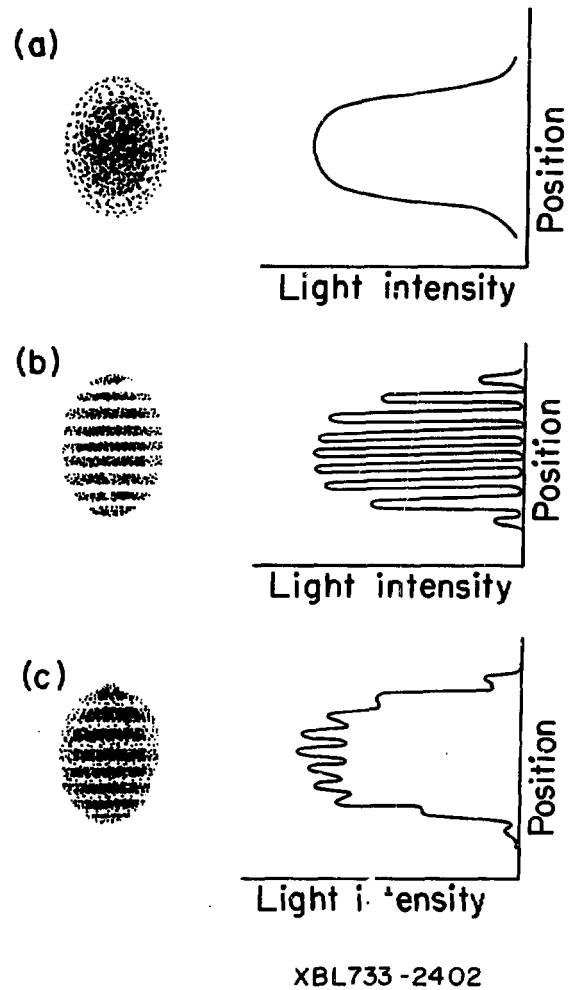

Fig. II-3. For legend, see page 31.

Fig. II-3. Patterns of illumination of the screen. (a) A smooth distribution of light intensity due to a source observed through one beam. (b) Two-beam interference fringes due to a source observed through both beams. (c) A pattern due to several separate sources.

If an optical system of this type, a two-beam spectrometer, were used to observe a plasma, and if the amplitude of the interference pattern, and not the total light intensity, were recorded as a spectral amplitude, the result would depend upon only those sources within the small, well localized common source volume. In this manner, one could observe exclusively a small selected region within a luminous volume of plasma. This is something which cannot be done with conventional spectroscopic apparatus.

The essential difference is that, in a single beam observation, unwanted light is stopped only by some system of masks and slits. Any light of the proper frequency which is admitted by the optical system--and this includes all the light radiated along certain rays--contributes to the output of the spectrometer. With two beams, however, it is possible to discriminate against a portion of that light which is admitted by the optical system. This is what gives the better resolution.

In a laboratory instrument, it is useful to observe an optical signal electronically. In a two-beam spectrometer, there are several ways in which this might be done. Most simply, the screen (in Fig. II-2) could be replaced by an array of slits placed at the positions of the maxima and minima of an expected two-beam interference pattern. Then a set of mirrors or light pipes could be used to direct the light from a set of maxima (which we shall call "beam 1") into one photomultiplier tube ("tube 1") and the light from the corresponding minima ("beam 2") into another phototube ("tube 2"). Then, if the illumination were uniform, the two

measured intensities would be equal, but if the expected two-beam interference pattern were present, most of the light would be received by one of the phototubes. One could then record, as the output of the system, not the total measured intensity, but rather the difference between the two phototube signals.

Any observation made with such an instrument would be a local measurement. Light from a source observed only through beam A or only through beam B would be divided equally between beams 1 and 2. Such light would not contribute to the recorded difference signal. Only light from common sources would (or might) be divided unequally between the two phototubes.

There is, however, a further complication. The apparatus of Fig. II-2 defines a common source volume which is at least as wide as a diffraction-limited focus of either of the two observed beams. To every point within this region there corresponds an expected set of two-beam interference fringes on the screen. But the patterns due to different sources might not coincide.

Indeed, it can be seen at once that all such patterns would not coincide. The locations of the maxima of such a pattern depend upon the difference between the lengths of the two optical paths from the source to a point on the screen. To estimate the effect of a displacement of the source, it is helpful to imagine interchanging source and screen. If a screen were placed at the common source volume and a point source were placed where we have drawn a screen, a set of two-beam interference fringes would again appear. The spacing of the fringes in this pattern would depend

upon α, the angle between the beams, and the size of the illuminated region would depend upon β, the angle subtended by either beam (see Fig. II-2). Since $\alpha \gg \beta$, there would be many fringes in the pattern. Because the various optical paths are unchanged by the interchange of source and screen, the maxima of the new pattern are just the locations in the original arrangement of sources which would have produced intensity maxima at the location of the new source. Such sources would have all produced coincident sets of interference fringes ("pattern 1"). Sources at intermediate points--the minima of the new pattern--would in the original arrangement have produced the opposite or complementary two-beam interference pattern ("pattern 2"). Finally, the region illuminated in the interchanged arrangement is just the original common source volume. Hence the multiplicity of fringes here implies the presence, in the system first considered, of different points from which light would contribute in opposing fashion to the output signal. Some common sources would radiate preferentially into phototube 1; other common sources would radiate preferentially into phototube 2.

If the common source volume were filled with luminous plasma, both types of source could be expected. The result might be a cancellation of effect. To understand the significance of this conclusion, it is helpful to recall some features of a laser light-scattering experiment. In that type of measurement, scatterers at different points necessarily contribute light of different phases to the observed beam and such contributions can

destructively interfere. As we have noted already, a uniform distribution of scattering centers would produce no scattered wave at all. The scattering is due to fluctuations in the density of scatterers. More particularly, according to Eq. (I.11), the light scattered by a plasma is due to one spatial Fourier component, the $\underline{k}_\Delta \equiv \underline{k}_s - \underline{k}_i$ component, of the electron density. Thus the partial cancellation of effect leads not to a null output but rather to a different and quite useful type of information.

The two-beam spectrometer of Fig. II-2 would in fact produce a similar result. From within the common source volume, light emitted into a narrow range of directions around $\hat{k}_A$ is accepted by beam A (see Fig. II-4). If a common source were displaced by $\underline{\delta}$, the optical path to the screen through beam A would be reduced by $\underline{\delta}\cdot\hat{k}_A$ and the change in phase along this path would be reduced by

$$(2\pi)\,\frac{\underline{\delta}\cdot\hat{k}_A}{(\text{wavelength})} = \frac{\underline{\delta}\cdot\hat{k}_A}{(\lambda/|k_A|)} = \underline{\delta}\cdot\underline{k}_A .$$

($\underline{k}_A$ = wave vector, at the source, of the light in beam A.) The same displacement $\underline{\delta}$ would reduce the difference in phase from the source to the screen along beam B by $\underline{\delta}\cdot\underline{k}_B$. Hence the relative phase of the light in the two beams would be changed by an amount

$$\underline{\delta}\cdot\underline{k}_B - \underline{\delta}\cdot\underline{k}_A = \underline{\delta}\cdot(\underline{k}_B - \underline{k}_A) = \delta\cdot\underline{k}_\Delta$$

($k_\Delta \equiv \underline{k}_B - \underline{k}_A$) which depends upon the displacement $\underline{\delta}$ and upon $\underline{k}_\Delta$, the difference wave vector, a quantity which appeared already in

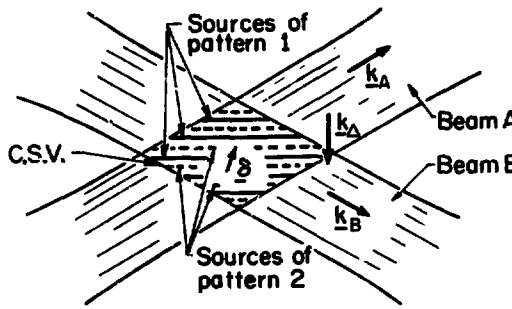

XBL733-2403

Fig. II-4a. The effect of a displacement of the source--detail of the source region. c.s.v. = common source volume.

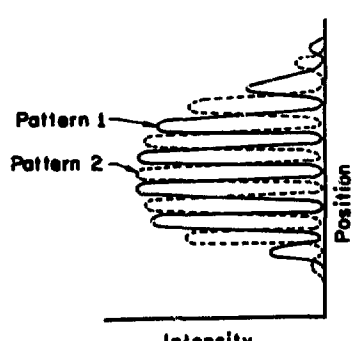

XBL 733-2404

Fig. II-4b. Corresponding patterns of illumination of the screen.

the analysis of scattering.

If the displacement $\underline{\delta}$ were normal to $\underline{k}_\Delta$, there would be no change in the relative phase of the light in the two beams. Hence all the common sources in a plane normal to $\underline{k}_\Delta$ would produce coincident interference patterns. Each such source plane would act as a single source. Furthermore, different source planes separated by an integral multiple of the distance $2\pi/|k_\Delta|$ would also produce the same pattern ("pattern 1"). But sources in an intermediate set of planes (see Fig. II-4) would all produce the opposite or complementary set of fringes ("pattern 2"). Hence the amplitude of the resulting two-beam interference--that is, of the mutual coherence between the light in the beams A and B--would be proportional not to the total intensity of common sources, but rather to the difference in intensity between these two groups of sources. This quantity is simply the amplitude of the $\underline{k}_\Delta$ spatial Fourier component of the source distribution.

Here it should be emphasized that although this result is similar to what is found in an analysis of scattering, the reasons for the same effect are somewhat different in the two cases. The result of a scattering measurement depends upon interference between the light scattered from different points within the scattering volume. The coherent incident beam provides a definite relation between the phases of waves scattered by different electrons. Beause of the resulting interference, the measured intensity of scattered light depends upon fine scale fluctuations in the plasma electron density.

To describe a spectroscopic observation, one must make the opposite assumption: The light from different sources is completely incoherent. There is no observable phase relation between the light emitted from one point and that from another point. In effect, two such waves would not interfere at all.

How then could one observe the source distribution? The answer is that if one looked from one direction only, one could not. But if a plasma were observed from two directions, with the instrument shown in Fig. II-2, (1) each common source would produce an interference pattern on the screen; and (2) if the sources were distributed in space according to $\underline{k}_{\Delta}$, these various interference patterns would coincide. Then an overall pattern would appear on the screen.

The light from each source would interfere only with itself, not with the light from another source. It is the relation between the different interference patterns which then gives information about the source distribution. But when one combines interference patterns, one adds intensities; one does not add electric fields. In this arrangement, it is the superposition of the various intensity patterns which corresponds to the interference of light waves (electric fields) in a scattering measurement.[32] A two-beam spectrometer could, of course, be considered without reference to a scattering measurement, but in any explanation it is important that points (1) and (2) should not be confused. Both steps are essential to the result.

The effect of the spatial distribution of sources has been

discussed as if it were stationary, which it would not be for times longer than $\tau_0 \approx 1/\omega_0$, where ω_0 is a frequency characterizing the $\underline{k}_\Delta$ component of the distribution. This affects the manner in which the signal must be received, but it also introduces the possibility of observing directly the frequencies characterizing the plasma.

We have assumed already that the observed light is a spectral line of width $\Delta\omega$. It follows that the measured light intensities cannot vary at frequencies greater than this. The time resolution of the system is further limited by the response times of photomultiplier tubes. If it is assumed that the signal does not vary over times shorter than $\tau = \left[c^{-1} \text{ (length of the common source volume)}\right]$ then the output of the system at any instant represents the (single) distribution of sources at the time the light was emitted. In this low frequency limit, the output signal would reproduce directly the (fluctuating) time dependence of the $\underline{k}_\Delta$ component of the distribution of common sources. (This is shown in Section II A 3 below.) If, for example, one had in the plasma a wave vector $\underline{k}_\Delta$ and (low) frequency ω_0, one would see in the signal an oscillation at ω_0 (provided, of course, that the light source intensity varied with the amplitude of the plasma wave). That is, a portion of the light accepted by the system would oscillate between beams 1 and 2 at ω_0, the frequency of the wave.

In the usual spectroscopic or light scattering measurement, it is sufficient to record an integrated intensity value. The fluctuation of the light intensity about the measured average is

not usually considered. In the present case, however, the fluctuation is important because the measured signal is the difference between two light intensities (beams 1 and 2). A long time average of this signal would produce a null result. It is essential to observe the signal over times less than $\tau_0 = 1/\omega_0$, the fluctuation time.

There are several ways in which this might be done. For pulsed experiments, the optimal procedure would be difficult to specify in general, but in a steady-state experiment one could simply record a frequency spectrum $Y(\omega)$ of the output signal $Y(t) \equiv \overline{I_2(t)} - \overline{I_1(t)}$. The recorded $Y(\omega)$ would be proportional to the spectrum of the $\underline{k}_\Delta$ component of the common source (intensity) distribution. (See Section II A 3.) For example, a plasma wave (in the common source volume) of wave vector $\underline{k}_\Delta$ and frequency ω_0 would produce a peak at ω_0 in the recorded signal spectrum $Y(\omega)$.

Finally, it should be noted that in several areas of research, methods are used which involve effects similar to those considered here. Interference between scattered waves is important, for example, in the scattering of x-rays by crystals[33] and in Brillon scattering of light by sound waves in liquids.[34] Theoretical analyses of the reflection of radar[35] waves also lead to many of the same results.

The suggested use of two-beam interference to resolve fluctuations in light source densities within a plasma is quite similar to the manner in which the diameters of stars can be measured with a Michaelson stellar interferometer.[36]

Another class of instruments which bear an interesting similarity to a two-beam spectrometer are the laser Doppler anemometers which are used to study gas and liquid flows. The literature on these devices is extensive, but the most common types of laser anemometers are mentioned in one conference review article by Durst, Melling, and Whitelaw.[37a] Those authors describe three arrangements (see their Fig. 1). The first is just a simple scattering experiment, but one in which the scattered light is combined with light from the incident beam before detection. This permits measurement of small frequency changes, which produce beats in the observed intensity. In the fluid systems on which these anemometers are used, the particle positions are essentially random over distances $\approx |\underline{k}_\Delta|^{-1}$, so the scattered light intensity is just the sum of contributions from the different particles. (See Section I C above.)

Durst et al. then describe another type of system in which only scattered light is seen, but in which the scattering region is illuminated with two beams from the same laser. The two incident beams interfere to give a pattern of fringes within the region observed. The scattered light is then found to be modulated by the motion of fluid density fluctuations across this pattern of varying illumination. This system is similar to the inverse of a two-beam spectrometer: Instead of a two-beam observation, one has two incident beams, but in each case the two beams interfere to define a source wavelength, and in each case the observed intensity is just the sum of contributions from the different

particles, in spectroscopy because of incoherence between sources and in scattering because of randomness in particle position. So for different reasons, one obtains quite similar results in the two cases.

Finally, the same authors mention also a system in which only a single incident beam is used, but in which the scattering is then observed from two directions. This system is the one which most resembles our two-beam system. A two-beam system used to measure random scattering is clearly similar to a two-beam spectrometer. However, in the laser anemometer, only one final light intensity is measured, so the signal contains contributions from each beam alone, as well as a correction due to interference. So even in the absence of coherence there would be an output (as from either tube 1 or 2 in our two-beam system) but in practice the effect of interference can be separated, since it gives a rapid time dependence to the measured signal.

Moreover, one can also use an intensity difference measurement to separate the interference in a laser anemometer. An arrangement which uses polarizing optics to do this has been studied by Bossel, Hiller, and Meier[37b] in an experiment of the two-incident-beam variety.

2. Some Comments on These Results

Thus a review of several widely used techniques illustrates the importance of an understanding of the coherence properties of an optical radiation field, and an analysis of a simple two-beam spectrometer shows that information about the local values of the

wavelengths and frequencies of fluctuations in light source densities is available, at least in principle, from measurements of the coherence of the emitted light. With this understanding, the present study was undertaken to explore the possibility of developing from these ideas a useful, practical diagnostic method.

Several general features of this type of measurement can be seen already from the first example. Only the effect of a single spectral line was described, but the same procedure could clearly be repeated for several portions of a spectrum. Since different spectral features are due to different types of sources, it should be possible to measure in this way the distributions in $\underline{k}$ and ω of various groups of particles. (In a scattering measurement, by comparison, only the electrons are observed directly.) With a two beam spectrometer, all of the information in the spectrum of the emitted light would still be available and one could measure at each optical frequency not only the total light intensity, but a whole set of optical correlations as well.

In a practical arrangement, the angle α between the beams could easily be made small by observing the plasma through two sections of one lens. This would permit observation of plasma wavelengths much larger than optical wavelengths. (Again, in comparison, a scattering study of long wavelength fluctuations requires the rather difficult observation of forward scattering.)

In comparison with the output of a conventional spectrometer, the level of the signal from a two-beam system would be much reduced. This, of course, simply reflects the improved resolution

of the instrument: Only a fraction of the sources observed through either beam contribute to the signal.

The problem is more serious, however, because in a real system, those sources which were observed, but which did not contribute to the signal, would produce a measured background noise. In the classical optical picture the "background light" (not to be confused with "stray light", which can be reduced by improvements in the optics) is divided equally between beams 1 and 2 and the effect is balanced out in the intensity difference signal. In a real system, the background light would contribute an irreducible amount of photon noise. The "signal" and "background" components differ simply in their photo count probability distributions and the separation of effects is a problem in statistics. The need for adequate photon statistics thus imposes a basic light intensity (and observation time) requirement which is considered in Chapter III of this discussion.

The need for adequate light intensity leads one to consider improvements in the design of the optical system. The two-beam spectrometer so far considered is extremely inefficient because the plasma is observed only through two narrow bundles of rays. Fortunately, one can design an equivalent system which presents a much larger solid angle of acceptance. In Appendix C, the preceding discussion is extended to include some more efficient arrangements. In Section II B below, the same problem is considered from a more abstract and general point of view.

Beyond the design of a more efficient version of the present system, it is also of interest to consider other possible observa-

tions. Selection of a single wavelength component of the distribution of sources within a local volume is not the only type of spatial resolution which could be achieved. Spectroscopic systems can be designed to use phase information for a variety of purposes. This possibility greatly extends the scope of the problem. It is important not only to consider a variety of optical systems, but also to describe in general terms the range of possible measurements. The necessary analysis is not completed in this study, but in the next few sections of the discussion, several ways of looking at the prolem are considered.

Many plasma phenomena occur at frequencies too high for direct time measurements. The low frequency assumption of the preceding analysis is thus a severe restriction on the utility of the suggested method. Fortunately, it does not appear to be a necessary limitation. Some modifications of the apparatus which would permit observation of higher frequency phenomena are proposed in Chapter V.

The low-frequency limit is nevertheless a convenient initial simplification. It essentially permits one to consider first the spatial or $\underline{k}$ dependence of the problem and to defer discussion of the time or frequency dependence. Both the analysis presented in this chapter and the observations described in Chapter IV pertain to this one aspect of the problem.

3. A Reformulation of the Two-Beam Problem

In the preceding discussion of a two-beam spectrometer, several assumptions are stated or implied:

1. The effect of the plasma is represented by a scalar source density, $s(\underline{r},t)$, which is not affected by other elements of the optical problem.

2. One linearly polarized component of the emitted light is accepted by the optical system. It is assumed that the amplitude $\xi(\underline{r},t)$ of this radiation is related to the source by a scalar wave equation Eq. (I.3),

$$\nabla^2\xi(\underline{r},t) - \frac{1}{c^2}\frac{\partial^2\xi(\underline{r},t)}{\partial t^2} = -4\pi s(\underline{r},t)$$

which has the retarded solution[38]

$$\xi(\underline{r},t) = \int d^3r' \frac{1}{|\underline{r} - \underline{r}'|} s\left(\underline{r}', t - \frac{|\underline{r} - \underline{r}'|}{c}\right). \qquad \text{(II.1)}$$

3. The plasma is observed through two beams which are restricted as to regions of observation, directions $(\hat{k}_A, \hat{k}_B)$ of emission of accepted light, and optical wavelength $(2\pi/|\underline{k}_A| + 2\pi/|\underline{k}_B|)$. The accepted light is conveniently described in terms of a spatial Fourier transform of the wave amplitude

$$\xi_{A,B}(\underline{k}_{A,B},t) \equiv \int_{\substack{\text{(all}\\ \text{space)}}} d^3r\, \xi_{A,B}(\underline{r},t) e^{-i\underline{k}_{A,B}\cdot\underline{r}} \qquad \text{(II.2a)}$$

$$= \int_{\substack{\text{(all}\\ \text{space)}}} d^3r \int_{\substack{\text{(region}\\ \text{observed)}}} d^3r' \frac{1}{|\underline{r} - \underline{r}'|} \cdot s\left(\underline{r}', t - \frac{|\underline{r} - \underline{r}'|}{c}\right) e^{-i\underline{k}_{A,B}\cdot\underline{r}}$$

$$= \int_{\substack{\text{(all}\\ \text{space)}}} d^3r' \; \xi_{A,B}(\underline{k}_{A,B}, t; \underline{r}'),$$

where

$$\xi_{A,B}(\underline{k}, t; \underline{r}') \equiv \begin{cases} \int d^3r \, \frac{e^{-i\underline{k}\cdot\underline{r}}}{|\underline{r} - \underline{r}'|} \, s\left(\underline{r}', t - \frac{|\underline{r} - \underline{r}'|}{c}\right) \\ \text{for points } \underline{r}' \text{ within the observed beam and} \\ 0 \quad \text{for all other points } \underline{r}' \end{cases} \tag{II.2b}$$

is the $\underline{k}$ component of the radiation from sources at points $\underline{r}'$ observed through beam A or B.

Since the negative frequency components of $\xi_{A,B}(\underline{k}_{A,B}, t)$ propagate in the $-\hat{k}_{A,B}$ direction, and since the source is observed from the $+\hat{k}_{A,B}$ directions, only the positive frequency components, $\xi^{(+)}_{A,B}(\underline{k}_{A,B}, t)$, are received by the detector. (This point is discussed in detail in Appendix E. 1.) The amplitudes of the transmitted waves, which are, of course, real valued quantities, may be expressed in terms of $\xi^{(+)}_{A,B}(\underline{k}_{A,B}, t)$. See Eq. (E.17) and discussion.) To within a multiplicative constant

$$\xi^{(\text{observed})}_{A,B}(\underline{r}, t) \propto \text{Re} \int_{\substack{\text{(directions}\\ \text{observed)}}} d^2\hat{k}_{A,B} \int_0^\infty d|\underline{k}_{A,B}| \, e^{i\underline{k}_{A,B}\cdot\underline{r}} f(|\underline{k}_{A,B}|c)$$

$$\cdot \frac{|\underline{k}_{A,B}|}{2\pi i c} \, \xi^{(+)}_{A,B}(\underline{k}_{A,B}, t) \tag{II.3}$$

where $f(|\underline{k}_{A,B}|c)$ is the transfer function of the spectral filter. The light in each beam may then be expressed as the superposition

of contributions from different points within the plasma. Combining Eqs. (II.2) and (II.3), we have

$$\xi^{(\text{observed})}_{A,B}(\underline{r},t) = \int d^3r' \; \xi^{(\text{observed})}_{A,B}(\underline{r},t;\underline{r}') \tag{II.4a}$$

where

$$\xi^{(\text{observed})}_{A,B}(\underline{r},t;\underline{r}') = \text{Re}\int d^2\hat{k}_{A,B} \int_0^\infty d|\underline{k}_{A,B}| e^{i\underline{k}_{A,B}\cdot\underline{r}} f(|\underline{k}_{A,B}|c)$$

$$\cdot \frac{|\underline{k}_{A,B}|}{2\pi i c} \xi^{(+)}_{A,B}(\underline{k}_{A,B},t;\underline{r}') \tag{II.4b}$$

4. The light in beams A and B is then combined and reseparated into two complementary "interference patterns," beams 1 and 2, whose time averaged intensities are measured. The optical system which combines the two beams serves to superimpose the light from different points: $\underline{r}_A$ within beam A and $\underline{r}_B$ within beam B.

$$I_{1,2}(t) = \overline{\left| \frac{1}{\sqrt{2}} \left[\xi^{(\text{observed})}_B(\underline{r}_B,t) \mp \xi^{(\text{observed})}_A(\underline{r}_A,t) \right] \right|^2}$$

$$= \frac{1}{2} \overline{\left| \int d^3r' \; \xi^{(\text{observed})}_B(\underline{r}_B,t;\underline{r}') \mp \int d^3r' \; \xi^{(\text{observed})}_A(\underline{r}_A,t;\underline{r}') \right|^2} . \tag{II.5}$$

5. Light emitted from different points within the plasma is completely incoherent. Each measured intensity is just the sum of intensities of light from different points. Thus Eq. (II.5) becomes

$$I_{1,2}(t) = \frac{1}{2}\int d^3r' \overline{\left| \xi_B^{(\text{observed})}(\underline{r}_B, t; \underline{r}') \mp \xi_A^{(\text{observed})}(\underline{r}_A, t; \underline{r}') \right|^2} \qquad \text{(II.6)}$$

Since beams A and B are transmitted through the same spectral filter, $f(|k_A|c) = f(|k_B|c)$ and Eqs. (II.4) and (II.6) reduce to

$$I_{1,2}(t) = \frac{1}{2}\int d^3r' \overline{\left| \text{Re} \int_0^\infty d|\underline{k}| \, \frac{|\underline{k}|}{2\pi i c} f(|\underline{k}|c) \right.}$$

$$\overline{\left. \left[\int d^2k_B e^{i\underline{k}_B \cdot \underline{r}_B} \xi_B^{(+)}(\underline{k}_B, t; \underline{r}') \mp \int d^2k_A e^{i\underline{k}_A \cdot \underline{r}_A} \xi_A^{(+)}(\underline{k}_A, t; \underline{r}') \right] \right|^2} \qquad \text{(II.7)}$$

6. Beams A and B are narrow bundles of rays, each subtending a small solid angle $\delta^2\Omega$. The amplitude $\xi_{A,B}$ does not vary over the width of either beam, so the integrations over direction $d^2k_{A,B}$ merely introduce a factor of $\delta^2\Omega$.

7. The integration time over which the intensities are averaged exceeds the coherence time of the light, so the measured intensities are just the sums of the intensities of different spectral components,

$$I_{1,2}(t) = \frac{1}{2}\int d^3r' \int_0^\infty d|\underline{k}| \left(\frac{|\underline{k}|}{2\pi c} \right)^2 (\delta^2\Omega)^2$$

$$\cdot \overline{\left| \text{Re } if(|\underline{k}|c) \left[e^{i\underline{k}_B \cdot \underline{r}_B} \xi_B^{(+)}(\underline{k}_B, t; \underline{r}') \mp e^{i\underline{k}_A \cdot \underline{r}_A} \xi_A^{(+)}(\underline{k}_A, t; \underline{r}') \right] \right|^2}. \qquad \text{(II.8)}$$

Since the wave amplitudes are real, their time-averaged

intensities can be expressed in terms of the associated analytic signal. [See Eq. (E.15).] It is convenient to make this substituion here. Doing so, and using the result obtain in Appendix E.2 leads, after a few algebraic steps, to the expression

$$I_{1,2}(t) = \int d^3r' \int_0^\infty d|\underline{k}| \; |f(|\underline{k}|c)|^2 I_{1,2}(t,|\underline{k}|;\underline{r}') \qquad \text{(II.9a)}$$

where

$$I_{1,2}(t,|\underline{k}|;\underline{r}') = \frac{1}{4}\left(\frac{|k|\delta^2\Omega}{2\pi c}\right)^2 \cdot \overline{\left| e^{i\underline{k}_B\cdot\underline{r}_B} \xi_B^{(+)}(\underline{k}_B,t;\underline{r}') \mp e^{i\underline{k}_A\cdot\underline{r}_A} \xi_A^{(+)}(\underline{k}_A,t;\underline{r}') \right|^2}. \qquad \text{(II.9b)}$$

8. Each location within the plasma is an isotropic source of light whose coherence length exceeds any differences in optical path through the system. The contributions to beams A and B from the same source point are completely coherent. Their combined effect is found by adding the two component amplitudes before time averaging.

The recorded output of the instrument is the difference between the two measured intensities,

$$Y(t) = I_2(t) - I_1(t)$$

$$= \int d^3r' \int_0^\infty d|\underline{k}| \; |f(|\underline{k}|c)|^2 \left[I_2(t,|\underline{k}|;\underline{r}') - I_1(t,|\underline{k}|;\underline{r}') \right]. \qquad \text{(II.10)}$$

Using Eq. (II.9b) gives, after a few algebraic steps,

$$I_2(t,|\underline{k}|;\underline{r}') - I_1(t,|\underline{k}|;\underline{r}') = \left(\frac{|\underline{k}|\delta^2\Omega}{2\pi c}\right)^2$$

$$\cdot \left\{ \mathrm{Re}\left[\overline{e^{-i\underline{k}_A\cdot\underline{r}_A \xi(+)^*(\underline{k}_A,t;\underline{r}')} e^{i\underline{k}_B\cdot\underline{r}_B \xi_B(+)(\underline{k}_B,t;\underline{r}')}} \right] \right\}$$

$$= \mathrm{Re}\ \Gamma_{BA}(0;|\underline{k}|,\underline{r}') \qquad \text{(II.11)}$$

where the correlation $\Gamma_{BA}(\tau;|\underline{k}|,\underline{r}')$ is defined

$$\Gamma_{BA}(\tau;|\underline{k}|,\underline{r}') \equiv \left(\frac{|\underline{k}|\delta^2\Omega}{2\pi c}\right)^2 \overline{\left[e^{i\underline{k}_A\cdot\underline{r}_A \xi_A(+)(\underline{k}_A,t;\underline{r}')}\right]^*}$$

$$\cdot \overline{\left[e^{i\underline{k}_B\cdot\underline{r}_B \xi_B(+)(\underline{k}_B,t+\tau,\underline{r}')}\right]} \ . \qquad \text{(II.12)}$$

Thus the observed signal is just an integral of correlations

$$Y(t) = \int_{\substack{\text{(common}\\ \text{source volume)}}} d^3r' \int_0^\infty d|\underline{k}|\ |f(|\underline{k}|c)|^2\ \mathrm{Re}\ \Gamma_{BA}(0;|\underline{k}|,\underline{r}') \qquad \text{(II.13)}$$

between the $\underline{k}_A$ and $\underline{k}_B$ components of the light. Since Γ_{BA} is clearly zero if either factor vanishes, the $\underline{r}'$ integration may be restricted to the common source volume as expected.

Equations (II.2b) can now be used to express the correlation $\Gamma_{BA}(0;|\underline{k}|,\underline{r}')$ in terms of the given source distribution, $s(\underline{r}',t)$:

$$\Gamma_{BA}(0;|\underline{k}|,\underline{r}') = \left(\frac{|\underline{k}|\delta^2\Omega}{2\pi c}\right)^2 e^{-i\underline{k}_A\cdot\underline{r}_A} e^{+i\underline{k}_B\cdot\underline{r}_B}$$

$$\cdot \overline{\int d^3r_1 \frac{e^{i\underline{k}_A\cdot\underline{r}_1}}{|\underline{r}_1 - \underline{r}'|} s^{(+)*}\left(\underline{r}', t - \frac{|\underline{r}_1 - \underline{r}'|}{c}\right)}$$

$$\cdot \overline{\int d^3r_2 \frac{e^{-i\underline{k}_B\cdot\underline{r}_2}}{|\underline{r}_2 - \underline{r}'|} s^{(+)}\left(\underline{r}', t - \frac{|\underline{r}_2 - \underline{r}'|}{c}\right)}$$

$$= \left(\frac{|\underline{k}|\delta^2\Omega}{2\pi c}\right)^2 e^{-i\underline{k}_A\cdot\underline{r}_A} e^{+i\underline{k}_B\cdot\underline{r}_B} e^{i\underline{k}_A\cdot\underline{r}'} e^{-i\underline{k}_B\cdot\underline{r}'}$$

$$\cdot \overline{\int d^3\rho_1 \frac{1}{|\underline{\rho}_1|} e^{i\underline{k}_A\cdot\underline{\rho}_1} s^{(+)*}\left(\underline{r}', t - \frac{|\underline{\rho}_1|}{c}\right)}$$

$$\cdot \overline{\int d^3\rho_2 \frac{1}{|\underline{\rho}_2|} e^{-i\underline{k}_B\cdot\underline{\rho}_2} s^{(+)}\left(\underline{r}', t - \frac{|\underline{\rho}_2|}{c}\right)} \qquad \text{(II.14)}$$

where $\underline{\rho}_1 \equiv \underline{r}_1 - \underline{r}'$

and $\underline{\rho}_2 \equiv \underline{r}_2 - \underline{r}'$.

This expression reduces to (see Appendix B.2 for details),

$$\Gamma_{BA}(0;|\underline{k}|,\underline{r}') \underset{t\to\infty}{\rightarrow} e^{-i\underline{k}_A\cdot(\underline{r}_A-\underline{r}')} e^{i\underline{k}_B\cdot(\underline{r}_B-\underline{r}')} (\delta^2\Omega)^2 \mathcal{S}(|\underline{k}|c;\underline{r}') \qquad \text{(II.15a)}$$

where

$$\mathcal{S}(|\underline{k}|c;\underline{r}') \equiv |s^{(+)}(\underline{r}', |\underline{k}|c)|^2 \qquad \text{(II.15b)}$$

is the spectrum of the light emitted from $\underline{r}'$. [$s^{(+)}(\underline{r}', |\underline{k}|c)$ is the temporal Fourier transform of $s^{(+)}(\underline{r}', t)$, i.e., the positive frequency portion of the transform of $s(\underline{r}', t)$. The spectrum $\mathcal{A}(|\underline{k}|c; \underline{r}')$ is thus defined over positive optical frequencies $|\underline{k}|c$.]

The time average in Eq. (II.15b) is actually superfluous, since the averaged quantity is constant. This is a consequence of the introduction of the analytic signal in Eq.(II.9); if the real field amplitude had been retained, an average would be needed to define a constant light intensity.

More important, however, is the fact that a real time average is always taken over a finite interval. In a real system, if $\Delta\omega$, the spectrometer bandwidth, is relatively narrow, the output light is nearly monochromatic. Then an average of the intensity over a time $T \sim \Delta\omega^{-1}$ eliminates the optical frequency variation but retains a slow time dependence in the measured spectrum. The result of this operation (which is considered more carefully in Appendix E.5) is a time varying signal, not a single long time limit as above. To describe this result, Eq. (II.15) can simply be rewritten in the form,

$$\Gamma_{BA}(0; |\underline{k}|, \underline{r}', t) = e^{-i\underline{k}_A\cdot(\underline{r}_A - \underline{r}')} e^{+i\underline{k}_B\cdot(\underline{r}_B - \underline{r}')} (\delta^2\Omega)^2 \mathcal{A}(|\underline{k}|c; \underline{r}', t) \tag{II.16}$$

Since the spectral amplitude is real, the phase of the correlation is determined by the factor,

$$e^{i\left[\underline{k}_B\cdot(\underline{r}_B - \underline{r}') - \underline{k}_A\cdot(\underline{r}_A - \underline{r}')\right]}. \tag{II.17}$$

The two terms in the exponent are just the phase differences along the paths from the source point $\underline{r}'$ to the two observation points. The phase of the correlation, that is, the relative phase of the components of the light observed through the two beams, is just determined by the difference between the lengths of the two optical paths.

In general, this difference would depend both upon $\underline{r}'$ and upon $|\underline{k}|$. However, it was assumed above that the light from each point $\underline{r}'$ is coherent, that its coherence length exceeds the differences in optical path. For a thermal plasma, the coherence length is just determined by the width of the spectrum of the transmitted light. The requirement of coherence simply means that the light is so nearly monochromatic and the path differeences are so small that the phase difference is the same for all components of the spectrum. Under this assumption, the phase of the correlation depends upon $\underline{r}'$, but not explicitly upon $|\underline{k}|$. The expression (II.17) may thus be written

$$e^{i\phi}\, e^{-i\underline{k}_\Delta \cdot \underline{r}'}$$

where

$$\phi \equiv \underline{k}_B \cdot \underline{r}_B - \underline{k}_A \cdot \underline{r}_A \qquad \text{(II.18)}$$

and

$$\underline{k}_\Delta \equiv \underline{k}_B - \underline{k}_A$$

may be defined for one typical optical wavelength and then treated as constants, independent of $|\underline{k}|$. Equations (II.13) and (II.16) then give the final form,

$$Y(t) = (\delta^2\Omega)^2 \int_0^\infty d|\underline{k}|\ |f(|\underline{k}|c)|^2$$

$$\cdot\ \mathrm{Re}\Big[e^{i\phi} \int_{\substack{\text{common}\\ \text{source volume}}} d^3\underline{r}'\ e^{-i\underline{k}_\Delta\cdot\underline{r}'}\, \mathcal{A}(|\underline{k}|c;\underline{r}',t)\Big]$$

$$= (\delta^2\Omega)^2\ \mathrm{Re}\Big[e^{i\phi} \int_0^\infty d|\underline{k}|\ |f(|\underline{k}|c)|^2 \mathcal{A}(|\underline{k}|c;\underline{k}_\Delta,t)\Big] \qquad \text{(II.19)}$$

$$\text{common sources}$$

So, to within a phase factor, the result depends only upon $\mathcal{A}(|\underline{k}|c;\underline{k}_\Delta,t)$, the $\underline{k}_\Delta$ spatial Fourier component of the distri-
common sources

bution of those sources of light of frequency $|\underline{k}|c$ which are observed through both beams, and upon $|f(|\underline{k}|c)|^2$, the transmission function of the spectral filter. The time dependence of the output simply follows the time dependence of the observed component of the light source distribution.

Only one phase of the complex valued $\mathcal{A}(|\underline{k}|c;\underline{k}_\Delta,t)$ is
common sources

here observed but, as explained in the next section, the optical system could easily be modified to provide both the real and the imaginary parts of $e^{i\phi}\mathcal{A}$.

It should be emphasized that the assumption of coherence does not imply that the interference must be the same for all accepted wavelengths. Sources of different portions of a spectral line, for example, might well be differently distributed in space. Different portions of a Stark broadened line, emitted from regions

of different electric field, or different portions of a Doppler broadened line, emitted by sources moving with different velocities could exhibit different dependence upon $\underline{k}_\Delta$ and t, even though the spectrum was quite narrow. The assumption of coherence simply means that the relation between the location of the source and the resulting interference pattern is the same for all accepted wavelengths. So long as this is true, the measured distribution will be just the sum of the distributions of all the sources which are observed in any single measurement.

If the spectrum of accepted light were so wide that the light was not coherent, the total signal would be due to <u>different</u> components of the distributions of sources of light of different wavelengths. This is not to say that such a measurement could not be useful, but only that it is not covered by the foregoing analysis. Some ways in which a larger portion of the spectrum might be used are considered in Chapters V and VI below.

For a two-beam spectroscopic observation, made with a narrow portion of the spectrum, Eq. (II.19) confirms the conclusions of our first analysis. The output, Y(t), gives a measure of $\mathcal{A}_{\text{common sources}}(|\underline{k}|c;\underline{k}_\Delta,t)$, the $\underline{k}_\Delta$ component of the common source distribution. If desired, a spectrum analyzer could be used to measure the (low) frequency spectrum $Y(\omega)$ of the output, which would give $\mathcal{A}_{\text{common sources}}(|\underline{k}|c;\underline{k}_\Delta,\omega)$, the complete Fourier transform of the distribution of light sources within the common source volume. According to the Wiener-Khintchine theorem, a complete

measurement of $\mathcal{S}(|\underline{k}|c;\underline{k}_\Delta,\omega)$ would provide the two-point, two-time correlation function of the source distribution. (common sources)

As in a scattering measurement (see Section I.C), only one $\underline{k}$ component, the $\underline{k}_\Delta$ component of the source density fluctuations would be observed at once, but with a two-beam spectrometer, one could examine a variety of plasma wavelengths by varying either the angle between the two beams or the optical wavelength accepted. In an arrangement like that of Fig. II-2, the angle between beams A and B could be changed by replacing the first lens by another of different focal length. The wavelength could be changed by changing the spectral filter, but of course it should be remembered that different optical wavelengths may be due to different types of source. As in any spectroscopic study, the relation between components of the spectrum and conditions in the plasma is a complicated matter which requires a separate analysis. With a conventional spectrometer, only the total intensity of each component of the spectrum is observed. With a two-beam spectrometer, one could, in principle, observe the two-point, two-time correlation function of the distribution of the sources of any feature in the spectrum of the light emitted by a plasma.

B. Multiple-Beam Systems

1. The Use of Polarization

The foregoing analysis was based upon a scalar wave equation, or, more precisely, upon a retarded Green's function solution to such an equation. This common, useful procedure is

easily interpreted: The scalar equation describes a single polarization component of the field. Such a description applies to many spectroscopic measurements, in which a single linearly or circularly polarized component of the light is used. Since, in many situations, light waves of different polarization remain distinct, a scalar analysis is often justified. However, even if the source is considered to be a scalar, and even if a scalar wave equation is used to calculate the amplitude of the emitted light, the fact that light is actually a vector wave is still important in the present problem.

The vector nature of the wave should be considered, first of all because the polarizability of light provides a most convenient way to measure phase relations. This fact is the basis of a class of instruments called polarization interferometers which are described in a recent book.[39] A polarization interferometer is a device in which two beams of light are differently polarized and then combined. The polarization of the resulting light depends upon the relative phase, as well as the polarization of the original component waves. Because of this dependence, a measurement of the resulting polarization gives information about the phases of the component waves, the same information which, in a conventional interferometer, is provided by a study of a pattern of interference fringes.

In most polarization interferometers, the interfering waves (waves A and B of the preceding discussion) are linearly polarized in orthogonal directions, as shown in Fig. II-5. If two

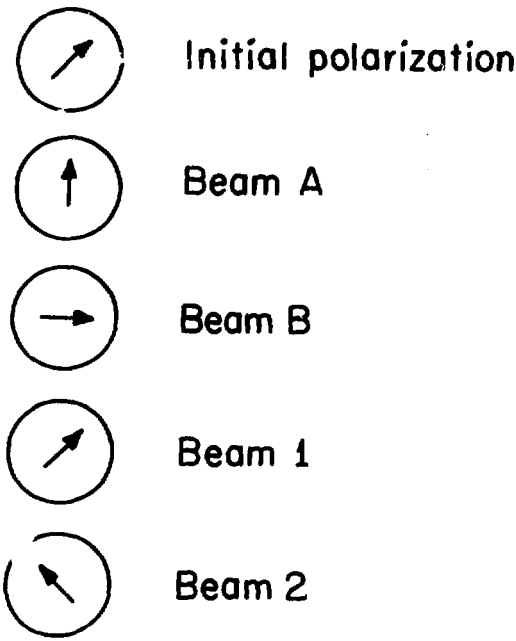

Fig. II-5. Polarization of the different beams.

such waves are equal in amplitude, and also equal in phase, their superposition will again be linearly polarized, in the direction "1" shown in Fig. II-5. If the interfering waves are 180 deg out of phase, their superposition will be linearly polarized in the orthogonal direction "2". These two polarization components are exactly equivalent to the "interference patterns 1 and 2" which were considered in detail in Section II.A above.

This equivalence provides a very convenient way to actually construct a two-beam spectroscopic system. Several possible designs for such an instrument are described in detail in Appendix C of this discussion. Essentially, one must use an initial polarizer to select one component of the emitted light, then polarize the observed beams A and B as shown in Fig. II-5, combine them, and separate the result into polarization components 1 and 2, which are observed with separate phototubes. Then, if beams A and I are coherent, their superposition will be polarized, and the light will be divided between phototubes 1 and 2 in a manner determined by the relative phase of A and B, exactly as described by the analysis of Section II.A.3. If the light in beams A and B is incoherent, their superposition will be unpolarized, the light will be divided equally between the two phototubes, and the output signal, $Y(t) = I_2(t) - I_1(t)$ will be zero. If the two observed beams are partially coherent, their superposition will be partially polarized, and, just as before, only the coherent portion of the light will contribute to the output of the system.

There are several advantages to this technique. A sorting out of different sets of interference fringes might be difficult,

but the orthogonally polarized components "1" and "2" can easily be separated. If beams A and B are distinguished by their polarization, they can be superimposed and portions of their paths made physically identical, insuring equality of path length and minimizing the effect of vibrations and misalignments in the system. Such a procedure also reduces the number of optical components needed, since, roughly speaking, every element then counts as two. Several other reasons for using polarization are examined later, in Appendix C.

One potential advantage, which we shall not consider further, but which should at least be mentioned, is the possibility of measuring the complete complex mutual coherence of the two observed light beams. Recall that the two-beam system analyzed above was shown to measure an integral over sources and frequencies of

$$\mathrm{Re}\left[e^{i\phi}\Gamma_{BA}(0;|\underline{k}|,\underline{r}')\right]$$

[see Eq. (II.13)], where Γ_{BA} is the mutual coherence and $e^{i\phi}$ is a constant factor. The restriction to the real part of the expression is a consequence of the way in which the interference was observed. The system separated "interference patterns 1 and 2," with pattern 1 produced if beams A and B were--apart from the phase difference ϕ--equal in phase and pattern 2 produced if they were 180 deg out of phase. However, if A and B were 90 deg apart in phase, the fringe pattern would be exactly intermediate between 1 and 2, the light would be divided equally between the two photo-

tubes, and a null output would result--exactly as if the light were incoherent. Such unobserved correlations are represented by the missing part of the mutual coherence,

$$\mathrm{Im}\left[e^{i\phi}\Gamma_{BA}(0;|\underline{k}|,\underline{r}')\right].$$

In a polarization interferometer, such a correlation would make the output circularly polarized. Since this effect could also be observed, both the real and the imaginary parts of the mutual coherence could, in principle, be measured, a possibility explained in more detail in Ref. 39.

After discussing a two-beam spectrometer, it is natural to imagine extending the method by designing a system to compare light emitted in many directions from a plasma. Such a multiple-beam spectrometer would certainly be more efficient than a two-beam system, since more light could be used, and furthermore, the more complex arrangement should make possible a great variety of spectroscopic measurements.

Thus one could proceed now to consider in succession three- and four- and five-beam spectroscopic systems. However, when the use of polarization is included, the simple two-beam system suggests a different kind of generalization. Since orthogonally polarized beams may be superimposed without loss of identity, one can, with a polarizing system, define not just more beams, but two whole sets of beams, "beams A" and beams B," polarized as A and B in Fig. II-5.

Within the optical system, the A and B components cannot only

be recognized, they can also be independently manipulated. If optical components made of birefringent materials are included in the system, the optics seen by the A and B components of the light can be completely different. This possibility, which is really the most important reason for using polarizing optics, leads us to replace the simple two-beam system by a much more general type of apparatus. In place of the two apertures which defined beams A and B, there can be two whole optical systems, A and B, followed by a polarization interferometer to measure the correlation between the two resulting waves.

2. Multiple-Beam Systems in the Huygens Approximation

A general spectroscopic system of this type is shown in Fig. II-6. There a lens, with focal point within the plasma, is followed by a linear polarizer, which insures that the system operates with only one component of the light. The amplitude of this transmitted wave, $\xi_0(\underline{r},t)$, may be treated as a scalar and related to a given scalar source by expression

$$\xi_0(\underline{r}^{(in)},t) = \int d^3r' \frac{1}{|\underline{r}^{(in)} - \underline{r}'|} \cdot s\left(\underline{r}', t - \frac{|\underline{r}^{(in)} - \underline{r}'| + \phi_1(\underline{r}^{(in)})}{c}\right) \qquad \text{(II.20)}$$

where $\underline{r}' = (x', y', z')$ refers to points within the plasma and $\underline{r}^{(in)} = (x^{(in)}, y^{(in)}, z^{(in)})$ denotes points immediately behind the lens. ($x' = x^{(in)} = y' = y^{(in)} = 0$ along the axis of the system.)

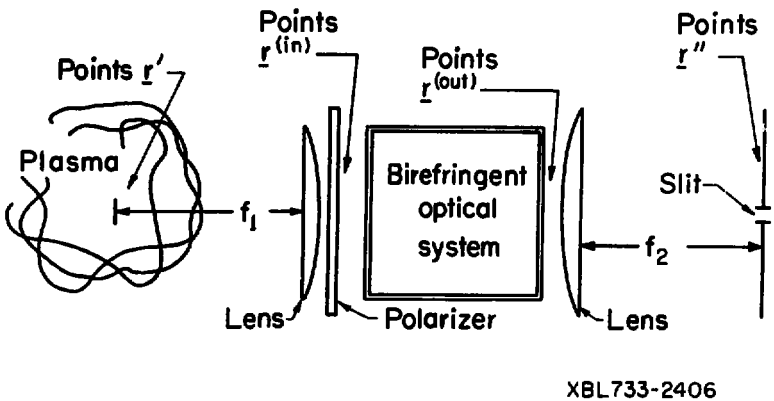

Fig. II-6. A multiple-beam spectroscopic system. (The slit shown at the right is the entrance to a spectrometer.)

$$\phi_1(\underline{r}^{(in)}) = \phi_{10} - \frac{1}{2} \frac{x^{(in)^2} + y^{(in)^2}}{f_1}$$

is the additional path introduced by the lens, which has a focal length of f_1.

This wave, ξ_0, is then considered to consist of A and B components, which are initially identical, except in polarization. The first lens is followed by an optical system which affects the A and B components differently. That is, the system contains birefringent elements with axes oriented so that the A and B components remain distinct and independent, but follow different paths. Assuming linearity and time-independence of the system, the effect of such an apparatus is described by two Green's functions, $g_A(\underline{r}^{(out)}, \underline{r}^{(in)}, \tau)$ and $g_B(\underline{r}^{(out)}, \underline{r}^{(in)}, \tau)$:

$$\xi_{A,B}(\underline{r}^{(out)},t) = \int d^3r^{(in)} \int_0^\infty d\tau \cdot g_{A,B}(\underline{r}^{(out)},r^{(in)},\tau)\xi_0(\underline{r}^{(in)},t - \tau). \quad \text{(II.21)}$$

Here $\underline{r}^{(out)} = (x^{(out)}, y^{(out)}, z^{(out)})$ denotes points across the output of the system.

The birefringent portion of the system is followed by a second lens of focal length f_2 which focuses parallel light onto a plane [of points $\underline{r}'' = (x'', y'', z'')$] containing the entrance to a spectrometer. The light at points $\underline{r}''$ is related to the light before the second lens by two Kirchoff integral expressions:[40]

$$\xi_{A,B}(\underline{r}'',t'') = \frac{1}{4\pi}\int d^2r^{(out)} \left[\frac{1}{|\underline{r}'' - \underline{r}^{(out)}|} \nabla\xi_{A,B}(\underline{r}^{(out)}, t^{(out)}) \right.$$

$$\left. - \frac{\underline{r}'' - \underline{r}^{(out)}}{c|\underline{r}'' - \underline{r}^{(out)}|^2} \frac{\partial}{\partial t^{(out)}} \xi_{A,B}(\underline{r}^{(out)}, t^{(out)}) \right]_{\text{Ret.}} \qquad \text{(II.22)}$$

$$\text{Ret.:} \quad t^{(out)} = t'' - \frac{|\underline{r}'' - \underline{r}^{(out)}| + \phi_2(\underline{r}^{(out)})}{c} .$$

Here

$$\phi_2(\underline{r}^{(out)}) = \phi_{20} - \frac{1}{2} \frac{x^{(out)^2} + y^{(out)^2}}{f_2}$$

is the added path length produced by the lens. $\left[x^{(out)} = x'' = y^{(out)} = y'' = 0 \text{ along the axis of the system.} \right]$ Here it is assumed that the normal component of $\nabla\xi(\underline{r},t)$ just after the lens is approximately given by

$$\nabla\xi \left[\underline{r}^{(out)}, t - \frac{\phi_2(\underline{r}^{(out)})}{c} \right] \cdot d^2r^{(out)}.$$

A term of higher order in $\left[(\text{wavelength})/|\underline{r}'' - \underline{r}^{(out)}| \right]$ has also been neglected. In this expression one can make the usual Huygens approximation by assuming that $\xi = 0$ behind any masks and is unperturbed at the points across an aperture.

Altogether, Eqs. (II.20), (II.21), and (II.22) determine $\xi_A(\underline{r}'',t'')$ and $\xi_B(\underline{r}'',t'')$ in terms of $s(\underline{r}',t')$. Since the different steps are linear relations, their combined effect is also linear. Hence if ξ_A, ξ_B, and s are Fourier transformed in time,

the fields at any point $\underline{r}''$ produced by a source at a point $\underline{r}'$ will be determined by two complex-valued transfer functions, $\phi_A(\underline{r}'',\underline{r}',\omega)$ and $\phi_B(\underline{r}'',\underline{r}',\omega)$.

$$\xi_{A,B}(\underline{r}'',\omega;\underline{r}') = \phi_{A,B}(\underline{r}'',\underline{r}';\omega)s(\underline{r}',\omega). \qquad \text{(II.23)}$$

Within the spectrometer, however, it is not the A and B components, but rather the intermediate polarizations "1" and "2" which are separated.

$$\xi_1 = 1/\sqrt{2}\ (\xi_B - \xi_A)$$

$$\xi_2 = 1/\sqrt{2}\ (\xi_B + \xi_A).$$

Since all of the light of the proper frequency which enters the spectrometer is reflected into one of the phototubes, each measured intensity is given by an integral over the spectrometer entrance aperture. Assuming that the light is nearly normal to this surface,

$$I_{1,2}(t';\underline{r}') = \int_{\substack{\text{(spectrometer}\\ \text{entrance)}}} d^2r'' \int_0^\infty \frac{d\omega}{2\pi} |f(\omega)|^2 \cdot |\xi_B(\underline{r}'',\omega;\underline{r}',t) \mp \xi_A(\underline{r}'',\omega;\underline{r}',t)|^2.$$

Here, as in the analysis in Section II.A.3, $|f(\omega)|^2$ is the spectrometer transmission function. Also as before, a slow time dependence has been included here in the measured spectra.

Since the plasma is an incoherent source, each intensity is just a sum of contributions from the different points $\underline{r}'$.

$$I_{1,2}(t) = \int d^3r'\ I_{1,2}(t;\underline{r}').$$

The output of the system is the difference signal

$$Y(t) = I_2(t) - I_1(t) = \int d^3r' \int_0^\infty \frac{d\omega}{\pi} |f(\omega)|^2 \int_{\substack{\text{(spectrometer}\\ \text{entrance)}}} d^2r''\ 2$$

$$\cdot\ \mathrm{Re}\left[\xi_A{}^*(\underline{r}'',\omega;\underline{r}',t)\xi_B(\underline{r}'',\omega;\underline{r}',t)\right].$$

As in the simple two-beam system, the output gives a measure of the correlation between the A and B components of the light.

Using Eqs. (II.23) to express the result in terms of the source distribution gives

$$Y(t) = \frac{2}{\pi}\int d^3r' \int_0^\infty d\omega |f(\omega)|^2 \int_{\substack{\text{(spectrometer}\\ \text{entrance)}}} d^2r''$$

$$\cdot\ \mathrm{Re}\left[\phi_A{}^*(\underline{r}'',\underline{r}',\omega)s^*(\underline{r}',\omega)\phi_B(\underline{r}'',\underline{r}',\omega)s(\underline{r}',\omega)\right]$$

$$= \int d^3r' \int d\omega |f(\omega)|^2 \cdot T(\underline{r}',\omega)\mathcal{S}(\omega;\underline{r}',t) \qquad \text{(II.24)}$$

where, as before,

$$\mathcal{S}(\omega;\underline{r}',t) = s^*(\underline{r}',\omega;t)s(\underline{r}',\omega;t) = |s(\underline{r}',\omega;t)|^2$$

is the spectrum of light emitted at $\underline{r}'$. So the output signal $Y(t)$ depends upon the quantity

$$T(\underline{r}',\omega) = \mathrm{Re}\,\frac{2}{\pi}\int_{\substack{\text{(spectromter}\\ \text{entrance)}}} d^2r''\ \phi_A{}^*(\underline{r}'',\underline{r}',\omega)\phi_B(\underline{r}'',\underline{r}',\omega).$$

This is the transmission function for the system as a whole. (This term seems appropriate, since the quantity is real, but it should be noted that this transmission function may be negative.)

Equation (II.24) is a generalization of Eq. (II.19). Comparing the two results, we see that the simple two-beam system is described by

$$T(\underline{r}',\omega) = \begin{cases} (c\delta^2\Omega)^2 \, \mathrm{Re}\left[e^{i\phi} \, e^{-i\underline{k}_\Delta \cdot \underline{r}'} \right] & \text{for points } \underline{r}' \text{ within the c.s.v.} \\ 0 & \text{for points outside the c.s.v.} \end{cases}$$

A two-beam spectrometer would observe the $\underline{k}_\Delta$ component of the distribution of common sources. But this is just one special case of the more general system shown in Fig. II-6. In general, any such arrangement would define some function $T(\underline{r}',\omega)$. According to Eq. (II.24), the output of the system is then given by an integral over points $\underline{r}'$ of the expression $T(\underline{r}',\omega)\,\mathcal{A}(\omega;\underline{r}',t)$. So any system of this type would select just one component of the light source distribution: the $T(\underline{r}',\omega)$ component of $\mathcal{A}(\omega;\underline{r}',t)$.

Many such systems are possible. In Appendix C of this discussion, a number of different multiple-beam spectrometers are proposed. In the next section of the present chapter, the mathematical techniques just outlined are applied to several of those same examples.

3. Three Particular Optical Systems

In using this description, it is convenient to first simplify the expressions for the optical path lengths. Treating

$\underline{r}'$, $x^{(in)}$, and $y^{(in)}$ as small quantities, assuming $z^{(in)}$ nearly equal to f_1, and keeping all small quantities through second order gives

$$|\underline{r}^{(in)} - \underline{r}'| + \phi_1(\underline{r}^{(in)}) \cong \phi_{10} + z^{(in)} - z' + \frac{x'^2 + y'^2}{2f_1} - \frac{x^{(in)}x' + y^{(in)}y'}{f_1} .$$

Keeping leading terms in the magnitude, and corrections in the phase through second order, Eq. (II.20) becomes

$$\xi_0(\underline{r}^{(in)},t) \cong \frac{1}{f_1}\int d^3r'\, s(\underline{r}',t')\Big|_{Ret.}$$

$$\text{Ret.:}\quad t' = t - \frac{1}{c}\left(\phi_{10} + z^{(in)} - z' + \frac{x'^2 + y'^2}{2f_1} - \frac{x^{(in)}x' + y^{(in)}y'}{f_1}\right) .$$

In all of the systems which we shall consider, the first lens is followed by a calcite rhomb. This element displaces one polarization component by a distance d, while leaving the other unaffected. (See Appendix C.) Thus, after the rhomb (at points $\tilde{\underline{r}}$), ξ_0 is split into two waves.

$$\xi_A(\tilde{\underline{r}},t) = \xi_0(\underline{r}^{(in)},t^{(in)})\Big|_{\substack{\underline{r}^{(in)} = \tilde{\underline{r}} - \hat{e}_z D \\ t^{(in)} = t - \tau_A}}$$

$$= \frac{1}{f_1}\int d^3r' s(\underline{r}', t - c_A) \qquad \text{(II.25a)}$$

$$c_A = \tau_A + \frac{1}{c}\left(\phi_{10} + \tilde{z} - D - z' + \frac{x'^2 + y'^2}{2f_1} - \frac{\tilde{x}x' + \tilde{y}y'}{f_1}\right),$$

$$\xi_B(\tilde{\underline{r}},t) = \xi_0(\underline{r}^{(in)},t^{(in)})\Big|_{\substack{\underline{r}^{(in)} = \tilde{\underline{r}} - \hat{e}_y d - e_z D \\ t^{(in)} = t - \tau_B}}$$

$$= \frac{1}{f_1}\int d^3r'\, s(\underline{r}',t - c_B) \qquad \text{(II.25b)}$$

$$c_B = \tau_B + \frac{1}{c}\left(\phi_{10} + \tilde{z} - D - z' + \frac{x'^2 + y'^2}{2f_1} - \frac{\tilde{x}x' + (\tilde{y} - d)y'}{f_1}\right).$$

Here τ_A and τ_B are delays due to the rhomb, and D is the length of the rhomb.

We shall also need the derivatives

$$\nabla\xi_{A,B}(\tilde{\underline{r}},t) = \frac{1}{f_1}\int d^3r'\, \frac{1}{c}\left(\hat{e}_x \frac{x'}{f_1} + \hat{e}_y \frac{y'}{f_1} - \hat{e}_z\right) \cdot \frac{\partial}{\partial t'} s(\underline{r}',t')\Big|_{t' = t - c_{A,B}} \qquad \text{(II.26a)}$$

and

$$\frac{\partial}{\partial t}\xi_{A,B}(\tilde{\underline{r}},t) = \frac{1}{f_1}\int d^3r'\, \frac{\partial}{\partial t'} s(\underline{r}',t')\Big|_{t' = t - c_{A,B}}. \qquad \text{(II.26b)}$$

The simplest system which we shall consider is one in which the rhomb is followed by a mask with a single slit, as shown in Fig. C-4 in Appendix C. In this case,

$$\xi_{A,B}(\underline{r}^{(out)},t) \begin{cases} = \xi_{A,B}(\underline{\tilde{r}},t)\big|_{\underline{\tilde{r}} = \underline{r}^{(out)}} \\ \qquad \text{for} \quad \tilde{x}_1 < x^{(out)} < \tilde{x}_2 \\ \qquad\qquad \tilde{y}_1 < y^{(out)} < \tilde{y}_2 \\ = 0 \quad \text{otherwise.} \end{cases}$$

From the discussion in Appendix C, it is expected that the effect of this arrangement should resemble that of a simple two-beam system.

Equations (II.22) can also be simplified. Assuming that $x^{(out)}$, $y^{(out)}$, x'', y'', and $(z'' - z^{(out)} - f_2)$ are all small quantities, one can approximate the last segment of the path,

$$|\underline{r}'' - \underline{r}^{(out)}| + \phi_2(\underline{r}^{(out)}) \tilde{=} \phi_{20} + z'' - z^{(out)} + \frac{x'' + y''}{2f_2} + \frac{x^{(out)}x'' + y^{(out)}y''}{f_2} .$$

Using this approximation, and the preceding expressions for $\nabla\xi$ and $\partial\xi/\partial t$, the two field amplitudes, $\xi_{A,B}(\underline{r}'',t)$ as the spectrometer entrance slit [given by Eq. (II.22)] may be written,

$$\xi_{A,B}(\underline{r}'',t) \tilde{=} -\frac{1}{2\pi c}\frac{1}{f_1}\frac{1}{f_2}\int_{\tilde{x}_1}^{\tilde{x}_2} d\tilde{x} \int_{\tilde{y}_1}^{\tilde{y}_2} d\tilde{y} \int d^3r' \cdot \frac{\partial}{\partial t'} s(\underline{r}',t')\Big|_{t' = t - c_{A,B} - c_0}$$

$$c_0 = \frac{1}{c}\left[\phi_{20} + z'' - \tilde{z} + \frac{x''^2 + y''^2}{2f_2} - \frac{\tilde{x}x'' + \tilde{y}y''}{f_2}\right].$$

To obtain the transfer functions $\phi_{A,B}$, one must then Fourier transform this expression

$$\xi_{A,B}(\underline{r}'',\omega) = \frac{-1}{2\pi c}\frac{1}{f_1}\frac{1}{f_2}\int_{\tilde{x}_1}^{\tilde{x}_2} d\tilde{x}\int_{\tilde{y}_1}^{\tilde{y}_2} d\tilde{y}\int d^3r'\int dt\, e^{i\omega t} \cdot \frac{\partial}{\partial t'}\, s(\underline{r}',t')\Big|_{t' = t - c_{A,B} - c_0}$$

$$= \frac{-1}{2\pi c}\frac{1}{f_1}\frac{1}{f_2}\int_{\tilde{x}_1}^{\tilde{x}_2} d\tilde{x}\int_{\tilde{y}_1}^{\tilde{y}_2} d\tilde{y}\int d^3r'\, i\omega e^{+i\omega(c_{A,B}+c_0)} s(\underline{r}',\omega).$$

This has the needed form Eq. (II.23) :

$$\xi_{A,B}(\underline{r}'',\omega) = \int d^3r'\, \phi_{A,B}(\underline{r}'',\underline{r}',\omega) s(\underline{r}',\omega).$$

Evaluating the $\tilde{x}$ and $\tilde{y}$ integrations gives,

$$\phi_{A,B}(\underline{r}'',\underline{r}',\omega) = \frac{+i}{2\pi}\left(\frac{c}{\omega}\right)\frac{1}{f_1}\frac{1}{f_2}\frac{1}{(y'/f_1 + y''/f_2)}\frac{1}{(x'/f_1 + x''/f_2)}$$

$$\left\{ e^{+i\omega\left[c_{A,B}(\tilde{x}_2,\tilde{y}_2) + c_0(\tilde{x}_2,\tilde{y}_2)\right]} - e^{+i\omega\left[c_{A,B}(\tilde{x}_1,\tilde{y}_2) + c_0(\tilde{x}_1,\tilde{y}_2)\right]} - e^{+i\omega\left[c_{A,B}(\tilde{x}_2,\tilde{y}_1) + c_0(\tilde{x}_2,\tilde{y}_1)\right]} + e^{+i\omega\left[c_{A,B}(\tilde{x}_1,\tilde{y}_1) + c_0(\tilde{x}_1,\tilde{y}_1)\right]} \right\}. \qquad \text{(II.27)}$$

Combining these gives the transmission function for this system,

$$T(\underline{r}',\omega) = \mathrm{Re}\,\frac{2}{\pi}\int d^2r''\,\phi_A^*\phi_B$$

$$= \mathrm{Re}\left\{\frac{2}{\pi}\right\}^3\left(\frac{\omega}{c}\right)^2\frac{1}{(f_1f_2)^2}\,e^{+i\omega(\tau_B-\tau_A)}\,e^{+i\left[(\omega/c)(dy'/f_1)\right]}$$

$$\cdot\int_{x_1''}^{x_2''}dx''\int_{y_1''}^{y''_2}dy''\,\frac{1}{X^2}\,\frac{1}{Y^2}$$

$$\cdot\,\sin^2\left(\frac{X\tilde{x}_2 - X\tilde{x}_1}{2}\right)\sin^2\left(\frac{Y\tilde{y}_2 - Y\tilde{y}_1}{2}\right)$$

where

$$X = \frac{\omega}{c}\left(\frac{x'}{f_1} + \frac{x''}{f_2}\right)$$

$$Y = \frac{\omega}{c}\left(\frac{y'}{f_1} + \frac{y''}{f_2}\right)$$

and $(x_2'' - x_1'')$ and $(y_2'' - y_1'')$ are the dimensions of the spectrometer entrance slit. The width $(y_2'' - y_1'')$ is assumed to be less than the width of a maximum of a diffraction pattern due to the first slit. (See Appendix C.) Thus Y may be considered constant in the integration over y". However, $(x_2'' - x_1'')$, the length of the entrance slit, is much larger than the width of $1/X^2$, so the x" integration may as well be taken over the whole line. Making these replacements gives,

$$T(\underline{r}',\omega) = \mathrm{Re}\left\{\frac{2}{\pi}\right\}^2\frac{\omega}{c}\,\frac{1}{(f_1f_2)^2}\,e^{+i\omega(\tau_B-\tau_A)}f_2(y_2'' - y_1'')(\tilde{x}_2 - \tilde{x}_1)$$

$$e^{+i\left[(\omega/c)(dy'/f_1)\right]}F(y') \qquad \text{(II.28)}$$

where

$$F(y') = \frac{\sin^2\left(Y \frac{(\tilde{y}_2 - \tilde{y}_1)}{2}\right)}{Y^2}$$

defines the source region observed. Assuming that the source is incoherent, one can used Eq. (II.24) to write the output of the system,

$$Y(t) = \int d^3r' \int d\omega \, |f(\omega)|^2 T(\underline{r}', \omega) \mathcal{A}(\omega; \underline{r}', t)$$

$$= C \int d\omega \left|\frac{\omega}{c}\right| |f(\omega)|^2 \, \mathrm{Re}\, e^{+i\omega(\tau_B - \tau_A)} \int d^3r' \, F(y') \, e^{+i\left[(\omega/c)(dy'/f_1)\right]} \mathcal{A}(\omega; \underline{r}', t)$$

$$= C \int d\omega \left|\frac{\omega}{c}\right| |f(\omega)|^2 \, \mathrm{Re}\, e^{+i\omega(\tau_B - \tau_A)} \mathcal{A}_{\text{observed}}(\omega; \underline{k}_\Delta, t) \qquad \text{(II.29)}$$

where

$$C = \left|\frac{2}{\pi}\right|^2 \frac{1}{(f_1 f_2)^2} \, (\tilde{x}_2 - \tilde{x}_1) f_2 (y_2'' - y_1'')$$

$$\mathcal{A}_{\text{observed}}(\omega; \underline{r}', t) = \mathcal{A}(\omega; \underline{r}', t) F(y')$$

and

$$\underline{k}_\Delta = -e_y \frac{\omega}{c} \frac{d}{f_1} \, .$$

So, assuming that $e^{+i\omega(\tau_B - \tau_A)}$ is constant over the range of frequencies considered (which is equivalent to saying that the path difference is less than the coherence length) this system observes the $\underline{k}_\Delta$ spatial Fourier component of the distribution of light sources within the observation region. Thus, at least near

the focal plane of the first lens, this setup is equivalent to the simple two-beam system which was discussed in Section II.A.

Moreover, the result is seen to depend upon the width, $(\tilde{y}_2 - \tilde{y}_1)$ of the aperture in the mask behind the rhomb, but not upon its location, since $\tilde{y}_1$ and $\tilde{y}_2$ could both be changed by a common amount and not affect the answer. This suggests using a mask with many slits, as shown in Fig. C-6a in Appendix C. This second system would give two transfer functions, [for n slits, separated by a distance $\Delta < (\tilde{y}_2 - \tilde{y}_1)$]

$$\phi_{A,B}(\underline{r}'',\underline{r}',\omega) = \frac{-i\omega}{2\pi c}\frac{1}{f_1}\frac{1}{f_2}\int_{\tilde{x}_1}^{\tilde{x}_2} d\tilde{x} \sum_{j=0}^{n}\int_{\tilde{y}_1+j\Delta}^{\tilde{y}_2+j\Delta} d\tilde{y}\, e^{+i\omega(c_{A,B}+c_0)}$$

$$= \frac{-i\omega}{2\pi c}\frac{1}{f_1}\frac{1}{f_2} e^{+i\omega\tau_{A,B}} e^{+i(\omega/c)\Phi}\int_{\tilde{x}_1}^{\tilde{x}_2} d\tilde{x}\, e^{-iX\tilde{x}}$$

$$\cdot \sum_{j=0}^{n}\int_{\tilde{y}_1+j\Delta}^{\tilde{y}_2+j\Delta} d\tilde{y}\, e^{-iY\tilde{y}} \begin{cases} \cdot\ 1 \text{ for A} \\ \cdot\ e^{+i\,(\omega/c)(dy'/f_1)} \text{ for B} \end{cases}$$

$$= \frac{-i\omega}{2\pi c}\frac{1}{f_1}\frac{1}{f_2}\frac{1}{X}\frac{1}{Y} e^{+i\omega\tau_{A,B}} e^{+i(\omega/c)\Phi} (e^{-iX\tilde{x}_2} - e^{-iX\tilde{x}_1})$$

$$\sum_{j=1}^{n} e^{-ij\Delta Y} (e^{-iY\tilde{y}_2} - e^{-iY\tilde{y}_1}) \begin{cases} \cdot\ 1 \text{ for A} \\ \cdot\ e^{+i(\omega/c)(dy'/f_1)} \text{ for B} \end{cases}$$

(II.30)

where

$$\Phi = \phi_{10} + \phi_{20} + z'' - z' - D + \frac{x'^2 + y'^2}{2f_1} + \frac{x''^2 + y''^2}{2f_2} .$$

Using these to calculate the transmission fuction for this system gives,

$$T(\underline{r}'\omega) = \mathrm{Re}\left(\frac{2}{\pi}\right)^3\left(\frac{\omega}{c}\right)^2 \frac{1}{(f_1 f_2)^2} e^{+i\omega(\tau_B-\tau_A)} e^{+i\left[(\omega/c)(dy'/f_1)\right]}$$

$$\int_{x_1''}^{x_2''} dx'' \frac{1}{X^2} \sin^2 \frac{X\tilde{x}_2 - X\tilde{x}_1}{2} \int_{y_1''}^{y_2''} dy'' \frac{1}{Y^2}$$

$$\cdot \frac{\sin^2\left(\frac{Y\tilde{y}_2 - Y\tilde{y}_1}{2}\right) \sin^2\left(\frac{n\Delta Y}{2}\right)}{\sin^2\left(\frac{\Delta Y}{2}\right)}$$

Assuming again that $(x_2'' - x_1'')$ is large, while $(y_2'' - y_1'')$ is small, one has,

$$T(\underline{r}',\omega) = \mathrm{Re}\ C \frac{\omega}{c} e^{+i\omega(\tau_B-\tau_A)} e^{+i\left[(\omega/c)(dy'/f_1)\right]}$$

$$\cdot F(y')\left[\frac{\sin^2\left(\frac{n\Upsilon\Delta}{2}\right)}{\sin^2\left(\frac{\Upsilon\Delta}{2}\right)}\right] \qquad \text{(II.31)}$$

with Y evaluated at y_1''.

This result is somewhat similar to that found for the simple two-beam system, but there is an important extra factor $\left[\sin^2\left(\frac{n\Upsilon\Delta}{2}\right)/\sin^2\left(\frac{\Upsilon\Delta}{2}\right)\right]$. Assuming that Δ, the distance between slits is comparable to d, the displacement due to the rhomb, and that $\Upsilon = \omega/c\left[(y'/f_1) + (y_1''/f_2)\right]$ is of the same order as $(\omega/c)(y'/f_1)$, the additional factor $\sin^2(n\Upsilon\Delta/2)$ will vary much more rapidly with y' than will the exponential, $e^{+i\left[(\omega/c)(dy'/f_1)\right]}$. Thus the

effect of such an apparatus would be very different from that of a simple two-beam system. The multiple slit arrangement would observe exclusively those regions where the extra factor is large.

As is explained in Appendix C, this difference in effect is caused by interference between light observed through different slits in the first mask. Because of this additional interference, the result is not just a sum of two-beam observations. To make a more efficient version of the two-beam system, one must avoid this interference between separate pairs of beams. As is suggested in Appendix C, one can do this by using a collimator to select the light from each pair of beams independently, before the point where the separate pairs of beams are all combined. Such an apparatus is shown in Fig. C-7 in Appendix C.

To describe this third arrangement, we denote points at the output of the collimator by $\underset{\sim}{\tilde{r}} = (\tilde{x},\tilde{y},\tilde{z})$. The light there consists of outputs from the different collimator slits,

$$\mathcal{E}_{A,B}(\underset{\sim}{\tilde{r}},t) = \begin{cases} \mathcal{E}^{(j)}_{A,B}(\underset{\sim}{r},t) & \text{for } \tilde{x}_1 < \tilde{x} < \tilde{x}_2 \\ & \quad \tilde{y}_1 + j\Delta < \tilde{y} < \tilde{y}_2 + j\Delta \\ 0 & \text{otherwise.} \end{cases}$$

The output of each slit is given by a Kirchoff integral across the entrance to the same section of the collimator

$$\mathcal{E}^{(j)}_{A,B}(\underset{\sim}{\tilde{r}},t) \approx \frac{1}{4\pi}\int_{\tilde{x}_1}^{\tilde{x}_2} d\tilde{x} \int_{\tilde{y}_1+j\Delta}^{\tilde{y}_2+j\Delta} d\tilde{y}\, \frac{1}{|\underset{\sim}{\tilde{r}} - \underset{\sim}{\tilde{r}}|}$$

$$\cdot \left[\nabla \mathcal{E}_{A,B}(\underset{\sim}{\tilde{r}},\tilde{t})\Big|_z - \frac{1}{c}\frac{\partial}{\partial \tilde{t}}\,\mathcal{E}_{A,B}(\underset{\sim}{\tilde{r}},\tilde{t})\right]_{\tilde{t} = t - \frac{|\underset{\sim}{\tilde{r}} - \underset{\sim}{\tilde{r}}|}{c}}$$

$$\approx \frac{1}{2\pi} \int_{\tilde{x}_1}^{\tilde{x}_2} d\tilde{x} \int_{\tilde{y}_1+j\Delta}^{\tilde{y}_2+j\Delta} d\tilde{y}\, \frac{1}{L}\, \frac{-1}{c}\, \frac{1}{r_1} \int d^3r'$$

$$\cdot \frac{\partial}{\partial t'} s(\underline{r}'t') \Big|_{t' = t - c_{A,B}\,\tilde{c}}$$

where

$$\tilde{c} = \frac{1}{c}\left\{ \tilde{z} - \tilde{z} + \frac{1}{2L}\left[(\tilde{x} - \tilde{x})^2 + (\tilde{y} - \tilde{y})^2 \right] \right\}$$

and L is the length of the collimator. Here Eqs. (II.26a,b) have been used to express the field $\xi(\underline{\tilde{r}},t)$ in terms of the source $s(\underline{r}',t')$ and the distances $(\tilde{x} - \tilde{x})$, $(\tilde{y} - \tilde{y})$, and $(\tilde{z} - \tilde{z} - L)$ have been treated as small quantities in an expansion of the path length.

The fields at the spectrometer entrance slit are a sum of contributions from the different collimator slits, contributions given by a Kirchoff integral across the collimator exit:

$$\xi_{A,B}(\underline{r}'',t) \approx \frac{1}{4\pi} \sum_{j=0}^{n} \int_{\tilde{x}_1}^{\tilde{x}_2} d\tilde{x} \int_{\tilde{y}_1+j\Delta}^{\tilde{y}_2+j\Delta} d\tilde{y}\, \frac{1}{r_2}$$

$$\cdot \left[\nabla \xi_{A,B}^{(j)}(\underline{\tilde{r}},\tilde{t}) \Big|_z - \frac{1}{c} \frac{\partial}{\partial \tilde{t}}\, \xi^{(j)}(\underline{\tilde{r}},\tilde{t}) \right]_{\tilde{t} = t - c_0'}$$

where

$$c_0' = \frac{1}{c}\left(\phi_{20} + z'' - \tilde{z} + \frac{x''^2 + y''^2}{2r_2} - \frac{\tilde{x}x'' + \tilde{y}y''}{r_2} \right).$$

Using the above expressions for $\xi^{(j)}(\tilde{\underline{r}},t)$, and Fourier transforming the result gives for this system the two transfer functions,

$$\phi_{A,B}(\underline{r}'',\underline{r}',\omega) = \frac{-1}{(2\pi)^2}\frac{1}{Lf_1f_2}\left(\frac{\omega}{c}\right)^2 \sum_{j=0}^{n} \int_{\tilde{x}_1}^{\tilde{x}_2} d\tilde{x} \int_{\tilde{y}_1+j\Delta}^{\tilde{y}_2+j\Delta} d\tilde{y}$$

$$\cdot \int_{\tilde{x}_1}^{\tilde{x}_2} d\tilde{\tilde{x}} \int_{\tilde{y}_1+j\Delta}^{\tilde{y}_2+j\Delta} d\tilde{\tilde{y}}\, e^{i\omega(c_{A,B}+\tilde{c}+c_0')}$$

$$= \frac{i}{(2\pi)^2}(1+i)\sqrt{\frac{\pi Lc}{\omega}}\frac{1}{Ly'y''} e^{i\omega\tau_{A,B}} e^{i(\omega/c)\Phi}$$

$$\cdot e^{-i(\omega/c)(L/2)(x'^2/f_1^2)} \frac{1}{X}\left(e^{-iX\tilde{x}_2} - e^{-iX\tilde{x}_1}\right)$$

$$\cdot \sum_{j=0}^{n} e^{-i\left[(\omega/c)(y'/f_1)j\Delta\right]} e^{-i\left[(\omega/c)(y''/f_2)j\Delta\right]}$$

$$\cdot \left(e^{-i(\omega/c)(y'\tilde{y}_2/f_1)} - e^{-i(\omega/c)(y'\tilde{y}_1/f_1)}\right)$$

$$\cdot \left(e^{-i(\omega/c)(y''\tilde{y}_2/f_2)} - e^{-i(\omega/c)(y''\tilde{y}_1/f_2)}\right)$$

$$\cdot \begin{cases} 1 & \text{for A} \\ e^{i(dy'/f_1)(\omega/c)} & \text{for B} \end{cases} \qquad \text{(II.32)}$$

where in the x and y integrations it has been assumed that $(x_2 - x_1)$ is large, while $(y_2 - y_1)$ is small in comparison with the widths of the respective integrands.

Combining these two transfer functions gives the transmission function for this system:

$$T(\underline{r}',\omega) = \mathrm{Re}\,\frac{2}{\pi}\int d^2r''\ \phi_A^*\phi_B$$

$$= \mathrm{Re}\left(\frac{2}{\pi}\right)^4 \frac{1}{L}\frac{c}{\omega}\, e^{i\omega(\tau_B-\tau_A)}\, e^{i(dy'/f_1)(\omega/c)} \int d^2r''$$

$$\cdot \frac{1}{X^2}\sin^2\left(\frac{X\tilde{x}_2 - X\tilde{x}_1}{2}\right)\frac{1}{(y'y'')^2}$$

$$\cdot \sin^2\left[\frac{\omega}{c}\frac{y'}{f_1}\frac{(\tilde{y}_2 - \tilde{y}_1)}{2}\right]\sin^2\left[\frac{\omega}{c}\frac{y''}{f_2}\frac{(\tilde{y}_2 - \tilde{y}_1)}{2}\right]$$

$$\cdot \sum_{j=0}^{n}\ \sum_{j'=0}^{n} e^{-iY(j-j')\Delta}$$

The reason for using a collimator is to avoid any effect of multiple-beam interference between light accepted through different slits in the collimator. For this reason, it is essential that no more light should be rejected after all the beams have been combined. Thus the spectrometer entrance slit should be made larger than the width of the illumination pattern there, and in the above expression the $\underline{r}''$ integration should be taken over the whole plane. Doing this one has,

$$T(\underline{r}'\omega) = \mathrm{Re}\left(\frac{2}{\pi}\right)^2 \frac{1}{L}\frac{c}{\omega}\, n(\tilde{x}_2 - \tilde{x}_1)(\tilde{y}_2 - \tilde{y}_1)\, e^{i\omega(\tau_B-\tau_A)}$$

$$\cdot e^{i(dy'/f_1)(\omega/c)}\ \frac{1}{y'^2}\sin^2\left[\frac{\omega}{c}\frac{y'}{f_1}\frac{(\tilde{y}_2 - \tilde{y}_1)}{2}\right]. \qquad (II.33)$$

Here the double sum has vanished. This occurs in the y'' integration, where one has expressions of the form,

$$\int_{-\infty}^{\infty} dy'' \frac{1}{y''^2} \sin^2\left[\frac{\omega}{c}\frac{(\tilde{y}_2 - \tilde{y}_1)}{2f_2} y''\right] \cos\left[\frac{\omega}{c}\frac{\Delta}{f_2}(j - j')y''\right].$$

This vanishes[41] for $j \neq j'$, provided that $\Delta > (y_2 - y_1)$, i.e., provided that the slit separation exceeds the slit width, which it obviously does. This leaves a single sum of identical terms, which gives the factor n.

Thus the effect of interference vanishes, as was expected, and the contributions from the different slits are seen to be identical, because, as noted earlier, each result is independent of the slit position. So the conclusion of Appendix C is verified: A spectrometer with many independently collimated pairs of beams provides a more efficient version of the simple two-beam system which was first considered. It should be remembered, however, that this is true only of regions near the focus of the system.

C. Higher Order Correlations

The elementary two-beam spectrometer discussed in Section II.A would give an output, Y(t), proportional to the mutual coherence $\Gamma_{BA}(0;|\underline{k}|,t)$ between light of wavelength $2\pi|\underline{k}|^{-1}$ emitted in directions $\hat{k}_A$ and $\hat{k}_B$ from the same region. In the analysis in Section II .3, this quantity was shown to be proportional to one Fourier component, $\mathcal{A}(|\underline{k}|c;\underline{k}_\Delta,t)$, of the distribution of observed light sources. According to the Wiener-Khintchine theorem,[21] measurement of $\mathcal{A}(|\underline{k}|c;\underline{k}_\Delta,t)$ is equivalent to measurement of the two-point correlation function of the light source distribution.

Hence a two-beam spectroscopic measurement of correlations in the light emitted by a plasma would give information about two-point correlations in the distribution of the source. So stated, this result suggests that there may be a much more general correspondence between correlation functions of a light field, $\xi(\underline{r},t)$, and correlation functions of the density of sources, $\mathcal{A}(|\underline{k}|c;\underline{r}',t)$.

In discussions of optical theory, higher order correlations, like the two-beam mutual coherence, are customarily defined in terms of an associated analytic signal. Wolf[42] has used this technique to define a complete set of complex correlations,

$$\Gamma^{(m,n)} \equiv 2^{(m+n)} \overline{\xi_1^{(+)*} \xi_2^{(+)*} \cdots \xi_m^{(+)*} \xi_{m+1}^{(+)} \cdots \xi_{m+n}^{(+)}} \quad . \quad \text{(II.34)}$$

(The use of this form here involves one change, however, since the definition was made to compare light at one point at different times, while the observations discussed here would compare light at one point in different beams with no delays.[43]) Similar definitions have been used by other authors. (see, for example, Ref. 1a.)

We shall not consider here the ways in which these higher order correlations might be measured. It is possible, at least in principle, to observe them (for example, by measuring higher order correlations of intensity), but that problem is beyond the scope of this investigation. However, the theory in Section II.A.3 is readily extended to some higher order quantities. Since this should be of interest by itself, such an extension of the theory is outlined in the next few pages.

It is shown in Appendix E.1 that light of wavelength $2\pi|\underline{k}|^{-1}$ emitted in direction $\hat{k}$ may be described by a field amplitude,

$$\xi^{(\text{observed})}(\underline{r},t) = \text{Re}\left[\frac{|\underline{k}|}{2\pi i c} e^{i\underline{k}\cdot\underline{r}} \xi^{(+)}(\underline{k},t)\right]$$

where $\xi^{(+)}(\underline{k},t)$ is the positive frequency, or analytic signal associated with the spatial Fourier transform of the field. (In this scalar model, the normalization is arbitrary, since the physical nature of ξ has not been specified.) The analytic signal associated with this field is

$$\xi^{(\text{observed})(+)}(\underline{r},t) = \frac{1}{2}\frac{|\underline{k}|}{2\pi i c} e^{i\underline{k}\cdot\underline{r}} \xi^{(+)}(\underline{k},t). \qquad \text{(II.35)}$$

This follows from the result shown in Appendix E.2. This form is now to be used in the expressions for the correlation functions.

To further simplify the problem, it is convenient to explicitly assume that the source, $s(\underline{r}',t)$, is quasimonochromatic:

$$s(\underline{r}',t) = 2\, a(\underline{r}',t)\, \cos\left[\omega_0 t + \phi(\underline{r}',t)\right] . \qquad \text{(II.36)}$$

The amplitude, $a(\underline{r}',t)$, is proportional to the square root of the source density and the phase, $\phi(\underline{r}'t)$, is random from point to point. The time variation of both a and ϕ is assumed to be much slower than the oscillation at the optical frequency, ω_0.

Using the Green's function expression for the field [Eq. II.1)] one has

$$\mathcal{E}^{(+)}(\underline{k},t) = \int d^3r\, e^{-i\underline{k}\cdot\underline{r}} \int d^3r' \, \frac{1}{|\underline{r}-\underline{r}'|}\, a\left(\underline{r}', t - \frac{|\underline{r}-\underline{r}'|}{c}\right)$$

$$\cdot\, e^{-i\omega_0\left[t-(|\underline{r}-\underline{r}'|)/c\right]}\, e^{-i\phi\left[\underline{r}', t-(|\underline{r}-\underline{r}'|)/c\right]}$$

$$= \int_{-\infty}^{t} c\,d\tau\, \frac{2\pi}{i|\underline{k}|}\left[e^{i|\underline{k}|c(t-\tau)} - e^{-i|\underline{k}|c(t-\tau)}\right] e^{-i\omega_0\tau}$$

$$\cdot \int d^3r'\, e^{-i\underline{k}\cdot\underline{r}'} a(\underline{r}',\tau) e^{-i\phi(\underline{r}',\tau)}.$$

As before, this integration over all preceding times is much idealized. If the finite size of the spectrometer grating is considered, the τ integration should be taken only over the preceding inverse optical bandwidth. Furthermore, since a and ϕ are slowly varying, they may be taken as constant over such an interval. From this more realistic form one obtains the result,

$$\mathcal{E}^{(+)}(\underline{k},t) = \frac{2\pi i c}{|\underline{k}|}\, e^{-i|\underline{k}|ct}\, \delta(\omega_0 - |\underline{k}|c) \int d^3r'\, e^{-i\underline{k}\cdot\underline{r}'} a(\underline{r}',t)$$

$$\cdot\, e^{-i\phi(\underline{r}',t)}. \qquad \text{(II.37)}$$

Using this expression to evaluate the two-beam mutual coherence [i.e., combining Eqs. (II.34) and (II.37)], one has

$$\Gamma^{(1,1)} = \frac{1}{4}\,\overline{\mathcal{E}_A^{(+)*}\mathcal{E}_B^{(+)}}$$

$$= e^{-i\underline{k}_A\cdot\underline{r}_A}\, e^{i\underline{k}_B\cdot\underline{r}_B} \int d^3r' \int d^3r''\, e^{-i\underline{k}_A\cdot\underline{r}'}\, e^{i\underline{k}_B\cdot\underline{r}''}$$

$$\cdot\, \overline{a(\underline{r}',t)a(\underline{r}'',t)e^{i\phi(\underline{r}',t)}\, e^{-i\phi(\underline{r}'',t)}}$$

$$= e^{-i\underline{k}_A\cdot\underline{r}_A} e^{i\underline{k}_B\cdot\underline{r}_B}\int d^3r' \, e^{-i(\underline{k}_B-\underline{k}_A)\cdot\underline{r}'}\overline{a^2(\underline{r}',t)}$$

$$= e^{-i\underline{k}_A\cdot\underline{r}_A} e^{i\underline{k}_B\cdot\underline{r}_B}\,\overline{n_s(\underline{k}_B-\underline{k}_A,t)}$$

where n_s is the (unnormalized) source density.

This result agrees with that obtained in Section II.A.3. But the assumption of Eq. (II.36) has so much simplified the derivation that it now can be extended without difficulty to some higher order quantities. For example, one can calculate a four-beam correlation,

$$\Gamma^{(2,2)} = 16\,\overline{\xi_C^{(+)*}\xi_A^{(+)*}\xi_B^{(+)}\xi_D^{(+)}}$$

$$= e^{-i\underline{k}_C\cdot\underline{r}_C} e^{-i\underline{k}_A\cdot\underline{r}_A} e^{i\underline{k}_B\cdot\underline{r}_B} e^{i\underline{k}_D\cdot\underline{r}_D}\int d^3r'\int d^3r''$$

$$\cdot\Big[e^{i\underline{k}_C\cdot\underline{r}'} e^{i\underline{k}_A\cdot\underline{r}''} e^{-i\underline{k}_B\cdot\underline{r}'} e^{-i\underline{k}_D\cdot\underline{r}''}$$

$$+ e^{i\underline{k}_C\cdot\underline{r}'} e^{i\underline{k}_A\cdot\underline{r}''} e^{-i\underline{k}_B\cdot\underline{r}''} e^{-i\underline{k}_D\cdot\underline{r}'}\Big]\overline{a^2(\underline{r}',t)a^2(\underline{r}'',t)}$$

$$= e^{-i\underline{k}_C\cdot\underline{r}_C} e^{-i\underline{k}_A\cdot\underline{r}_A} e^{i\underline{k}_B\cdot\underline{r}_B} e^{i\underline{k}_D\cdot\underline{r}_D}$$

$$\cdot\Big[\overline{n_s(\underline{k}_B-\underline{k}_C,t)n_s(\underline{k}_D-\underline{k}_A,t)} + \overline{n_s(\underline{k}_D-\underline{k}_C,t)n_s(\underline{k}_B-\underline{k}_A,t)}\Big].$$

So this four-beam optical correlation is seen to be proportional to a sum of mean products of source density fluctuation components. Here the remaining exponential factors are just constants. The source density components, $n_s(\underline{k},t)$, are complex valued spatial Fourier transforms. Hence the indicated average products depend upon the phases of the factors. If there were a correlation between two such quantities due, for example, to an

interaction between plasma waves with wave vectors $(\underline{k}_B - \underline{k}_C)$ and $(\underline{k}_D - \underline{k}_A)$, the measured averages would differ from a product of the averages of the two factors. Such a correlation corresponds to higher order correlations in the light source distribution.

Again, this all assumes an incoherent source. There is no correlation between the phases of the light from different points. But there can be correlations between the light observed through different beams, because the same sources contribute to them all. This was shown to be the case for the two-beam coherence, and the same thing is now seen to be true also of some higher order quantities.

The foregoing derivation of $\Gamma^{(1,1)}$ and $\Gamma^{(2,2)}$ is easily extended to still higher order quantities. Any of the correlations defined by Eq. (II.34) can be obtained in the same manner.

III. SIGNAL, NOISE, AND LIGHT INTENSITY

A. Quantum Optics and Intensity Correlations

The analyses in the preceding chapters have all been done within a framework of purely classical optics. But, of course, a classical theory is merely a limiting expression of the more fundamental quantum optics. The present chapter takes up the question of estimating the ratio of signal to noise in the output of a multiple-beam spectrometer. In this analysis, the discreteness of light quanta is important.

Such discussions usually assume that photon detection is a random process whose probability density is proportional to the classical light intensity. This assumption received some attention at the time of the first intensity correlation measurements, which were done by Hanbury Brown and Twiss.[44] In their analysis of that experiment,[45] Hanbury Brown and Twiss used both classical and quantum theories. They interpreted the agreement of the classical and quantum calculations as an expression of the principle of complementarity: One can interpret the interference process in terms of waves and then explain the detection process in terms of discrete particles. Since interference involves the wave aspect of light, a classical analysis is valid for that part of the experiment. The same experiment was again analyzed by Purcell,[46] who also equated classical intensity with photon probability. In both of these papers, the point was made that one can also analyze the interference process while discussing photons, but that a wave picture is more convenient because a light wave

may be treated as a classical field, while photons cannot be treated as classical particles.

It perhaps should be emphasized that the multiple-beam spectrometers which we are considering here are not intensity correlation devices. The spectrometers discussed in Chapter II select two observed waves, A and B, which are combined and then reseparated into interference patterns 1 and 2, giving information about the phase of A and B. To make an intensity correlation measurement, on the other hand, one would not combine beams A and B at all. One would simply measure the intensity of A with one phototube and the intensity of B with another phototube and then record the correlation of the outputs. This is the technique which was first demonstrated by Hanbury Brown and Twiss. It provides a different way of getting information about the mutual coherence of two light waves. Intensity correlation measurements have replaced the other methods in certain applications, but the multiple-beam spectrometers which we are considering belong to the older, standard class of interferometric instruments.

But this is not to say that an intensity correlation measurement could not be useful in the observation of a plasma. Indeed, this technique should be important there for the same reasons for which it was developed in the first place. Intensity correlation methods were first developed for use in stellar interferometry. It had long been known that one could use an interferometer to measure the apparent diameter of a star, but the utility of this technique was limited by the effect of atmospheric scintillation.

Variations in the Earth's atmosphere cause variations in the phase of starlight, and at points too widely separated these variations are uncorrelated, destroying the effect of interference. This limits the useable baseline, and hence the resolution of a conventional stellar interferometer. But an intensity interferometer is largely unaffected by this difficulty. The intensity is a much more slowly changing quantity than the amplitude, and changes in path of many wavelengths can be tolerated.

In a plasma, variations in the index of refraction could produce the same effect. If the index of refraction were not exactly unity, differences in n along the different lines of sight could cause phase changes and destroy the interference.[47] As in observations of a star, the use of an intensity interferometer would permit extension of the method to such cases.

Since the first intensity correlation measurements, the invention of the laser and improvements in other optical devices have led to renewed interest in the quantum theory of optics. The present state of this subject is described in several recent books.[2]

The interpretation of photodetection data, and the relation between classical and quantum optics--both topics of particular importance for our discussion here--are considered in detail in one paper by Glauber.[48] Strictly speaking, only radiation fields containing many quanta are described by classical theory, and, moreover, there are many quantum states which even with large quantum numbers do not seem to correspond to any classical descrip-

tion. Noting this, Glauber then describes a certain class of states (states whose density operators can be written in a form which he calls a "P representation", with a positive weight function) whose averaged behavior--in particular, their quantum mechanical correlation functions--may be written in a form similar to classical theory, even in the limit where the occupation numbers of the states are very small. The light emitted by chaotic sources, he observes, is always of this form.

The same paper also analyzes the significance of photon counting measurements. Using a simple model of a photon counter, Glauber obtains an expression for the factorial moments of the photocount probability distribution in terms of the correlation functions of the radiation field. [His Eq. (51).] This result is much more general than any which we will be using here, but for the first moment it just gives the mean number of counts expected in a given interval. This mean is proportional to the time integral of the first correlation function, i.e., to the quantity which corresponds to classical intensity. For fields which correspond to classical descriptions, Glauber then goes on to obtain an expression for the complete photocount probability distribution. This he shows to be an integral over Poisson distributions, a result which can also be obtained from semiclassical analysis. (See Ref. 49.)

The quantum theory, of course, provides much more than just a basis for a classical description. But for our problem here, a full quantum treatment is not really needed, so long as one

accepts the two assumptions that a classical analysis describes the interference of the light and that the classical intensity may then be taken as a photon probability in analyzing the detection process. One can then explain both interference and photon statistics. We will not discuss the basis of this simple (and quite standard) picture any further here. More complete explanations of the link between this semiclassical description and the full quantum theory can be found in the paper by Glauber just outlined[48] and in the books on quantum optics mentioned earlier.[2]

B. Classical Noise

Even if a completely classical description of the light were adequate, a multiple-beam spectrometer, like any other instrument, would generate some noise. Before beginning an analysis of photon statistics, one should obtain at least an estimate of the amount of noise to be expected from such other sources as stray light, mechanical vibrations, and fluctuations in the electronics.

Ideally, in the classical picture, the light in either beam A or beam B alone should contribute nothing to the output signal. Such light should be divided equally between beams 1 and 2, adding nothing to their intensity difference.

It perhaps should be emphasized that one actually could balance out the separate effects of both of the beams A and B. One could obviously zero either one of them by adjusting the phototube gains, but the same setting which balanced A would probably not be exactly right for B. There is, however, a second possible adjustment. One could also rotate slightly the polariza-

tions of A and B with respect to 1 and 2. This would put more of A into 1 and more of B into 2 or vice versa. By using this "differential" control, together with the "common" calibration of the phototubes, one could, in principle, precisely null out the effect of each of the two beams.

In reality, this balancing would not be perfect, but the effect of noise could then be minimized by signal processing. In many observations, the spectrum $Y(\omega)$ of the signal $Y(t)$ would have sharp maxima at certain frequencies. For example, if the observed source density component were produced by a plasma wave of frequency ω_0, this would appear in the recorded signal spectrum. The noise, on the other hand, should be spread out over some wider band of frequencies. (Remember that the signal comes from only one component of the source distribution. Thus the signal spectrum would usually be much narrower than the whole spectrum of plasma disturbances. Thus even if the noise came from the plasma, it would still be spread over a wider band.)

So there are, so to speak, two "lines of defense" against unwanted background light. First, one can null out beams A and B alone. Ideally, this should eliminate everything except the signal. Then any noise which does get through (or which is generated later in the system) can be removed in an analysis of the time or frequency dependence of the signal. Roughly estimating, it should be possible to balance the phototubes to within one percent. Then if the signal spectrum is at all unique, one should be able to do at least as well again in the signal spectrum

analysis. Together, this would give discrimination of one part in 10^4, and probably several orders of magnitude more.

Furthermore, if it were possible to modulate the observed phenomenon, one could use phase sensitive detection, which would give a large additional improvement. Another way to use this same technique, if the phenomenon were stationary, would be to modulate the light with a toothed wheel or other shutter and then phase lock onto that signal. This would not discriminate against the background light, but it would stop noise generated later in the system (e.g., in the amplifier or the spectrum analyzer).

One cannot say much more in general. The sensitivity of any given measurement would depend upon the apparatus used and upon the spectral properties of the selected signal. But it does not appear that "classical" noise would present any major problem. It seems evident that in almost any situation in which a multiple-beam spectrometer could be used, the observation would be limited by photon statistics, rather than by other types of noise.

C. An Estimate of Photon Statistics

For an analysis of photon statistics, it is convenient to express each light intensity in terms of a mean counting rate. Our system measures two intensities, $I_1(t)$ and $I_2(t)$, and these in turn consist of two distinct components: "background light" and "signal light". The background light is that which classically is just divided equally between beams 1 and 2 (e.g., light from a source observed only through beam A. This is not to be confused with "stray light" which can be reduced by optical im-

provements). The signal light is that emitted by the one observed component of the light source distribution $\left[T(\underline{r}',\omega)\right.$ in the terminology of Section II.B.2$\left.\right]$. Describing both of these in terms of photon flux, we have

2Q background photons/second

P signal photons/second.

2Q is divided equally between phototubes 1 and 2; P is unequally divided and varies between the two in a manner determined by the time dependence of the observed source density component. These two intensities, whose values were obtained from classical analysis are now to be treated as photon detection probabilities. For an ideal photon counter, this description can be justified by semiclassical analysis, as explained in the preceding section.

A photomultiplier tube is not a perfect photon counter, but for many such devices, a similar description of the output is appropriate. This can be seen from an investigation of photomultiplier properties reported recently by Robben.[50] After measuring the pulse charge spectrum and the fluctuations in the outputs of a variety of different photomultiplier tubes, Robben was able to describe the noise properties of each tube in terms of three parameters: the overall quantum efficience, ηF; a photoelectron noise factor, S; and an effective dark rate, D. The quantum efficiency η and photoelectron collection F were used as usually defined. The factor S was defined in terms of excess measured noise, but in the simple model of a phototube producing

pulses with a range of amplitudes, followed by a discriminator which accepts all those above some threshold, S is just the inverse of the fraction of the total pulses which are counted. D is the measured dark rate at the same discriminator setting. These quantities were found to be independent of frequency, except for periods longer than about 10 seconds. Thus, for many observations, P and Q, the signal and background contributions to the counting rates could just be modified to take into account the fractional detection and the dark rate:

$$P' = \frac{\eta F}{S} P \qquad \text{(III.1a)}$$

$$Q' = \frac{\eta F}{S} Q + D. \qquad \text{(III.1b)}$$

So in the following analysis, the measured light intensities, which will be specified in terms of P and Q may be interpreted as photon fluxes (measured by a perfect photon counter) or, more realistically, as photomultiplier output pulse rates, given by P' and Q' in Eqs. (III.1a,b).

If the signal were at zero frequency, the photon statistics would be simple. Assuming that P went entirely into beam 2, one would have

$$I_1 = Q$$

$$I_2 = Q + P.$$

Provided that $Q \gg P$ (which is assumed throughout the following), the signal to noise ratio would be

$$\frac{S}{N} = \left[\frac{(PT)^2}{2QT}\right]^{1/2}$$

where T is the total time of observation.

In general, the problem is more complicated than this, since the signal Y(t) is time dependent. In such situations one would be likely to record a signal spectrum $Y(\omega)$. To analyze this operation, consider now a case in which the observed component of the light source density is all due to a plasma wave of frequency ω_0. Then P, the signal light, would oscillate between the phototubes at this rate and the spectrum would show a peak at ω_0.

We represent a spectrum analyzer by the model shown in Fig. III-1. In such a device the signal Y(t) is first mixed with the output of a reference oscillator and the result is then averaged over a time τ. Since the mixing heterodynes the signal down in frequency by an amount equal to the frequency of the reference oscillator, and since the τ average transmits only those frequencies below $1/\tau$, the result represents the signal frequency components in a band of width $1/\tau$ around the reference frequency. To measure the amplitude of the signal within this band, the output of the τ average, Y'(t) is squared, giving a signal Z(t). This quantity is then averaged over the observation time, which we again denote by T.

Thus the observation of a signal spectrum involves two time intervals, an inverse bandwidth, τ, and T, the total time of observation at one signal frequency. (If the reference frequency

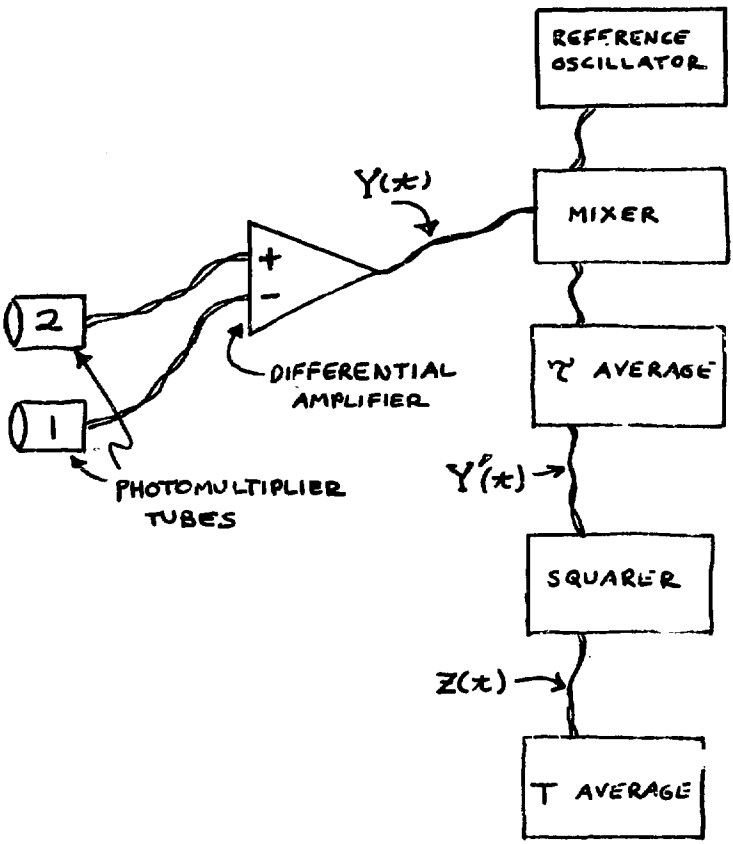

Fig. III-1. A model of the electronic apparatus.

is swept, T is the time needed to sweep across one bandwith.) Since all transmitted frequency components lie within $1/\tau$ of the reference, their phase relative to the reference cannot change within a τ interval. *In terms of counting* statistics, the signal probability is roughly constant over any τ interval, so for such times the problem is effectively at zero frequency. On the other hand, at times differing by much more than τ, Y'(t) is an average of different inputs, so such values represent completely separate samples of the signal spectrum.

To describe these two extremes, it is convenient to divide the observation time into a set of T/τ discrete τ intervals. As an approximation, one can then consider each τ interval separately, assuming that Z(t) at the end of each depends only upon signals received during that same interval, and also that all such inputs may be weighted equally. Since these are then completely independent samples, the signal-to-noise ratio expected in the T average is

$$\left(\frac{S}{N}\right)_T = \sqrt{\frac{T}{\tau}} \left(\frac{S}{N}\right)_\tau \qquad \text{(III.2)}$$

where $(S/N)_\tau$ is that expected from the counting distribution due to Z(t). In figuring these quantities, we shall consider all counts equal in magnitude, but since the phototube signals are differences, and also multiplied by a reference signal which takes either sign, one must include both positive and negative pulses. If n is the recorded algebraic sum of counts, one has for a τ interval

$$\left|\frac{S}{N}\right|^2_{\tau} = \frac{\left[\langle n\rangle_{Z \text{ with signal}} - \langle n\rangle_{Z \text{ without signal}}\right]^2}{\langle n^2\rangle_Z - \langle n\rangle_Z^2} . \qquad \text{(III.3)}$$

Here $\langle\rangle$ denotes an average and the subscript Z refers to the associated probability distribution. As indicated, the "signal" is not the spectral amplitude; it is the difference between the amplitude with signal (i.e., with the reference frequency $\approx \omega_0$) and that without signal (or with the reference oscillator at another frequency). In either case there will be some spectral amplitude due to the randomly distributed background counts. To be observable, the effect of the signal must exceed the fluctuations in the measured background spectral amplitude.

Since $Z(t) = Y'(t)^2$,

$$\langle n\rangle_Z = \langle n^2\rangle_{Y'} \qquad \text{(III.4a)}$$

$$\langle n^2\rangle_Z = \langle n^4\rangle_{Y'} . \qquad \text{(III.4b)}$$

Y' in turn is equal to the difference between $Y_2(t)$ and $Y_1(t)$, the positive and negative components of the output of the filter. (In a zero frequency observation, these would be just I_1 and I_2. In an observation at a higher frequency, the multiplication by a reference oscillation switches I_1 and I_2 between Y_1 and Y_2 at the reference frequency.) Over a τ interval, the signal P is divided unequally between Y_1 and Y_2. By definition,

$$Y'(t) = \int_{t-\tau}^{t} dt' \left[Y_2(t) - Y_1(t)\right] .$$

Hence the counting distributions are related by an integral

$$P_{Y'}(n) = \int dn'\ P_{Y_1}(n')P_{Y_2}(n + n').$$

From this it follows that

$$\langle n^2\rangle_{Y'} = \langle n^2\rangle_{Y_2} + 2\langle n\rangle_{Y_1}\langle n\rangle_{Y_2} + \langle n^2\rangle_{Y_1} \qquad \text{(III.5a)}$$

and that

$$\langle n^4\rangle_{Y'} = \langle n^4\rangle_{Y_2} + 4\langle n^3\rangle_{Y_2}\langle n\rangle_{Y_1} + 6\langle n^2\rangle_{Y_2}\langle n^2\rangle_{Y_1} + 4\langle n\rangle_{Y_2}\langle n^3\rangle_{Y_1} + \langle n^4\rangle_{Y_1}. \qquad \text{(III.5b)}$$

Finally, the distributions for $Y_1(t)$ and $Y_2(t)$ we take to be Poissonian. If the signal is all contained in $Y_2(t)$ this gives,

$$P_{Y_1}(n) = \frac{(Q\tau)^n}{n!}\, e^{-Q\tau} \qquad \text{(III.6a)}$$

$$P_{Y_2}(n) = \frac{\left[(Q + P)\tau\right]^n}{n!}\, e^{-(Q+P)\tau} \qquad \text{(III.6b)}$$

This is an approximation too, since it ignores the rapid fluctuations in the classical intensity, but since the times considered here are all much longer than the coherence time of the light, the neglected increase in $\langle n^2\rangle$ and other moments, the "excess photon noise", is relatively small. (See Ref. 49.)

All the needed moments can be calculated from these distributions. Using Eqs. (III.5a,b) to write the moments of Y', and keeping only leading terms, one obtains

$$\langle n^2 \rangle_{Y' \text{ with signal}} - \langle n^2 \rangle_{Y' \text{ without signal}} = (P\tau)^2$$

$$\langle n^4 \rangle_{Y'} - \langle n^2 \rangle_{Y'} = 8(Q\tau)^2 .$$

From Eqs. (III.3) and (III.4a,b) one can then calculate the signal-to-noise ratio for the τ average,

$$\left(\frac{S}{N}\right)^2_{\tau} = \frac{(P\tau)^4}{8(Q\tau)^2} .$$

Then from Eq. (III.2) one obtains the signal-to-noise ratio for the whole measurement

$$\left(\frac{S}{N}\right)^2_{T} = T\tau \frac{P^4}{8Q^2} . \qquad \text{(III.7)}$$

So, for the effect to be observable, one must have

$$P \sqrt{T\tau} > \sqrt{8}\, \frac{Q}{P} . \qquad \text{(III.8)}$$

Here the numerical factor should not be taken seriously, since several simplifying approximations have been used, but the result shows the dependence on the different factors and indicates when such an observation should be feasible.

IV. EXPERIMENTAL RESULTS

A. Tests of the Optical System

1. The Calcite Rhomb

To test the conclusions of the foregoing analysis, several multiple-beam spectrometers were assembled and studied. A central element in all of the arrangements used was a calcite rhomb, 1 cm^2 in aperture, which is shown in Fig. IV-1.

As a first step, the optical properties of the rhomb alone were examined, using light from a small He-Ne laser. The laser was equipped with a beam-expanding telescope, which when focused at infinity produced a beam 2 cm in diameter--large enough to illuminate the whole face of the rhomb. To observe the effect of the rhomb, a ground glass screen was placed approximately 1 m behind the rhomb and a camera behind the screen was used to photograph the illumination patterns.

The laser light was initially linearly polarized at 45° to the principal axes of the rhomb. A second linear polarizer was placed before the ground glass screen, to permit observation of different polarization components of the final pattern.

Altogether, the ordering of elements was:

laser,

beam-expanding telescope,

linear polarizer (at 45° to the axes of the rhomb),

calcite rhomb,

linear polarizer (varied to display the different patterns),

ground glass screen,

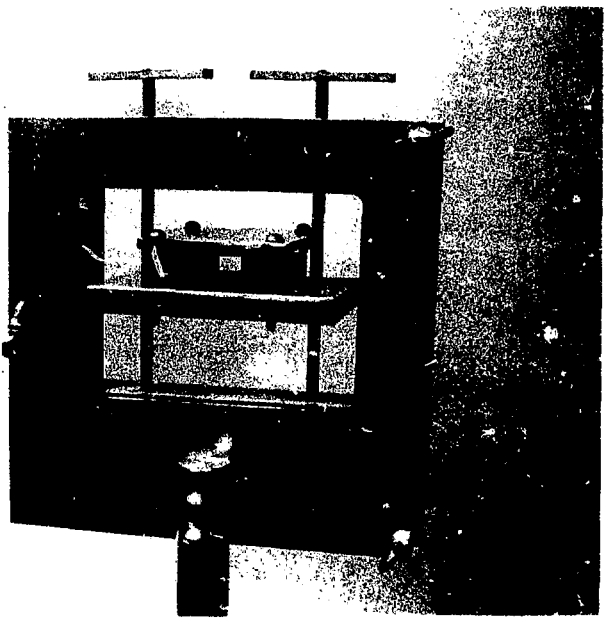

XBB 735-3039

Fig. IV-1. Calcite rhomb in mount.

camera, focused on the screen.

Thus this arrangement was like that shown in Fig. C-2 of Appendix C, except that in the present case the telescope was defocused to give a slightly expanding beam, a mask was not used, so the whole rhomb was illuminated, and the lens in Fig. C-2 was not needed, since the beams already overlapped.

The incident laser light was divided by the rhomb into two equally intense, orthogonally polarized components--"A" and "B" in the terminology of Chapter II. When the polarizer before the glass screen was oriented to select either of these components, a smooth distribution of intensity resulted, as is shown in the photographs in Fig. IV-2. But the intermediate component, "1" revealed a set of distinct interference fringes, and the orthogonal component "2" displayed the opposite or complementary set of fringes, as is shown in Fig. IV-3.

These are polarization fringe patterns, produced by interference between the A and B components of the light. Since A and B were orthogonally polarized, the total light intensity (also shown in Fig. IV-2) was just the sum of the intensities of A and B. But since A and B were coherent, they could interfere to give a pattern of varying polarization.

To display such results more concisely, one can place two orthogonally oriented polarizers side by side, so that each covers half the pattern. Then both the A and B components, or both the 1 and 2 components of the light can be observed. Such results are shown in Fig. IV-4. There the left frame shows the A and B com-

XBB 733-2372

Fig. IV-2. Illumination patterns with the rhomb alone. Top left: polarization A; top right: polarization B; bottom: total light intensity.

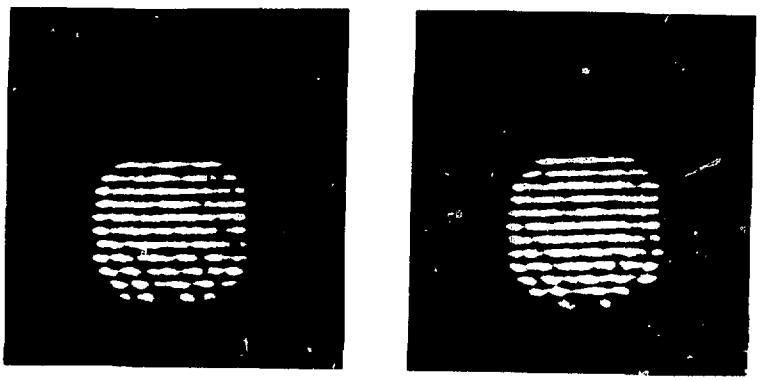

XBB 733-2374

Fig. IV-3. Illumination patterns with the rhomb alone.

Left: polarization 1; right: polarization 2.

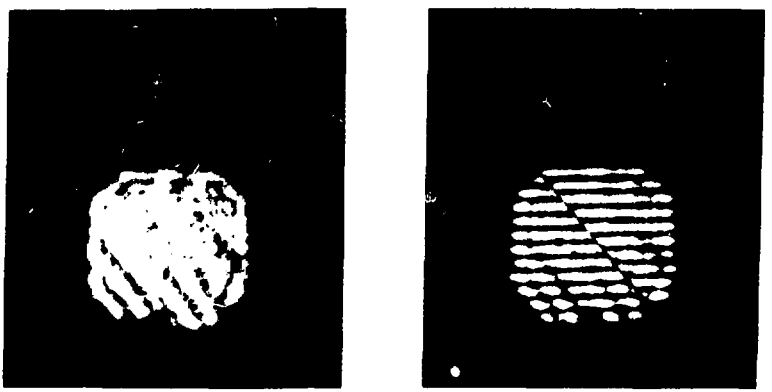

XBB 733-2373

Fig. IV-4. Illumination patterns with the rhomb alone.

Left: polarizations A and B; right: polarizations 1 and 2.

ponents (the left and right halves of the pattern) and the right frame shows components 1 and 2. Here it is particularly evident that patterns 1 and 2 are complementary.

These results are illustrations of the kind of polarization interference effects which we propose to use to measure correlations in the light emitted by a plasma. Moreover, since all of patterns in these figures were made while illuminating the entire rhomb, the sharpness of the fringes served to demonstrate that this rhomb was of sufficient quality for use in such a system.

2. A Two-Beam Spectroscopic System

As the next step, an elementary two-beam spectroscopic system was assembled. In this arrangement, the calcite rhomb was used in series with a monochromator. A mask behind the rhomb served to define the two observed beams, a lens before the rhomb defined a common source volume, and finally a second lens focused the light onto the entrance slit of the monochromator, exactly as illustrated in Fig. C-4 of Appendix C.

If this system had been used to observe a plasma, a linear polarizer would have been placed behind the first lens, causing the transmitted light to be divided into equal A and B components by the rhomb. These components would have been recombined at the monochromator entrance and the light which was transmitted by the monochromator would have been separated into 1 and 2 components by a prism placed behind the exit slit.

However, for testing the system it is much more convenient to interchange the roles of source and observation point. If the

exit slit of the monochromator is illuminated with light polarized as 2, that light will retrace the optical path in reverse, will be divided into A and B components by the rhomb and these components will be recombined at the former location of the common source volume. There all those points for which the path lengths of the A and B components differ by an integral number of wavelengths will be illuminated by light polarized as 2, while all the points for which the two path lengths differ by a half integral number of wavelengths will receive light polarized as 1. Since none of the path lengths is changed by reversing the direction of the light, these points are exactly the locations from which sources would, in the original arrangement, have contributed light of the same 1 or 2 polarization to the output of the system. Thus, in this way, one can obtain directly a display of the observed component of the light source distribution.

This procedure was used to test a variety of systems. For the two-beam system, the arrangement was:

He-Ne laser,

linear polarizer (with the orientation "2"),

lens, focused on the exit slit of the monochromator,

monochromator,

lens, focused on the entrance slit of the monochromator,

mask with one slit,

calcite rhomb,

lens, focused on the screen,

two orthogonal linear polarizers side by side (varied

to display the different patterns),

ground glass screen,

camera, focused on the screen.

In normal operation, all of the light transmitted by the monochromator would contribute to the signal. Hence in the present reversed operation, the entire exit slit should be illuminated. This was accomplished by sweeping the focus of the laser beam along the exit slit during exposure of each photograph. Sweeping the focus in effect expands the laser beam, but in a way which prevents interference between light from different points along the slit.

The illumination patterns which this system gave are shown in Fig. IV-5. There the upper pattern shows polarizations 1 and 2, while the lower pattern shows polarizations A and B. Again, the A and B components produced smooth patterns (the faint vertical bands are due to unsteadiness in sweeping the beam), but the 1 and 2 components gave sets of sharp interference fringes.

As just explained, the patterns 1 and 2 in Fig. IV-5 show the locations from which sources would contribute light of that polarization to the output when the system was operated normally. The final measured quantity in normal operation is, of course, the difference, $Y(t) = I_2(t) - I_1(t)$, between the intensities of these two components of the output light. Hence, in Fig. IV-5 it is the <u>difference</u> between fringe patterns 1 and 2 which corresponds to the component of the density of light sources which would be measured by this system if it were used to observe a

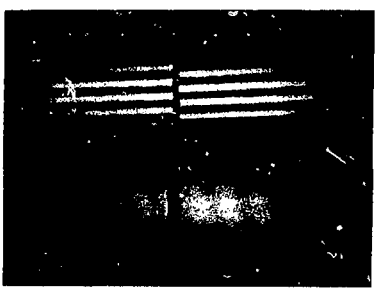

XBB 734-2425

Fig. IV-5. The effect of a two-beam spectrometer. Top: polarizations 1 and 2; bottom: polarizations A and B.

plasma. It is clear from the patterns that this difference is just one wavelength or $\underline{k}$ component of the distribution of light sources near the focus of the system. Thus these photographs agree with the predictions of the theory, with the result described in Sect. II.A by Eqs. (II.13) and (II.15) and described in Sect. II.B by Eq. (II.29).

The theory also predicts that the signal from a two-beam spectrometer will be due exclusively to sources within a restricted "common source volume". Indeed, the achievement of spatial localization was the first objective of the whole project. Thus, although the result is fairly certain, it is still important to check the effect of this system away from focus. This was done by moving the ground glass screen and the camera closer to the other optical components. (The distance between the screen and the last lens was roughly halved.)

The result is shown in Fig. IV-6. There the top frame shows again some patterns taken at the focus, while the lower frame shows the results away from focus. In the lower frame beams A and B are clearly separated, and patterns 1 and 2, which now do not exhibit fringes, are seen to be identical. Hence, the intensity difference signal, Y(t), will always vanish for sources this far from the focus. This region makes no contribution to the signal, irrespective of the distribution of the sources there. Thus the result of a two-beam spectroscopic observation would not be an average along a line of sight. Sources this far from the focus would not be observed.

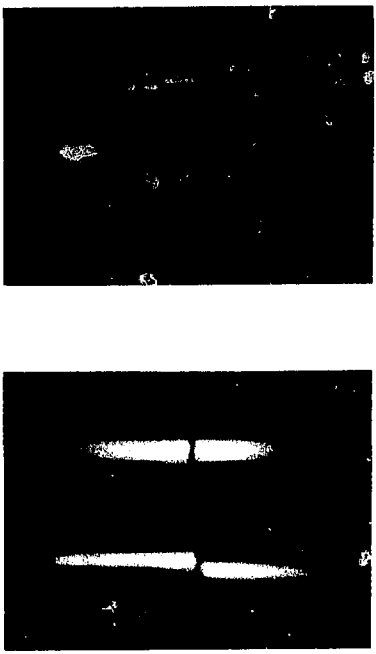

XBB 734-2424

Fig. IV-6. Spatial resolution with a two-beam system.

Top frame--patterns in the focal plane of the system (upper pattern: polarizations 1 and 2; lower pattern: polarizations A and B).

Bottom frame--patterns at a distance from the focus (upper pattern: polarizations 1 and 2; lower pattern: polarizations A and B).

Although one can thus make a local measurement, our theory predicted that--at least with a two-beam system--one can observe only fluctuations in the light source density. One cannot observe the total number of light sources in some region, essentially because the wavelength of the observed source density component ($2\pi/|\underline{k}_\Delta|$) is necessarily smaller than the width of the focal region. This is true because the former varies inversely with the angle between beams A and B, while the latter varies inversely with the angle subtended by either beam alone (angles α and β, respectively, in Fig. C-4). This conclusion was also checked experimentally, and the results are shown in Fig. IV-7. In our apparatus, the angle between the beams was determined by the focal lengths of the lenses and by the lateral displacement of one beam by the rhomb. This was left unchanged. The angle subtended by each beam, however, was determined by the width of the slit in the mask before the rhomb, and this was varied to produce the three sets of patterns shown in Fig. IV-7 (again taken at focus). The upper pattern was made with the largest slit, the center pattern with a narrower slit, and the lower pattern with a still narrower slit. Thus the angle β subtended by each beam was progressively decreased, and, as expected, the number of fringes in the pattern is seen to vary inversely with this angle.

Beyond a simple confirmation of the theory, the importance of these results is that they showed that an optical system of the type envisioned could be made from components of quite ordinary quality. The width of the beams A and B covered a substantial

XBB 734-2433

Fig. IV-7. The effect of the width of the beam-defining slit. Top frame: widest slit; bottom frame: narrowest slit.

portion of the diameter of the lenses used (and in the multiple-beam systems described below, the whole set of beams covered a large part of the lens area), yet the interference patterns obtained were sharp and clear. This occurred because the displacement due to the rhomb was fairly small and thus the interfering components of different beams passed through adjacent portions of the lens. It is only necessary that the different interference patterns coincide, but that is in essence a requirement on the imaging quality of the lens: So long as the lens is good enough to image a point to a spot much smaller than the desired fringe spacing, then the interference patterns produced by pairs of beams which go through different portions of the lens will coincide and the whole pattern will be sharp and clear.

I want to emphasize this point. At no time in this experimental work was any difficulty due to poor lens quality encountered. The production of polarization interference fringe patterns does not require "interference quality" components. Our systems were made with lenses already in the laboratory and they always produced fringe patterns like those shown in the photographs presented here.

3. Some Multiple-Beam Systems

Thus the two-beam system performed as expected. This apparatus could be used to observe fluctuations in a plasma, but such an observation would be difficult because the two-beam system is so inefficient in its use of the available light. It was for this reason that some more complicated systems were designed (as

described in Appendix C) and analyzed (as described in Sect. II.B). In the experimental work, several multiple-beam systems were also constructed and tested.

To simplify these observations, only the interferometric portion of these systems was constructed. The results of the work with the two-beam system proved that the inclusion of the monochromator did not degrade the polarization fringe patterns. In those studies, however, the first part of the optical train,

laser

lens, focused on the exit slit of the monochromator

monochromator

lens, focused on the entrance slit of the monochromator,

simply served to produce a beam of parallel monochromatic light. It was important to establish that this could be done with the required accuracy, but once that had been demonstrated, this part of the system could be replaced by just the laser and a beam-expanding telescope.

To make a multiple-beam system of the first type considered in Appendix C, one need only replace the mask behind the rhomb with one containing many slits. This was done in the simplified system:

He-Ne laser,

beam-expanding telescope,

linear polarizer (oriented at 45° to the axes of the rhomb),

mask with slits to define the beams,

calcite rhomb,

lens, focused on the screen (except when the patterns were observed away from focus),

linear polarizer (varied to display the different patterns),

ground glass screen,

camera, focused on the screen.

In tests of the two-beam system, the focus of the light was swept along the exit slit of the spectrometer. This caused an image to sweep along the entrance slit, and the lens focused there produced a collimated beam swept in direction. Thus the effect of illuminating the entire slit could be simulated in the present simplified system by rotating the laser and telescope during exposure of the photographs. However, the work with the two-beam system showed that this would only spread the patterns horizontally. Since all the features of interest can be seen without such a spreading, the multiple-beam patterns studied next were simply photographed at one position of the laser beam. The results thus show a single vertical slice of the complete fringe patterns.

The design of a multiple-beam system actually began when it was realized that the effect of a simple two-beam system should be independent of the exact position of the slit which defines the beams. In Appendix C it was argued that a change in the position of the slit in the mask behind the rhomb would not change the result. This led to the idea of using many slits at once, defining many pairs of beams which would use more of the available light. Thus, as a first experiment, it was essential to check

the effect of changing the position of the beam-defining slit.

To do this, a mask with one slit was mounted between the laser and the calcite rhomb. This just produced a two-beam system, but this time, in photographing the result, the beam-defining slit was swept across the rhomb while the camera was open. Thus, if the pattern had varied with slit position, the effect would have been washed out. Instead, the sharp pattern in Fig. IV-8 resulted. (Again, this is a vertical section of a pattern like those shown in the preceding few figures.) This clearly shows that our essential supposition is correct: The position of the slit is inconsequential.

Since all of the points behind the rhomb thus give the same observation, one might wonder why the mask there cannot be removed entirely. A pattern produced without the mask is shown in Fig. IV-9. The result shown there is clearly not the same as that of a two-beam system. The reason for this difference is that a larger aperture permits the system to focus the light down to a smaller spot. (c.f. Fig. IV-7. What we now have is a pattern which contains less than one fringe.) Thus almost all the sources observed radiate into beam 1. This in itself might be desirable, but the trouble with this arrangement becomes apparent when the pattern is observed away from focus (Fig. IV-10). There the light is <u>still</u> all polarized as 1. (The order of the two polarizations was reversed between these figures. The light is, in fact, polarized the same way in both cases.) Thus this system does not provide spatial localization. Sources all along the

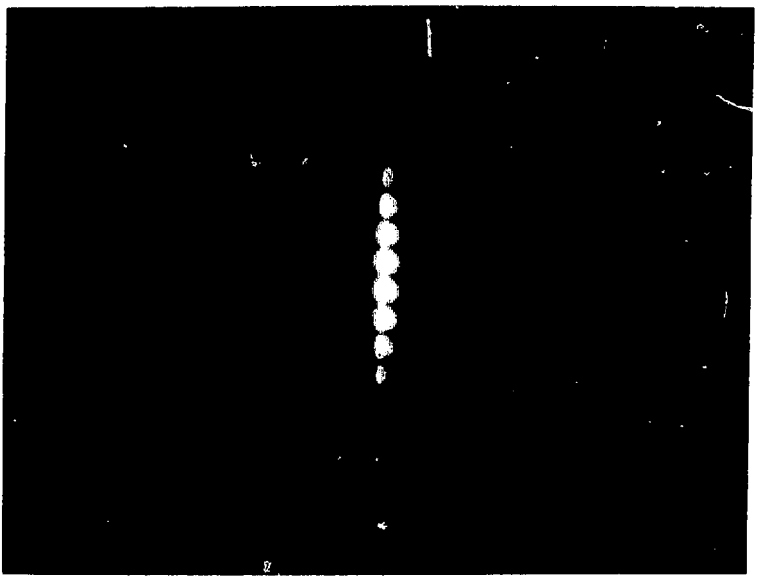

XBB 735-3032

Fig. IV-8. Lack of dependence of a two-beam pattern upon slit position. A photograph in which the beam-defining slit was swept across the rhomb during exposure.

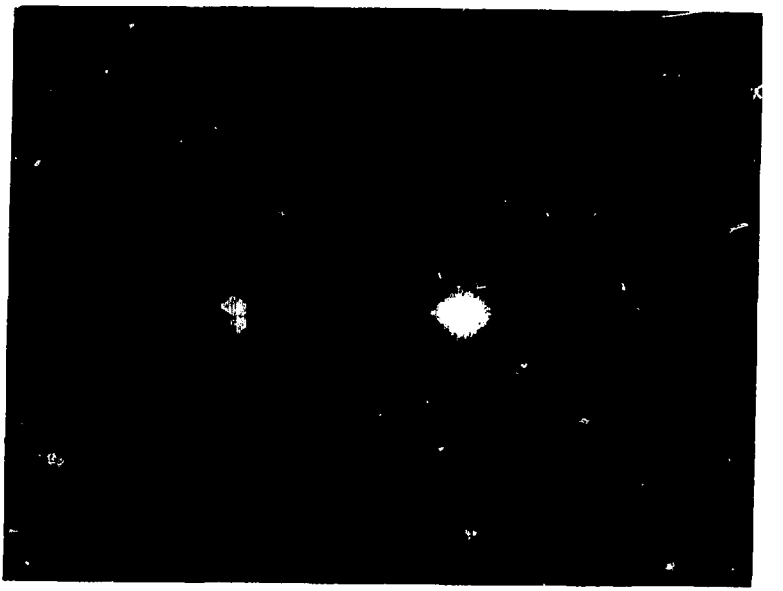

XBB 735-3033

Fig. IV-9. The effect of the whole rhomb without a mask--polarizations 1 and 2 observed at focus.

XBB 735-3034

Fig. IV-10. The effect of the whole rhomb without a mask--polarizations 1 and 2 observed away from focus.

line of sight would be observed. In the two-beam system, localization was provided by having separate beams which intersected only near the focus of the system. Without the mask, "beams A and B" completely overlap.

To avoid this difficulty one might consider inserting behind the rhomb a mask with many slits--defining separate beams but using more than two beams to accept more light. The effect of such a system is shown in Fig. IV-11.

The result shown there is again different from that of a two-beam system. In the new patterns, polarizations 1 and 2 give narrow, widely separated fringes. The reason for the difference is apparent from the patterns of A and B shown in the lower frame. Unlike the two-beam case, these patterns are not uniform, but now themselves consist of fringes. As explained in Appendix C, these fringes are produced by multiple-beam interference of the light transmitted through the different slits. Thus the overall effect is not the same as would be found for any of the slits considered singly.

This system was also analyzed in Sect. II.B (it is the second of the "three particular systems" of Sect. II.B.3) and the conclusion obtained there is given in Eq. (II.31). In the system of Fig. IV-11, the number of slits, n was 4, and Δ, the slit spacing, was approximately twice as much as d, the relative displacement of components A and B after the rhomb. When these values are inserted into Eq. (II.31), it then describes correctly the difference between the patterns 1 and 2 in Fig. IV-11. (Note, for

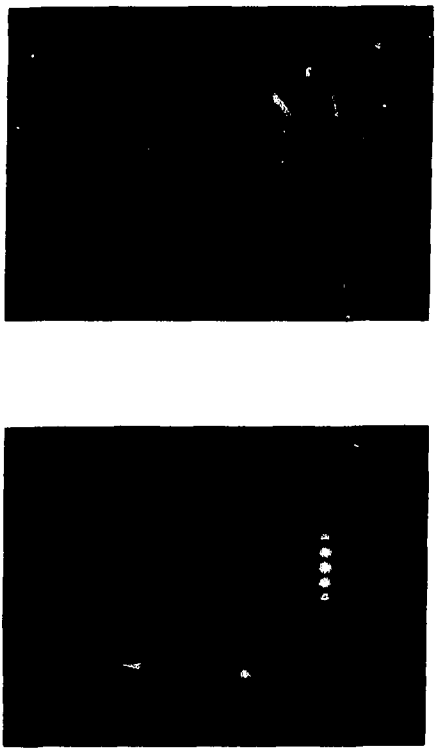

XBB 735-3037

Fig. IV-11. Patterns at the focus of a multiple-beam system. Top: polarizations 1 and 2; bottom: polarizations A and B and total light. Here $n = 4$ and $\Delta = 2d$.

example, that Eq.(II.31) says that the polarization fringes should be twice as widely spaced as are the maxima of total light intensity. In the photographed patterns, this is the case.) Thus this result also agrees with the predictions of our theory.

Although it differs from a two-beam system, this multiple-beam system also defines separate beams and hence should also give a local measurement. This it would do, as can be seen from Fig. IV-12, which shows the effect of the same system away from focus. There beams A and B are physically separated, components 1 and 2 are identically distributed, and hence the difference signal Y(t) would always vanish for sources this far from the focus.

Thus this system could be used to make a local spectroscopic measurement. The result might well be useful, but since it would be due to the irregular component of source density described by Eq. (II.31), the information obtained from this system would be in an inconvenient form.

4. A System with Several Independently Collimated Pairs of Beams

In our theoretical analysis it was concluded that one could make a multiple-beam spectroscopic system which would observe just one $\underline{k}$ component of the distribution of light sources within a local region. This system, which is described in Appendix C and was analyzed in Sect. II.B.3, was to include a collimator, a device which would define completely independently a whole set of pairs of beams A and B. By avoiding any interference between light accepted through the different slits, it was concluded that one could produce a more efficient version of a simple two-beam system.

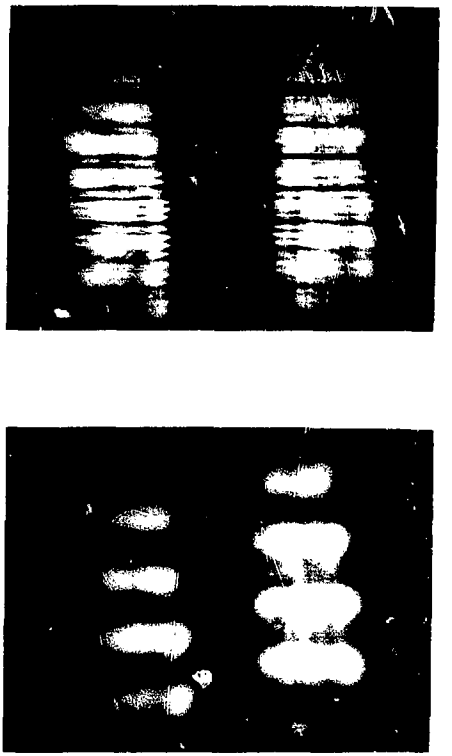

XBB 735-3036

Fig. IV-12. Patterns at a distance from the focus of a multiple-beam system. Top: polarizations 1 and 2; bottom: polarizations A and B. Here $n = 4$ and $\Delta = 2d$.

To actually build such a system it was only necessary to construct the collimator. Since this device was made with some care, a few words on its design may be appropriate. The collimator was made from sheets of 10 mil hard copper. From this were cut thirty plates 1-7/8 x 4 in. and thirty pairs of spacers 5/8 x 4 in. To form the collimator, these pieces were assembled in a stack of 0.600 x 1-7/8 x 4 in. To make the structure rigid, two pieces of 3/16 in. brass were cut to the length and width of the plates and mounted at the top and bottom of the collimator. To reduce reflections, two holes 5/8 x 1-1/16 in. were cut in each of the 10-mil plates. (i.e., the center 5/8 in. of the length of each plate consisted of three strips 5/8 in. wide, 1-1/16 in. apart. To cut the holes, the plates were clamped together in a stack and milled.) The assembled collimator was held together with both pins and screws. After assembly the device was electrolytically blackened in a chemical bath. The collimator ready for use is shown in Fig. IV-13.

As a first test, the collimator was used in place of the mask in a multiple-beam system like those discussed in the preceding section. The result is shown in the upper fram of Fig. IV-14. There polarizations 1 and 2 again show sharp, widely spaced fringes. This is not the effect of a system with many independently collimated pairs of beams. Since the laser beam was already collimated, the collimator simply acted as a mask with many slits, and since the laser light was coherent across the width of the beam, the light which went through different

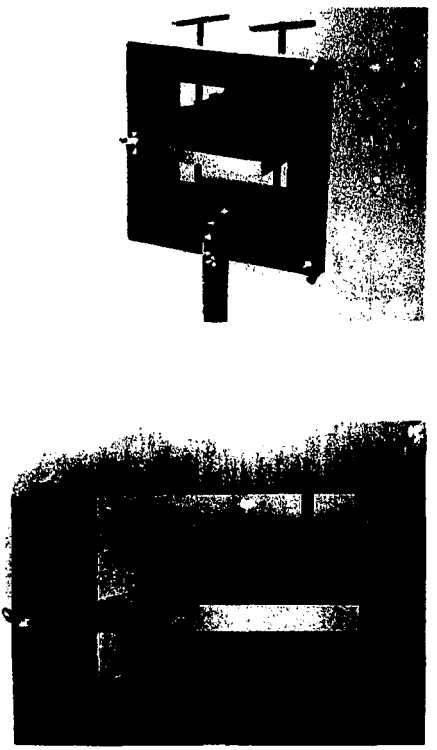

XBB 735-3038

Fig. IV-13. Two views of the collimator.

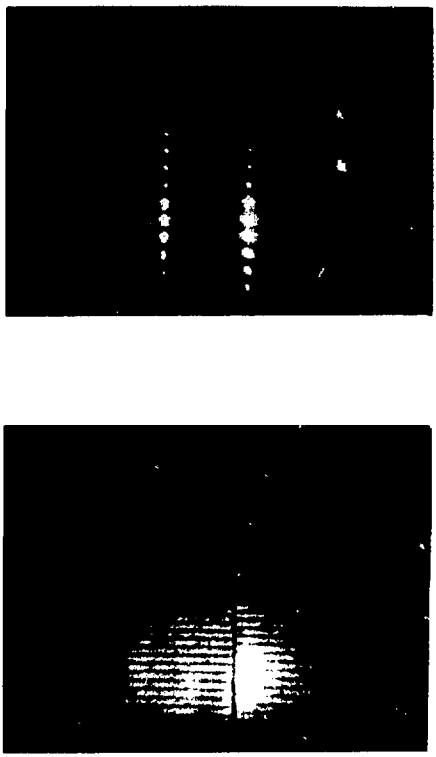

XBB 735-3035

Fig. IV-14. Two effects of the collimator.

Top frame--a multiple-beam pattern, $n = 15$, $\Delta \approx d/2$, made with the slits coherently illuminated.

Bottom frame--the effect of many independently collimated pairs of beams.

(Polarizations 1 and 2 shown in each case.)

collimator slits interfered to give the result shown. This is another example of a pattern described by Eq. (II.31). Here $\Delta \approx d/2$ and $n = 15$. (The collimator was taller than the rhomb, so only 15 slits were used.) Since, according to Eq. (II.31), the polarization fringe spacing should be roughly half the intensity fringe spacing, one might expect that only one polarization would be seen. This is almost true. Near the center of the pattern the light is mostly polarized as 2, but since d was not exactly twice Δ, the two patterns "get out of phase" and near the top the light is mostly polarized as 1.

This result again confirms the calculations which led to Eq. (II.31). It also shows what could happen if interference between light accepted through the different slits of the collimator were permitted to affect the result. In use in a spectrometer, the collimator is to be followed by a lens focused on the monochromator entrance slit. It is absolutely essential that this entrance slit be large enough to accept all of the light transmitted by the collimator. If only part of the light at that surface were accepted by the monochromator, the result of the measurement would depend upon multiple-beam interference and the observed source density component would be similar to that shown by the difference between the two patterns in the upper frame of Fig. IV-14.

When the collimator is correctly used, all of the light transmitted through the different slits will be accepted, so the result will not be affected by any multipe-beam interference. To model

this in an inverted system, it is necessary to illuminate the collimator incoherently. This was done by shining the laser onto a ground glass screen. A lens, focused on the screen, then gave an approximately collimated beam, but one in which the light was spread over a range of directions greater than that accepted by the collimator. Altogether, the test system was:

He-Ne laser,
ground glass screen,
lens, focused on this screen,
linear polarizer (oriented at 45° to the axes of the rhomb),
collimator,
calcite rhomb,
lens, focused on the following screen,
two orthogonally oriented linear polarizers, side by side (to show patterns 1 and 2),
ground glass screen,
camera, focused on the screen.

The result of this system is shown in the lower frame of Fig. IV-14. There polarizations 1 and 2 show simple sets of fringes like those obtained in the two-beam system. This is the desired result. In use as a spectrometer, this system would select a single $\underline{k}$ component (more precisely, a narrow range of components) of the distribution of light sources within the region observed.

This system is discussed in Appendix C and in Sect. II.B.5, where the conclusion is given by Eq. (II.55). The patterns in

Fig. IV-14 agree with the predictions of the theory. (The fine-scale graininess is just laser speckle, which has nothing to do with the spectroscopic system. Use of a ground glass screen does not really make the laser light incoherent, it merely complicates the phase relations so that unwanted interference produces only this easily ignored effect.)

As with the other systems tested, this result confirms the theory and also shows that the optical components were of sufficient quality for use in such a system. In the present case, this was particularly important, because in the formal theory it was assumed that all paths through a given collimator slit were equal to within a fraction of a wavelength, but the collimator actually used was not quite this restrictive. This difference did not appear to affect the result. As can be seen from Fig. IV-14, the fringe patterns produced agreed quite well with the predictions of the theory.

B. Observations of a Plasma

In the final part of the experimental work, the last optical system tested was used to observe fluctuations in a plasma. The plasma which was used for this purpose was produced in the Berkeley electron beam-plasma machine, which had previously been used in other experimental work.[51] Photographs of the machine and of the plasma are shown in Fig. IV-15.

In this device, an electron gun, biased to 4 kV negative,

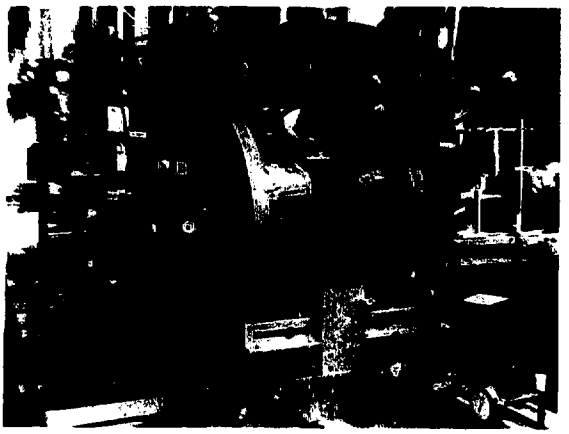

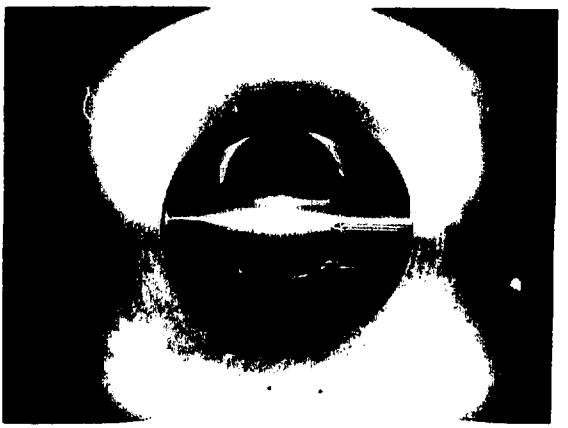

XBB 722-3344

Fig. IV-15. For legend, see page 134a.

Fig. IV-15. The electron beam-plasma experiment.

Top: The machine. The electron gun is to the left of the glass tee. The plasma chamber is between the two large magnet coils.

Bottom: Plasma with probes.

produced a 30 mA beam which was injected through two successive apertures (separating three independently pumped vacuum chambers) into a chamber filled with 300 microns of helium. The resulting beam-plasma instability produced a plasma with an electron temperature of a few eV and an electron density of a few times 10^{13} cm^{-3}. (See Ref. 51 and Appendix D below.) The plasma was confined by a magnetic field of 7 kG produced by two coils in Helmholz configuration. (The magnetic field also served to guide and focus the electron beam.) The electron beam was less than 1 mm in diameter and the resulting cylindrical plasma was approximately 0.5 cm in diameter and more than 10 cm long.

For a controlled test of the spectroscopic system, it was desired to produce in the plasma a disturbance of known frequency and of relatively large amplitude. This was done by using a negatively biased Langmuir probe with which one could vary the plasma density. This technique had already been used successfully to study the propagation of pulses in this plasma (see Appendix D). The pulse propagation work had shown that a density perturbation would be transmitted through the plasma at a speed slightly in excess of 10^6 cm/sec, the expected ion sound speed.

In the multiple-beam spectroscopic observations a sinusoidal signal rather than a pulsed signal was used. Frequencies in the range 10-50 MHz were chosen, since at the indicated ion sound speed this would give disturbances with wavelengths of a fraction of a millimeter--a convenient wavelength to observe with the multiple-beam system.

To improve the signal-to-noise ratio, two stages of phase-sensitive detection were employed. First, the transmitted signal was modulated at 50 kHz and this modulation was used as the reference signal to a lock-in amplifier. Secondly, the observed light was modulated at 1 kHz with a mechanical chopper and a reference signal from the chopper was used by a second lock-in amplifier (both were PAR Hr-8's).

The spectroscopic system was tuned to the neutral helium line at 4471 Å. To provide the needed aperture, the entrance and exit slits of the monochromator were removed entirely, a change which did not appreciably reduce the coherence length of the light, since most of the light was still in the 4471 Å line (see Appendix D). The neutral density was not expected to vary with plasma density, but since the neutral light emission was caused by excitation of neutral atoms by the plasma, it was expected that the light intensity would vary with the fluctuations in the plasma density.

The plasma was observed from a distance of 61 cm through a 13 cm focal length lens. This was followed by another lens of focal length of 26 cm which imaged the plasma at infinity. Later in the system, this light passed through the calcite rhomb of 1 cm^2 aperture which displaced one polarization laterally by 1.1 mm. In the multiple-beam system the effect of this was to select from within the plasma a source-density component of wavelength of 0.391 mm and to observe this through an aperture 0.64 cm^2, 61 cm from the plasma.

The collimator, the rhomb, and the monochromator were mounted so that beams A and B would be horizontal fans, vertically displaced. This would permit one to observe a vertical $\underline{k}$ vector component of the source distribution. Since the magnetic field lines in the plasma were horizontal, and since it was desired to observe propagation along the field, a Dove prism was included in the system to rotate by 90° the image of the plasma.

Altogether, the optical train was:

plasma,

lucite vacuum window,

objective lenses

linear polarizer (oriented at 45° to the axes of the rhomb),

calcite rhomb,

collimator,

lens, focused on the entrance to the monochromator,

mechanical chopper,

monochromator,

Glan-Thompson prism (separating polarization components 1 and 2),

lenses, focused on the exit of the monomchromator,

photomultiplier tubes.

The last few elements in the optical train are shown in Fig. IV-16. There can be seen the monochromator, the preceding lens, and chopper wheel, and the "Y" structure containing the Glan-Thompson prism, the two lenses, and the two photomultiplier tubes.

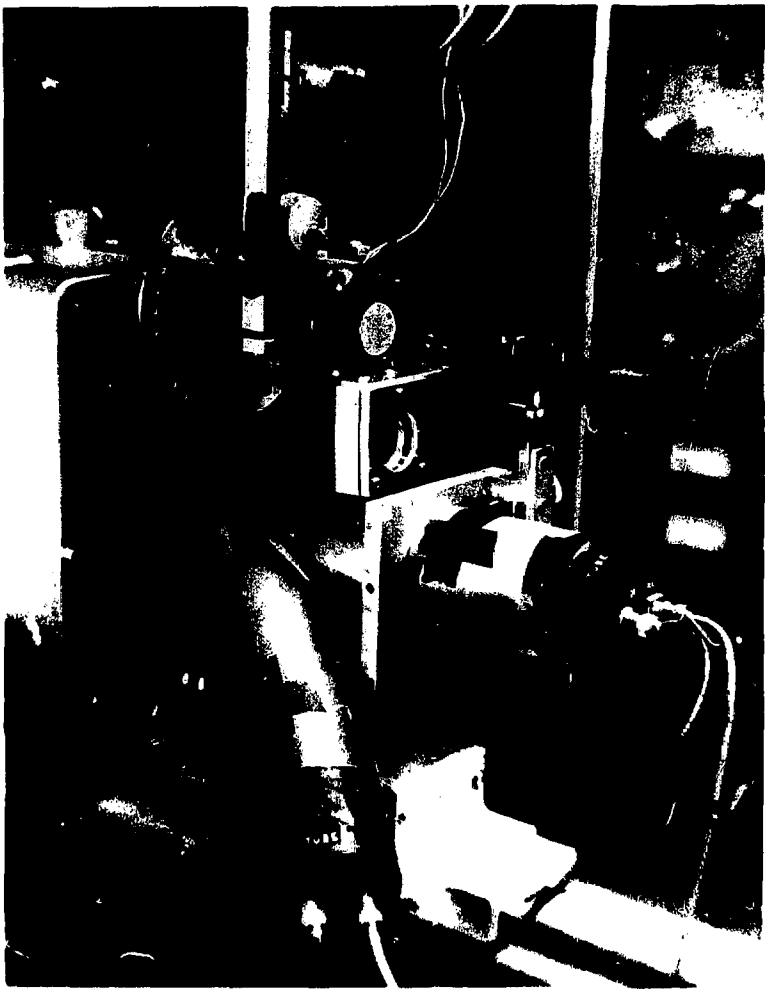

XBB 735-3343

Fig. IV-16. For legend, see page 138a.

Fig. IV-16. A view of the optical system showing the chopper wheel, the photomultiplier tube assembly, and one end of the monochromator.

A diagram of the entire apparatus is given by Fig. IV-17. As indicated there, the phototube outputs were compared by a differential amplifier, the resulting signal was fed into a spectrum analyzer, the output of this was processed by two lock-in amplifiers, and the result of this was then plotted by an X-Y recorder driven by the spectrum analyzer sweep.

The output was thus in the form of signal spectra. The disturbance in the plasma was injected at one frequency and the optical system was designed to observe one $\underline{k}$ component of the resulting plasma oscillations. Hence if the transmitter produced a disturbance at the observed $\underline{k}$, the signal spectrum would show a peak at the injected frequency.

Such a result is seen in Fig. IV-18. Each of the signal spectra shown there covers a range 39.5-41 MHz, which includes the transmitter frequency (40 MHz). The phototube difference signal (i.e., the intended output of the system) is shown in the upper trace, which does in fact exhibit a peak at the imposed frequency. This peak disappeared when the light path was blocked and it disappeared when the transmitting probe was rotated out of the plasma.

A spectrum of the output of a single one of the phototubes is shown by the second trace in Fig. IV-18. There the amplitude of the peak is reduced by half. This is as expected, since a wave at the observed $\underline{k}$ in the plasma will cause the light to oscillate between the phototubes (i.e., between the "interference patterns" observed by the phototubes). In the intensity difference signal, these two oscillations, which are out of phase, will add. So in

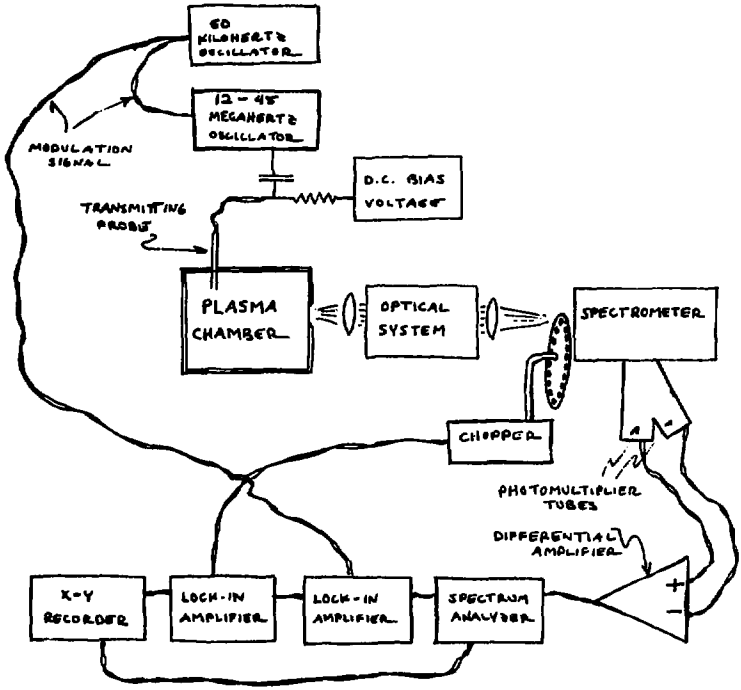

Fig. IV-17. Principal elements of the apparatus.

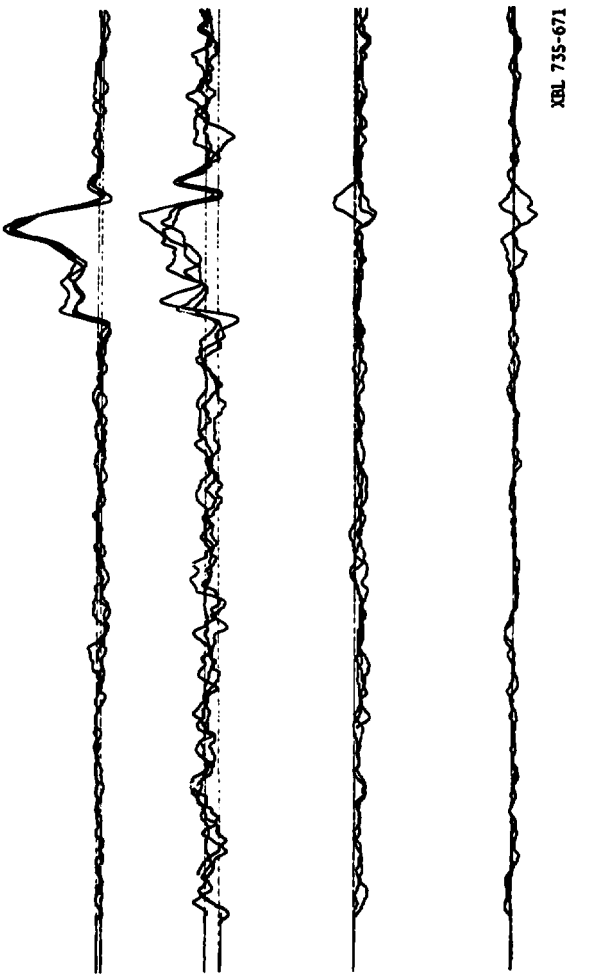

Fig. IV-18. For legend, see page 141a.

Fig. IV-18. Signal spectra (approximately 39.5 MHz with lower frequencies at right).

Top trace: The intensity difference signal.

Second trace: The output of one photomultiplier tube.

Third trace: The intensity difference signal with the light path blocked.

Bottom trace: The output of one photomultiplier tube with the light path blocked.

Each trace is three spectra superimposed (except the bottom trace, which is two spectra). This is a photograph of the X-Y recorder graph.

the spectrum of the output of each phototube alone, one ought to see exactly half the total signal amplitude.

Of equal interest is the change in the noise level all across the spectrum. The second trace is clearly noisier than the first. Nothing in the apparatus was changed between these to measurements (actually six measurements, as each spectrum is three traces). The differential amplifier was simply switched from (2-1) to 2. The increased noise is due to random variations in the plasma luminosity. When the two phototube signals are differenced, the fluctuations in the total light level are cancelled out. When only one of the tubes is used, the noise in the output is much greater. This is a useful thing to note in setting up the apparatus, because the cancellation of the noise shows that the system is correctly balanced at the frequencies of interest.

To be sure that the increased noise was not an electronic effect, the same spectra were again recorded, with the light path blocked (transmitter still on). The result is shown in the third and bottom sets of trances in Fig. IV-18. There the noise in the output of one phototube is less than that in the intensity difference signal, just as one would expect. Interestingly enough, the noise in the third set of traces (the difference signal with the light path blocked) is not much less than that in the top set of traces. Evidently most of the noise in the system came from the electronics, and hence it could have been eliminated by refinements in the apparatus.

On close inspection of the first two sets of traces, one sees

two small peaks, one on either side of the main peak, which increased when the system was switched from (2-1) to 2. Unlike the random noise, these features show a systematic change. This almost certainly is due to modulation of the total plasma luminosity by the transmitter. In Langmuir probe observations of pulse propagation in this plasma (see Appendix D) a fast signal was always seen. This was attributed to a potential fluctuation. That alone should not change the light emission, but there certainly are other mechanisms, such as a change in the electron temperature, which would cause the fast signal to make at least a slight change in the plasma luminosity. Since this would be seen with the same phase by both phototubes, the effect would be seen by each one alone, but would be balanced out in the intensity difference signal.

The presence of what appear to be the same two small peaks in the first set of traces may be due to a slight imbalance between the phototubes. A second possibility is that the plasma oscillation at the observed $\underline{k}$ merely had similar components in its spectrum. i.e., that the second set of traces is the sum of two components, one equal to half the upper traces and the other caused by modulation of the total luminosity.

There is, however, a third possibility which should also be mentioned. If there were a stationary or a slowly varying plasma disturbance at the observed $\underline{k}$, then the total light from the plasma would be divided unequally between the two phototubes. This by itself is just like any other fluctuation which the spectroscopic

system might observe. In this case the effect would appear at the low-frequency end of the signal spectrum. However, if the total plasma luminosity is modulated at a higher frequency, then the phototube which sees more light will see the modulation with a larger amplitude, and hence the modulation will appear in the intensity difference signal.

In other words, a high-frequency modulation of the total plasma luminosity would "illuminate" low-frequency density variations and these would then appear to have the higher frequency. Now, as far as the optical analysis is concerned, there is nothing to explain here. The high-frequency intensity modulation and the low-frequency density inhomogeneity combine to produce a fluctuation of the light source density at the observed wavelength and frequency. Then $n_s(\underline{k},\omega)$ actually exists in the plasma, and so, of course, the multiple-beam system sees it. But in interpreting such results it is important to realize that not every observed fluctuation corresponds to a wave in the plasma (except, perhaps, in a very broad sense of the term). Some features in the signal spectrum could be due to fast disturbances illuminating slower ones.

In our data, the location of the two small peaks at the sides of the main peak is not necessarily an indication of a difference in frequency. These data were taken with a lock-in amplifier which selected one phase component of the output of the spectrum analyzer. Since the phase and the amplitude of the (50 kHz) analyzer output would both change as the analyzer swept in frequency, the exact

shapes of features in these spectra did vary somewhat with the phase setting of the first lock-in amplifier. All the curves shown here were taken at a single phase setting.

It is also of interest to note the amplitude of these oscillations. When the gains of all the elements in the system are considered, the amplitude of the largest signals observed (at 29.5 MHz) is found to correspond to about a 10^{-10} A oscillation in photocurrent. The mean phototube output (measured directly) was 10^{-7} A. Hence the strongest signals were due to a 0.1% oscillation of the observed light intensities. In the pulse propagation studies (see Appendix D) in which the transmitter voltage was roughly the same as that used here, the peak of the pulse identified as an ion wave also represented a 0.1% change in the probe current. Now the width of that pulse was about five times the width of the transmitted pulse, so this amplitude represented about one-fifth of the whole disturbance. Judging by the interference patterns photographed in the test program (see Fig. IV-14) the spectroscopic system would observe a region about 40 fluctuation wavelengths wide. Thus the resolution in $\underline{k}$ was a few percent. Hence if the spread in transmitted wavelengths were about 10%, the spectral amplitude would also represent one-fifth of the disturbance. In a sweep through different frequencies (see Fig. IV-19) the maximum seen around 29.5 MHz did extend over roughly a 10% range of frequencies.

So the amplitude of the pulses seen with probes was roughly equal to the amplitude of oscillations observed spectroscopically.

In fact, this agreement must be at least in part fortuitous, if only because the dependence of the light intensity upon the plasma density is not known. An attempt was made to measure this dependence by changing the transmitter amplitude. It turned out that at large amplitudes (larger than where the data shown here were taken) the spectroscopic signal actually decreased as the transmitter amplitude increased. At lower amplitudes, the signal increased with the oscillation voltage, but the increase was much more rapid than linear. So the amplitude calibration has not been related to the plasma density disturbance. Still, it is worth noting that the observed 0.1% modulation of the light is reasonable and is similar to the density modulations seen with probes in the pulse studies.

Finally, to gain some information about the plasma response, the amplitude of these signals was observed over a range of frequencies. For each measurement the transmitter was set at one frequency and the spectrum analyzer was swept past that frequency. A set of the results is shown in Fig. IV-19. There one can see that the amplitude of the observed response did vary quite sharply with frequency. Of particular interest is a peak in response at about 29.5 MHz (the seventh trace in this set). Since the observed wavelength was 0.391 mm, this frequency corresponds to a phase velocity of 1.15×10^6 cm/sec. This is roughly equal to the ion sound speed, as computed from the measured temperature and as observed in the pulse propagation studies (see Appendix D). This suggests that these data show plasma density disturbances trans-

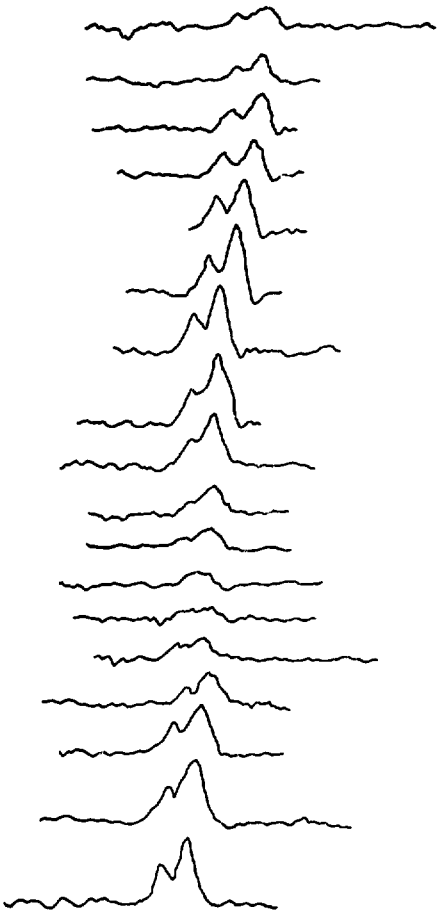

XBL 735-672

Fig. IV-19. For legend, see page 147a.

Fig. IV-19. Signal spectra taken at 0.5 MHz intervals from 26.5 through 35 MHz. These are tracings of the X-Y recorder plots.

mitted at the ion sound speed.

There are, however, several unknowns in the problem. The electron temperature, and hence the sound spped were known to vary with the distance from the center of the plasma column. The probe pulse data were taken just outside of the electron beam. The spectroscopic measurements presumably refer to the same region, if only because the transmitter was located there, but the effect of the hotter plasma within the beam remains unknown. Furthermore, the efficiency of the probe as a transmitter may be frequency dependent. Some of the observed variation in signal amplitude could have been due to the transmitter, rather than to propgation properties.

Clearly, an understanding of the dynamics of this plasma would require much more information that is contained in these few spectra. One could proceed now to use this spectroscopic system to do a complete study of the plasma--looking at different wavelengths, different frequencies, and different portions of the plasma column. But this would be a project in itself. Our purpose here is to show the utility of the spectrometer. These data should serve to illustrate the kind of information which can be obtained with such a diagnostic instrument.

V. HIGH-FREQUENCY PHENOMENA

A. The Effect of a Moving Source and the Use of a Time-Varying Optical System

The need to observe relatively high-frequency phenomena is a fundamental consideration of plasma diagnostics. Characteristic frequencies of many laboratory plasmas lie in the megahertz or gigahertz range. In pulsed experiments, the entire plasma may exist for only a small fraction of a second. We have noted already that the need for a probe with a rapid response suggests, in general, the consideration of optical diagnostic techniques.

In the multiple-beam spectrometers described in Chapter II, a component of the light would oscillate between two photomultiplier tubes in a manner characteristic of one component of the source distribution. Frequencies of plasma oscillations would be observed in the time dependence of the outputs of the phototubes. Yet phototubes, and other elements of the system, have a finite bandwidth which would, in practice, interfere with the measurement of frequencies above a few hundred megahertz. This is a serious limitation.

The present discussion began with an analysis of a simple two-beam spectrometer. A two-beam spectroscopic measurement was found to resemble a light-scattering experiment in several ways. A scattering measurement, however, is not restricted to low-frequency phenomena. Indeed, scattering provides a most convenient way to measure higher frequencies, which can be seen as optical frequency differences in the Doppler broadened spectrum of the

scattered light (see Sect. I.C). On the other hand, there are scattering measurement techniques (which we have not discussed) in which one does observe directly in a measured light intensity the time dependence of low-frequency phenomena. (See, for example, Ref. 52.) This similarity suggests that the low-frequency restriction of the multibeam spectrometers of Chapter II is due to our choice of apparatus, and not a necessary feature of a spectroscopic measurement.

To see how higher frequency, or higher phase velocity phenomena might be observed spectroscopically, consider first the effect of a single moving source. In Fig. V-1 is shown a small monochromatic light source which moves with a velocity $\underline{v}_s$. If the source has frequency ω_s, then the light emitted in a direction $\hat{k}_A$ must have a Doppler shifted frequency (to first order in $|\underline{v}_s|/c$)

$$\omega_A = \frac{\omega_s}{1 - \frac{\underline{v}_s}{c} \cdot \hat{k}_A} . \qquad (V.1)$$

Light which is emitted into different directions $\hat{k}_A$ and $\hat{k}_B$ will differ in frequency by an amount

$$\Delta\omega = \omega_B - \omega_A = \omega_s \left(\frac{1}{1 - \frac{\underline{v}_s}{c} \cdot \hat{k}_B} - \frac{1}{1 - \frac{\underline{v}_s}{c} \cdot \hat{k}_A} \right)$$

$$\approx \underline{v}_s \cdot (\underline{k}_B - \underline{k}_A) = \underline{v}_s \cdot \underline{k}_\Delta . \qquad (V.2)$$

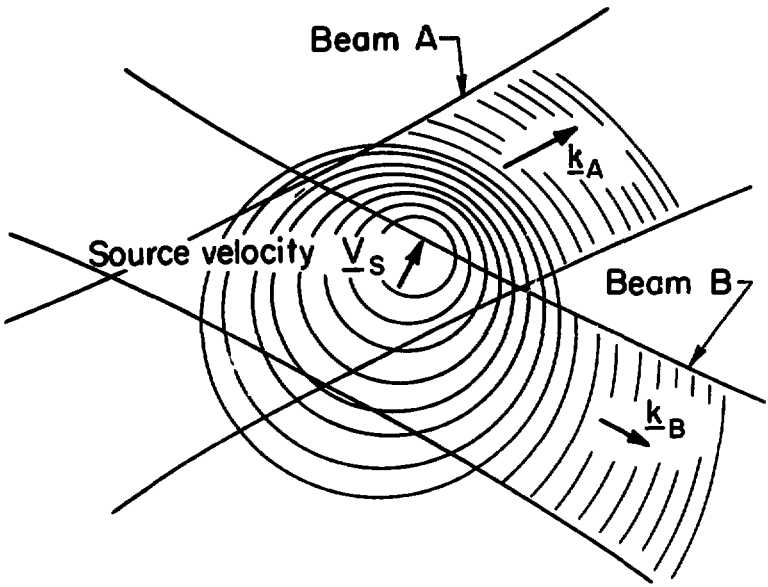

Fig. V-1. Two-beam observation of a moving source.

Here $\underline{k}_\Delta$ is the familiar difference wave vector [c.f. Eq. (I.9) or (II.18)].

So, at least for nonrelativistic motion, the difference in frequency which would be seen in a two-beam observation of a moving source depends upon the same $\underline{k}_\Delta$ which describes the fluctuations in source density observed in the low-frequency limit. The same source wavelength characterizes both the mutual coherence and the frequency difference observed with a two-beam spectrometer. This suggests that it should be possible to extend the low-frequency technique and observe rapid motions of a light source distribution by comparing light emitted in different directions at different optical frequencies.

In fact, the low-frequency system discussed in Sect. II.A already involves exactly this. In the simple two-beam arrangement, the observed beams A and B were combined and their superposition was separated into two complementary interference patterns--beams 1 and 2. It was shown that an oscillation of the $\underline{k}_\Delta$ component of the light source density would produce a corresponding oscillation of the light intensity between beams 1 and 2. This oscillation of the light is due to a steady variation in the relative phase--more precisely, in the phase of the mutual coherence--between beams A and B. Yet a steadily increasing phase difference is exactly the same thing as a difference in frequency. The low-frequency system simply measures a small frequency difference by observing the time dependence of the beats which result when the two waves are combined.

One can certainly measure differences in frequency between the two beams, but to extend the concept of a multiple-beam spectrometer, the phase must also be observed. The optical systems described in Chapter II were designed to measure the mutual coherence of light of equal, or at least nearly equal frequency. An obvious way to extend the method is to add to the system a moving mirror or other time-varying element which would Doppler shift the frequency of one of the beams. The remainder of the system could then be left unchanged.

Such a modified two-beam arrangement is shown in Fig. V-2 . The spectral filter again accepts the same $|\underline{k}|$ components of each beam, but since beam B is first shifted in frequency, the light accepted through the two beams is emitted at different frequencies from the plasma.

The analysis of Sect. II.A.3 is easily amended to describe this new arrangement. The light accepted through beam A, is, as before

$$\xi_A^{(\text{observed})}(\underline{r},t) = \text{Re}\, \delta^2\Omega \int_0^\infty d|\underline{k}_A| e^{i\underline{k}_A\cdot\underline{r}} f(|\underline{k}_A|c)\, \frac{|\underline{k}_A|}{2\pi i c}\, \xi_A^{(+)}(\underline{k}_A,t)$$

$$= \text{Re}\, \delta^2\Omega \int_0^\infty d|\underline{k}_A| e^{i\underline{k}_A\cdot\underline{r}} f(|\underline{k}_A|c)$$

$$\cdot \frac{|\underline{k}_A|}{2\pi i c} \int d^3r'\, \xi_B^{(+)}(\underline{k}_A,t;\underline{r}').$$

Because of the moving mirror, beam B is, in effect, observed from a moving frame of reference

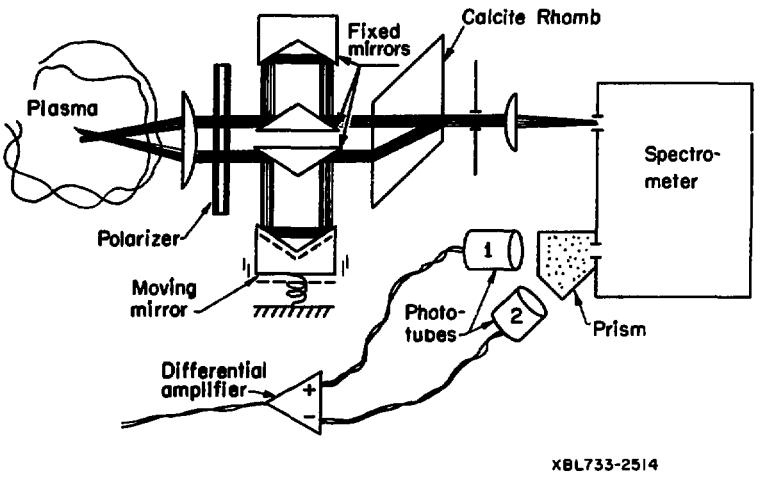

Fig. V-2. The use of a moving mirror in a two-beam system.

$$\xi_B^{(\text{observed})}(\underline{r},t) = \text{Re}\, \delta^2\Omega \int_0^\infty d|\underline{k}_B| e^{i\underline{k}_B\cdot\underline{r}} f(|\underline{k}_B|c) \cdot \frac{|\underline{k}_B|}{2\pi ic} \int d^3r'\, \tilde{\xi}_B^{(+)}(\underline{k}_B,t;\underline{r}'), \qquad (V.3a)$$

where

$$\tilde{\xi}_B^{(+)}(\underline{k}_B,t;\underline{r}') = \int d^3r_1\, e^{-i\underline{k}_B\cdot\underline{r}_1}\, \xi_B^{(+)}(\underline{r}_1 + \underline{v}_0 t, t;\underline{r}')$$

$$= \int d^3\rho\, e^{-i\underline{k}_B\cdot\underline{\rho}}\, e^{+i\underline{k}_B\cdot\underline{v}_0 t}\, \xi_B^{(+)}(\underline{\rho},t;\underline{r}')$$

$$= e^{+i\underline{k}_B\cdot\underline{v}_0 t}\, \xi_B^{(+)}(\underline{k}_B,t;\underline{r}'). \qquad (V.3b)$$

So, the effect of the moving mirror is to introduce in the observed field amplitude an additional factor of $e^{-i\underline{k}_B\cdot\underline{v}_0 t}$.

As before, the two waves are combined to produce two interference patterns

$$I_{1,2}(t) = \overline{\left| \frac{1}{\sqrt{2}} \left[\xi_B^{(\text{observed})}(\underline{r}_B,t) + \xi_A^{(\text{observed})}(\underline{r}_A,t) \right] \right|^2}$$

and the difference between these intensities provides the output of the system,

$$Y(t) = I_2(t) - I_1(t).$$

Assuming that $f(|\underline{k}_A|c) = f(|\underline{k}_B|c)$, describing the intensity in terms of an analytic signal, and assuming again that the light from each point $\underline{r}'$ is coherent, but that light from different

points is incoherent, leads, as before, to the expression

$$Y(t) = \int_{\substack{\text{common source}\\ \text{volume}}} d^3r' \int_0^\infty d|\underline{k}|\ |f(|\underline{k}|c)|^2\ \mathrm{Re}\ \tilde{\Gamma}_{BA}(0;|\underline{k}|,\underline{r}')$$

where now

$$\tilde{\Gamma}_{BA}(0;|\underline{k}|,\underline{r}') = \left(\frac{|\underline{k}|\delta^2\Omega}{2\pi c}\right)^2 \overline{\left[e^{i\underline{k}_A\cdot\underline{r}_A}\ \xi_A^{(+)}(\underline{k}_A,t;\underline{r}')\right]^*} \cdot \overline{\left[e^{i\underline{k}_B\cdot\underline{r}_B}\ e^{+i\underline{k}_B\cdot\underline{v}_0 t}\ \xi_B^{(+)}(\underline{k}_B,t;\underline{r}')\right]}\ . \qquad (V.4)$$

Expressing $\xi_{A,B}^{(+)}$ in terms of $s(\underline{r}',t)$, the source gives

$$\tilde{\Gamma}_{BA}(0;|\underline{k}|,\underline{r}') = \left(\frac{|\underline{k}|\delta^2\Omega}{2\pi c}\right)^2 e^{-i\underline{k}_A\cdot\underline{r}_A}\ e^{+i\underline{k}_B\cdot\underline{r}_B}\ e^{+i\underline{k}_A\cdot\underline{r}'}\ e^{-i\underline{k}_B\cdot\underline{r}'} \cdot \overline{\int d^3\rho_1\ \frac{1}{|\underline{\rho}_1|}\ e^{i\underline{k}_A\cdot\underline{\rho}_1}\ s^{(+)*}\left(\underline{r}', t - \frac{|\underline{\rho}_1|}{c}\right)} \cdot \overline{\int d^3\rho_2\ \frac{1}{|\underline{\rho}_2|}\ e^{+i\underline{k}_B\cdot\underline{v}_0 t}\ e^{-i\underline{k}_B\cdot\underline{\rho}_2}\ s^{(+)}\left(\underline{r}', t - \frac{|\underline{\rho}_2|}{c}\right)}\ .$$

Using again the result of Appendix B.2, we have,

$$\tilde{\Gamma}_{BA}(0;|\underline{k}|\underline{r}') \underset{t\to\infty}{\rightarrow} e^{-i\underline{k}_A\cdot(\underline{r}_A-\underline{r}')}\ e^{i\underline{k}_B\cdot(\underline{r}_B-\underline{r}')}\ (\delta^2\Omega)^2 \cdot \overline{\left[s^{(+)*}(\underline{r}',|\underline{k}|c)\ e^{+i\underline{k}_B\cdot\underline{v}_0 t}\ s^{(+)}(\underline{r}';|\underline{k}|c)\right]}\ . \qquad (V.5)$$

If the velocity $\underline{v}_0$ is not too large, the factor $e^{-i\underline{k}_B\cdot\underline{v}_0 t}$ will be nearly constant over the interval of the time average. In such cases, the above result becomes,

$$\tilde{\Gamma}_{BA}(0;|\underline{k}|,\underline{r}',t) = e^{i\phi}\, e^{-i\underline{k}_\Delta\cdot\underline{r}'}\, e^{+i\underline{k}_B\cdot\underline{v}_0 t}\, \mathcal{A}(|\underline{k}|c;\underline{r}',t)(\delta^2\Omega)^2$$

where ϕ, $\underline{k}_\Delta$, and $\mathcal{A}(|\underline{k}|c;\underline{r}',t)$ are defined as in Chapter II.A.3. If the light is so nearly monochromatic that ϕ and $\underline{k}_\Delta$ may be treated as constants, as was done before, the output of the system is

$$Y(t) = \int d|\underline{k}|\ |r(|\underline{k}|c)|^2\ \mathrm{Re}\left[e^{i\phi}\, e^{+i\underline{k}_B\cdot\underline{v}_0 t}\ \underset{\substack{\text{common}\\ \text{source}}}{\mathcal{A}}(|\underline{k}|c;\underline{k}_\Delta,t)\right](\delta^2\Omega)^2. \qquad \text{(V.6a)}$$

So the spatial resolution is unchanged. The system still observes the $\underline{k}_\Delta$ component of the distribution of common sources, but the introduction of a moving mirror has changed the time dependence of the output. Taking a frequency spectrum of the signal,

$$Y(\omega) = \int dt\, e^{i\omega t} Y(t)$$

$$= \int d|\underline{k}|\,|r(|\underline{k}|c)|^2\ \mathrm{Re}\left[e^{i\phi}\ (|\underline{k}|c;\underline{k}_\Delta,\omega + \underline{k}_B\cdot\underline{v}_0)\right](\delta^2\Omega)^2. \qquad \text{(V.6b)}$$

So the time dependence of the observation has been "heterodyned" in frequency. The ω frequency component of the output corresponds to the $\omega + \underline{k}_B\cdot\underline{v}_0$ frequency component of the $\underline{k}_\Delta$ wave vector component of the source distribution. The addition of a moving mirror has shifted the observed frequency range from near dc to an equal band around $\underline{k}_B\cdot\underline{v}_0$, thus permitting observation of higher frequency phenomena.

It should be remembered, however, that the factor $e^{i\underline{k}_B\cdot\underline{v}_0 t}$ was treated as constant in the time average which defined the light intensity. Such an assumption is, in fact, required for

consistency, because it was assumed that the light from each point $\underline{r}'$ was coherent, that the spectrum was so narrow that the differences in optical path were the same for all accepted wavelengths. The requirement of a narrow spectrum is, in itself, a low-frequency restriction. The above result is still significant, since the time dependence of even a narrow spectral feature may be too rapid to be easily observed, but to observe still higher frequencies, one must accept a larger portion of the spectrum and the requirement of coherence must be modified.

B. Correlations Between Light of Different Frequencies

Before continuing with the general analysis, it seems appropriate to say a little more about the ways in which these higher frequency correlations could be measured. The use of a moving mirror, or some similar device,[53] is only one of several possibilities, and a few other options might be mentioned.

One way in which the observation could be heterodyned in frequency is by employing a fast shutter. If an electro-optic element or some other rapid gate[54] were placed before the system and switched at a frequency Ω, the entire observation would then be shifted in frequency by that amount. This can be seen quite simply. Just imagine that the plasma wave observed had frequency Ω. Then the light would oscillate at this frequency between beams 1 and 2. If the spectrometer were gated, so that the window was open only when the light was polarized as 1, the signal would appear at zero frequency.

Another way in which high-frequency effects could be observed

is suggested by a more careful examination of the system shown in Fig. V-2. There a moving mirror is used to shift the frequency of the light in beam B, the light in beams A and B is then processed by the same spectrometer, and the mutual coherence of the two is measured by combining A and B and measuring the intensities of the intermediate polarizations--"interference patterns 1 and 2". Now the observation of interference is not the only way in which this mutual coherence could be measured. The magnitude of Γ_{BA} could also be obtained from an intensity correlation measurement. (See Sect. III.A.) In that case one would not combine beams A and B at all, but would observe the two with separate phototubes and then record the correlation of the two intensities. This is something which could be done with light of different frequencies. The moving mirror in Fig. V-2 does not affect the intensity of B, it only shifts the frequency. One could separate the same light without the mirror if the spectrometer were readjusted to the original, unshifted frequency of B. Since A is unaffected, one would then require two spectrometers or spectral filters set to different frequencies, as shown in Fig. V-3. If an intensity correlation measurement were practical, one could just select one frequency component of beam A and another frequency component of beam B and then observe a correlation of the two intensities. However, care should be taken to determine the usable aperture, which might be severely limited by requirements of coherence, and a more detailed analysis of the significance of an intensity correlation measurement--which is really beyond the domain of the

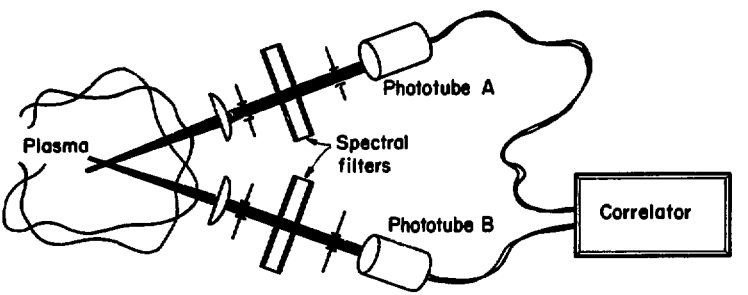

XBL733-2513

Fig. V-3. The use of intensity correlations to observe high-frequency phenomena.

present study--should also be done before attempting this type of experiment.

In whatever way the experiment is done, the object is to measure the coherence between two beams of light of different frequencies. This concept itself is not new. As has been noted by several authors,[55] there is nothing inconsistent about the idea of coherence between light waves of different frequencies. One can always imagine Doppler shifting the frequency and then comparing phases, and any of the other techniques just mentioned would also serve to introduce the same idea.

In a formal analysis, it is only necessary to include a time dependence in the correlation function. Thus where we had before

$$\Gamma_{BA}(\tau \mid \underline{k} \mid) = \left(\frac{|\underline{k}|\delta^2\Omega}{2\pi c}\right)^2 \cdot \overline{\left[e^{i\underline{k}_A\cdot\underline{r}_A}\xi_A^{(+)}(\underline{k}_A,t)\right]^* \left[e^{i\underline{k}_B\cdot\underline{r}_B}\xi_B^{(+)}(\underline{k}_B,t+\tau)\right]},$$

we should consider now

$$\Gamma_{BA}(\tau,|\underline{k}_A|,|\underline{k}_B|) = \left(\frac{|\underline{k}_A|\delta^2\Omega_A}{2\pi c}\right)\left(\frac{|\underline{k}_B|\delta^2\Omega_B}{2\pi c}\right) \cdot \overline{\left[e^{i\underline{k}_A\cdot\underline{r}_A}\xi_A^{(+)}(\underline{k}_A,t)\right]^* e^{i\Delta\omega t}\left[e^{i\underline{k}_B\cdot\underline{r}_B}\xi_B^{(+)}(\underline{k}_B,t+\tau)\right]} \tag{V.7a}$$

where the frequency difference,

$$\Delta\omega = |\underline{k}_B|c - |\underline{k}_A|c. \tag{V.7b}$$

To simplify the following equations, it is assumed here that

the light accepted through each beam is quasi-monochromatic. Then only one value of $|\underline{k}_A|$ and one value of $|\underline{k}_B|$ need by considered. The two frequencies, however, are not equal, and hence the total spectrum is not narrow. Indeed, this is required for the observation of high-frequency phenomena, since the frequencies of the phenomena observed cannot exceed the bandwidth of the light.

In all of our preceding calculations, light from different points $\underline{r}'$ within the plasma was considered incoherent, while light from the same source point was assumed to be completely coherent and, in effect, was treated as monochromatic. That assumption clearly is not valid in this high-frequency analysis, since light from each point is far from monochromatic, and hence our former, simple picture of the source is not appropriate. The easiest way to generalize the picture is to represent the plasma as a set of moving sources. Each source may still be considered monochromatic in its own frame of reference, but since the source is moving, the emitted light will be Doppler shifted to produce a broadened spectrum. One could do this by replacing the source density (in $\underline{r}$-space) by a distribution function (dependent also on velocity), but for simplicity we shall consider only a discrete set of sources:

$$s(\underline{r},t) = \sum_j \cos \omega_j t + \phi_j(t)\left[\delta\ \underline{r} - \underline{r}_j(t)\right]. \qquad (V.8)$$

Here the phases $\phi_j(t)$ are independent, so the different sources are all incoherent. Hence the mutual coherence Γ_{BA} may be written as a sum of contributions from the separate sources. Making this assumption, and then evaluating Γ_{BA} gives

$$\Gamma_{BA}(0,|\underline{k}_A|,|\underline{k}_B|) = -\,\delta^2\Omega_A\delta^2\Omega_B\, e^{-i\underline{k}_A\cdot\underline{r}_A}\, e^{+i\underline{k}_B\cdot\underline{r}_B}$$

$$\cdot \sum_j \int_{-\infty}^{t} d\tau_1 \left[e^{i|\underline{k}_A|c(t-\tau_1)} - e^{-i|\underline{k}_A|c(t-\tau_1)} \right] \overline{e^{i\underline{k}_A\cdot\underline{r}_j(\tau_1)}}$$

$$\cdot \overline{e^{i\left[\omega_j\tau_1+\phi_j(\tau_1)\right]}}\, e^{i\Delta\omega t} \int_{-\infty}^{t} d\tau_2 \left[e^{i|\underline{k}_B|c(t-\tau_2)} - e^{-i|\underline{k}_B|c(t-\tau_2)} \right]$$

$$\cdot \overline{e^{-i\underline{k}_B\cdot\underline{r}_j(\tau_2)}\, e^{-i\left[\omega_j\tau_2+\phi_j(\tau_2)\right]}} \,.$$

Since each source is nearly monochromatic, the phases ϕ_j are all slowly varying quantities. More precisely, they vary only at frequencies less than the optical bandwidth. But this implies that these phases may be taken constant in the τ_1 and τ_2 integrals which define the spectra, since these integrals are really taken only over the preceding inverse bandwidth interval. Hence it is admissable to replace $\phi_j(\tau_1)$ and $\phi_j(\tau_2)$ by $\phi_j(t)$.

It also greatly simplifies the result to assume that all the sources move without acceleration and set

$$\underline{r}_j(t) = \underline{r}_{j0} + \underline{v}_j t.$$

Under these assumptions the above result reduces to

$$\Gamma_{BA}(0,|\underline{k}_A|,|\underline{k}_B|) = \delta^2\Omega_A\delta^2\Omega_B\, e^{-i\underline{k}_A\cdot\underline{r}_A}\, e^{+i\underline{k}_B\cdot\underline{r}_B} \cdot \sum_j e^{-i(\underline{k}_B-\underline{k}_A)\cdot\underline{r}_{j0}}$$

$$\cdot\, \delta(\omega_j + \underline{k}_B\cdot\underline{v}_j - |\underline{k}_B|c)\delta(\omega_j + \underline{k}_A\cdot\underline{v}_j - |\underline{k}_A|c). \qquad (V.9)$$

Except for normalization, this expression just denotes the $\underline{k}_\Delta = \underline{k}_B - \underline{k}_A$ component of the distribution of those sources which have frequency and velocity such that

$$\omega_j + \underline{k}_B \cdot \underline{v}_j = |\underline{k}_B| c$$

$$\omega_j + \underline{k}_A \cdot \underline{v}_j = |\underline{k}_A| c.$$

Putting these relations in a more convenient form, we have the two conditions

$$(\underline{k}_B - \underline{k}_A) \cdot \underline{v}_j = |\underline{k}_B| c - |\underline{k}_A| c = \Delta\omega \qquad \text{(V.10a)}$$

$$\omega_j + \frac{1}{2} (\underline{k}_A + \underline{k}_B) \cdot \underline{v}_j = \frac{1}{2} (|\underline{k}_A| c + |\underline{k}_B| c). \qquad \text{(V.10b)}$$

The first condition, Eq. (V.10a), just restates our earlier result, Eq. (V.2), which was obtained from a much more elementary argument. The point is the same: The frequency difference between light emitted in the $\hat{k}_A$ and $\hat{k}_B$ directions depends upon that component of the source velocity which is parallel to $\underline{k}_\Delta$. Hence, by correlating light of different frequencies emitted in these two directions, one selects one value of this source velocity component. Only sources with such motion can contribute to the signal.

The second condition, Eq. (V.10b), just gives the usual effect of Doppler broadening, as is seen in conventional spectroscopy. Here it is the $(\underline{k}_A + \underline{k}_B)$ velocity component which changes the apparent frequency of the source.

What this calculation shows is that the effect of Doppler

broadening could be deduced from correlation measurements--even with a spectrum further broadened by another mechanism. We assumed that each source was monochromatic in its frame of reference, but did not assume that all the frequencies ω_j were equal. These frequencies could differ and this difference would produce a broadened spectrum. If such broadening concealed the Doppler shift, the source velocities could not be measured by conventional spectroscopy.

This is something which does happen in a plasma. In any plasma there are electric fields, fluctuating fields which through the mechanism of the Stark effect can broaden spectral lines. (we mean here the quasi-static, or Holtsmark type of Stark broadening, not collisional broadening which spreads the spectrum of the light emitted from each atom.) This broadening can exceed the Doppler broadening and conceal the Doppler line shape in the spectrum. Then the Doppler broadening cannot be seen--at least not without some kind of unfolding.

In such cases, nevertheless, a detailed record of the source velocities is still present in the radiation. As the preceding calculation shows, such information could be found from observation of the phase relations--of the correlations--between different frequency components of light emitted in directions $\hat{k}_A$ and $\hat{k}_B$. When differences in frequency are allowed, a two-beam spectroscopic observation could provide the distribution, not just in space, or k, but also in velocity, of the sources of each feature in the spectrum.

This result, of course, suggests some interesting experiments. Moreover, the analysis which we have done is only a beginning, for the effect of other optical arrangements and of other correlation measurements remains to be determined. We shall not pursue these questions further here; that would be a separate project. The foregoing discussion illustrates that an extension of the method to high frequencies is possible. An exploration of this possibility could be the subject of a later study.

VI. CONCLUSIONS AND SUGGESTIONS

A. A Summary of Results

This project began with the realization that spatially localized information about particle correlations--information of the type provided by a scattering experiment--is in fact present in the light emitted by a plasma. The initial objectives were to prove this fact and then to demonstrate that such information could be obtained with a practical, convenient diagnostic instrument. The facts about phase measurements could probably have been shown with a simple two-beam system, but since the two-beam arrangement is so inefficient, the development of a more efficient design was crucial to the question of practicality.

The multiple-beam system which was ultimately constructed involved two design principles: the use of polarization interference and the use of many independently-collimated pairs of beams. Our particular system could, of course, be improved, but these two techniques should be worth considering in the design of any such device.

The particular system described here can be claimed to have served its intended purpose: The optical tests verified the theory of the design and the plasma observations showed that such a system can be used for plasma diagnostics.

Regarding the experimental work, three comments seem worth making in conclusion. Firstly, as we have already noted, the optical system which was used was made from components of quite ordinary quality. The lenses were all single elements; the patterns

shown in Sect. IV.A were made using sheets of plastic polarizing material. Furthermore, the plasma was observed through a lucite vacuum window which was certainly not of high optical quality. It was originally thought that this window would have to be replaced, but before doing so the lucite was placed in the optical train of a test system like those described in Sect. IV.A. A pattern like that shown in the lower fram of Fig. IV-14 was produced, and the presence of the lucite seemed to have no effect whatsoever. The reason is that the lateral displacement between interfering beams was so small that the lucite (and the other elements) did not have to be very flat for the optical paths to be equal. After this discovery, the lucite window was put back in place and all the plasma observations were made right through it.

The second point is that the total solid angle subtended in our plasma observations was extremely small. The apterture was 0.64 cm square at 61 cm from the plasma. This amounts to 1.1×10^{-4} sterradians, or less than one-thousandth of one percent of the whole solid angle. Thus, although our system was more efficient than a two-beam setup, it was still extremely weak in terms of the total light available. The design which we used could be extended to a system with a much larger aperture. With more expense, but with the same approach, one could obtain orders of magnitude more light. (Also, the plasma used here was not particularly luminous. An arc discharge, for example, would be much brighter than the beam-plasma system on which these measurements were made.)

Finally, it should be remembered that a multiple-beam system of the design used here requires that all the light transmitted by the collimator be accepted by the monochromator. This means that the entrance slit cannot be too small, and hence that the spectral resolution is restricted. (In principle, of course, the resolution could be improved by using a more dispersive grating.) In our case this was not important, since the observed spectral line was stronger than any nearby feature, but in planning such a system, one should make sure that the intended phase and frequency measurements are compatible, and that the coherence length of the accepted light will exceed any difference between the lengths of the paths of the A and B components of the light.

In the course of studying these systems, it has become increasingly apparent that this problem involves much more than just the spectroscopic analogue of a light scattering experiment. The spectroscopic problem is much broader to begin with, because the variety of sources is much greater. Scattering is due mainly to the plasma electrons, but the emission spectrum includes light from many different groups of plasma particles. But beyond this difference, the spectroscopic problem is more diverse because the number of possible optical systems is much greater. In principle, one could construct multiple-beam spectrometers which would observe many different components of a light source distribution. The selection of one $\underline{k}$ component of the sources within a local region is only one among many possibilities.

To be better able to discuss the problem in some generality,

two different mathematical descriptions of this type of optical system have been presented. Reviewing briefly, the first approach was based upon spatial Fourier transforms. In a preliminary analysis of scattering (in Sec. I.C) it was shown that the light of one wavelength emitted in a given direction could be expressed in terms of the positive frequency portion of one $\underline{k}$ component of the radiation from within the observed region. This description was then used (in Sect. II.A.3) to analyze a two-beam spectroscopic system. Assuming that the light from each point was coherent but that light from different points was incoherent, it was shown how the measured correlation between light in the two beams could be written as an integral over source points and wave numbers [Eq. (II.13)]

$$Y(t) = \int_{\left(\begin{array}{c}\text{common}\\ \text{source volume}\end{array}\right)} d^3\underline{r}' \int_0^\infty d|\underline{k}|\ |f(|\underline{k}|c)|^2\ \mathrm{Re}\ \Gamma_{BA}(0;|\underline{k}|,\underline{r}').$$

The mutual coherence, $\Gamma_{BA}(0;|\underline{k}|,\underline{r}')$ was then expressed in terms of the source distribution:

$$\Gamma_{BA}(0;|\underline{k}|,\underline{r}') \underset{t\to\infty}{\rightarrow} e^{i\phi} e^{-i\underline{k}_\Delta\cdot\underline{r}'} (\delta^2\Omega)^2\, \mathcal{S}(|\underline{k}|c;\underline{r}')$$

Here $\mathcal{S}(|\underline{k}|c;\underline{r}')$ the spectrum of the light emitted by sources near $\underline{r}'$ and $e^{-i\underline{k}_\Delta\cdot\underline{r}'}$ is a complex phase factor which appears because the lengths of the optical paths depend upon the source position. Because of this factor, the integral over $\underline{r}'$ is just a Fourier transform of $\mathcal{S}(|\underline{k}|c;\underline{r}')$. Thus the measured signal, Y(t), is found to be due to one Fourier component of the source distri-

bution.

This analysis was later extended to high-frequency effects (in Chapter V) and to higher order correlations (in Sect. II.C).

The second description presented (in Sect. II.B.2) was not limited to narrow pencils of rays. Instead, it was assumed that the accepted light (initially polarized) could be divided into two orthogonally polarized components which would be treated separately by the optical system. The system was assumed to be linear, so that each effect could be described by a transfer function [Eq. II.23)]

$$\xi_{A,B}(\underline{r}'',\omega;\underline{r}') = \phi_{A,B}(\underline{r}'',\underline{r}',\omega)s(\underline{r}'\omega).$$

Here $\underline{r}'$ denotes points within the source volume and $\underline{r}''$ denotes points across the entrance to a monochromator. Y(t), the output from the system was then shown to be given by an integral over $\underline{r}''$ of the coherence between the waves ξ_A and ξ_B. Assuming the light from different points to be completely incoherent, we obtained the result, [Eq. (II.24)]

$$Y(t) = \int d^3r' \int d\omega |f(\omega)|^2 T(\underline{r}',\omega) \mathcal{L}(\omega;\underline{r}'t)$$

where

$$T(\underline{r}',\omega) = \mathrm{Re}\ \frac{2}{\pi} \int_{\substack{\text{(spectrometer} \\ \text{entrance)}}} d^{2-"} \qquad \phi_A^*(\underline{r}'',\underline{r},'\omega)\phi_B(\underline{r}'',\underline{r}',\omega).$$

Thus the function $T(\underline{r}',\omega)$ describes the effect of the correlation measurement. Since many transfer functions $\phi_{A,B}(\underline{r}'',\underline{r}',\omega)$ can

obviously be produced, a great variety of functions $T(\underline{r}',\omega)$ could be gene.ated.

Several spectroscopic systems were analyzed (in Sect. II.B.3) by this technique and the conclusions were later confirmed by optical tests done in the course of the laboratory work (described in Sect. IV.A).

Finally, the effect of photon noise in a model system was analyzed in Chapter III. There it was concluded that if the observed component of the source density oscillated at a frequency ω_0, and if a spectrum analyzer were used to select a band around ω_0, the effect should be measurable if [inequality(III.8)],

$$P\sqrt{T\tau} > \sqrt{8}\,\frac{Q}{P}\,.$$

Here P and Q are the signal and background photocount rates, τ is the analyzer inverse bandwidth, and T is the time of observation. In our plasma observations, phase-sensitive detection was used to reduce the noise, so the above result does not apply directly to the data, but it does imply that the signal could not have been observed without the lock-in amplifier. When measurements of plasma luminosity (see Appendix D) are scaled to our experimental conditions, the total photon counting rate deduced is roughly 10^6/sec. The signal level was one-tenth of one percent of background (see Sect. IV.b) so $Q = 10^6$ and $P = 10^3$. The inverse bandwidth τ was roughly 10^{-5} sec and the observation time was about 10 sec. Since these numbers do not satisfy the above criterion, it appears that the effective aperture of the system

would have to be increased before an unmodulated signal of this level could be observed.

The theoretical analysis developed here is clearly more than was needed to explain our measurements, but the general formalism should be useful if this work is to be carried any further. If the project were to be continued, it would not be necessary to go on with all of the topics which we have mentioned. By discussing a number of related problems, it was hoped to provide here an overview of some of the broader implications of these correlation measurements. But now it should be possible to concentrate on one or a few aspects of the problem without losing sight of the whole picture. Such a greater specialization should permit reasonably rapid progress from this point.

B. Extensions of This Work

There is no shortage of directions in which this work could be continued. One obvious next step is to now use such a system for detailed observations of a plasma. Only a few simple features of the plasma used in this work were considered. We have concentrated on the optics of the spectroscopic system. The other half (or perhaps the other ninety percent) of the problem is to see what can be learned with such a system when it is used to observe a plasma. The availability of this new tool should permit a variety of interesting experiments.

The multiple-beam spectroscopic system described here could be improved in several ways. One could use a system with a larger aperture, or with better spectral resolution, or with better

electronics to reduce the noise.

As noted in the preceding section, the photon noise analysis presented in Chapter III has not been tested. In any further study of these spectrometers, the level of noise, including photon noise, should certainly be examined in more detail.

The range of possible multiple-beam systems--i.e., of possible transmission functions $T(\underline{r}',\omega)$ has only begun to be explored. One could construct and test a much greater variety of systems, and the analysis presented here could also be continued. Our calculations (in Sect. II.B.3) were limited by several simplifying assumptions, including a restriction to points near the focal plane of the system. The calculation of the functions ϕ_A, ϕ_B, and T for systems of this type could be done more completely, without such restrictions as were used here. This is a problem which seems well suited for the use of some numerical analysis, which we have not emplcyed at all.

Also, in the general analysis, it would be valuable to know what type of systems are possible in principle. Given any desired $T(\underline{r}',\omega)$, could one design a system which would produce it, or are there basic mathematical restrictions on the transfer functions $\phi_{A,B}$ and the transmission function T which can be generated?

One property of the light sources which we have not discussed at all is angular coherence. All of the analyses done here assumed an isotropic source. This is acceptable when the range of angles actually used is small, but if the observations were extended over larger angles, the effect of the source radiation pattern would

have to be included. This would give an added complication in the theory, but it would also provide a way in which radiation patterns could be measured. A measurement of single-source radiation patterns would be of interest, for example, in observing bremsstrahlung or cyclotron radiation where the patterns depend upon particle energies.

Another property which could also be observed is the lateral coherence of the source. We have assumed throughout that any difference between the lengths of the interfering beams was less than the coherence length of the accepted light. One might, however, want to deliberately introduce a path length difference in order to measure the coherence length, thereby obtaining information about the spectrum. This, in itself, is nothing new. The point is simply that when one had a multiple-beam system it would be relatively easy to add a path length difference. This should be particularly useful since a multiple-beam system would otherwise be limited in spectral resolution (see Sect. VI.A above). The addition of a coherence length measurement could be a convenient way to avoid exactly this restriction.

Another possible extension is suggested by the origins of the multiple-beam technique. The development began with an analogy with scattering, where it was argued that one could obtain similar information from measurements of correlations in the light emitted by an incoherent source. Having used both methods, one might wonder whether it would not be of interest to combine the two techniques, using a multiple-beam system to observe scattered light.

To understand such a measurement, one would have to do a separate analysis, since the assumption of an incoherent source is not valid in scattering, but a part of the answer can be seen already. In scattering, the amplitude of the light of wave vector $\underline{k}_s$ is due to one Fourier component, $n_e(\underline{k}_\Delta, \omega_\Delta)$, of the electron density. (See Sect. I.C.) Such fluctuations typically are due to plasma waves. Thus if a two-beam system were used to measure the coherence between two components of the scattered light, the result would be a measure of the correlation between two waves in the plasma, a result which would in turn give information about higher order correlations between particles. Clearly, both the optics and the photocount statistics should be analyzed with care before attempting any such experiment. Success would probably require a very strong incident light beam, but there may well be situations (for example, in laser-produced plasma experiments) where correlations in the scattered light could be observed.

In our plasma observations, the light used was a neutral helium emission line. This was convenient because, in this weakly ionized gas, the strongest neutral line was narrow enough to provice coherence and strong enough to give a high intensity. In more fully ionized gases, however, line radiation would be weaker or even lacking altogether. To observe such a plasma, one would have to make use of the continuum. With our system this would be more difficult, because the spectral resolution would become critical and because the amount of light available in any narrow band would be limited. Thus it would be of value to see whether the

optical band of the system could be increased. In our system a broad spectrum could not be used, even if all the paths through the apparatus were made exactly equal, because the paths of the A and B components within the plasma would still differ by more than the coherence length of the light. What this means is that light of different wavelengths would have different phase changes and hence would produce different interference patterns--i.e., that the observed source density component $T(\underline{r}',\omega)$ would in fact be a function of ω. If too broad a spectrum were used the effect would wash out. This suggests an answer: If $T(\underline{r}',\omega)$ could be made independent of ω, then it would be possible to use a broad optical band.

In our system the observed source density component had a wavelength $(\lambda f_1/d)$, where λ was the optical wavelength, f_1 was the focal length of the first lens, and d was the displacement of one of the interfering beams. If the displacement d were not a constant, but were instead proportional to wavelength, then the whole expression would be wavelength independent. This would happen if the calcite rhomb were replaced by an element which gave an offset proportional to the wavelength of the light. Interestingly enough, our system already contained a device which gives a wavelength dependent displacement--namely, the grating spectrometer. If the entrance and exit apertures were made large enough, one polarization component could be put through the spectrometer and then recombined with the other component to give a wavelength-independent interference effect. Such a change would greatly

extend the utility of multiple-beam systems.

The possibility of making the device broad band is also interesting conceptually. Up to this point, we have considered a correlation measurement as something additional to a frequency measurement. Physically, our interferometric apparatus was mounted in series with a standard spectroscopic instrument. But now it appears that the technique could be made broad band and could be used to extract useful information from light whose spectrum is flat and uninformative. This possibility clearly shows that what we are dealing with here is really a separate aspect of the light--one which may have little or nothing to do with the frequency spectrum.

C. Final Comments

In comparison with a conventional spectrometer, a multiple-beam system has the advantage of providing spatial resolution. The output from a multiple-beam system is a local measurement, not just an average along a line of sight. However, a multiple-beam spectroscopic system is certainly not the only optical device which has such an effect. An ordinary camera also provides depth perception. By noting which objects in a photograph are in focus and which are out of focus one can tell something about distances along the line of sight. In closing our discussion here it might be of interest to examine the relation between the depth of field provided by a camera and the spatial reolution of our spectroscopic system.

The depth of field of a camera is the range of distances over

which objects are in focus, i.e., the distances over which a small source is imaged to a small spot on the film. According to physical optics, an image is simply a diffraction maximum, a sharp peak in intensity produced by interference between the Huygens wavelets of the light behind the lens. Thus a statement about the sharpness of an image is really a statement about the amplitude and width of a diffraction maximum.

To see how this effect could be simplified, one might try to reduce the number of interfering waves by masking off portions of a camera lens. If the lens were masked down to one small aperture, the result would be a pinhole camera in which depth perception would be lost. There the light coming through the aperture would contain information about direction (the slope of the wavefronts), but information about source distance (the curvature of the wavefronts) would be lost. To avoid this one might try masking off most of the lens, but leaving several small apertures. Then the light coming through each hole would have a direction and the different directions combined would imply the distance of the source. The result on the film would no longer be a clear image, but would be a set of interference fringes. Most simply, one could leave just two apertures in the lens. Then if the source were away from the focus of the system the two beams of light would strike the film at different points, but if the source were in the focal plane, the two beams would intersect on the film to give a set of interference fringes, a result which thus would constitute the most rudimentary precursor of an image. But now we

are right back to the two-beam system with which this whole discussion started!

It is important to realize that in order to detect any property like the sharpness of an image, one has to observe at least two light intensities. With one light intensity value, one has no way of knowing whether the source is in focus or not, but two intensities give an additional piece of information--namely whether they are equal or different. From that one can say something about the sharpness of an interference pattern, a statement which is similar in kind to statements about the sharpness of images. In this sense, the "multiple-beams" of importance in our system were not so much the observed beams A and B, but rather the two measured light intensities, 1 and 2.

One can think of a scale, an ordering of optical techniques according to the number of intensities observed. At one end of the scale are spectroscopic methods in which, at least at each wavelength, only a single light intensity is observed. At the other end of the scale are photographic methods in which many light intensity values are recorded on the film. The subject of the present study lies between these two extremes. We have shown that by taking the single step from one to two intensities, one can obtain new types of information. Two is a convenient number of intensities to use, because as we have seen, it is then only necessary to consider the single difference signal Y(t). Two is a convenient number also because such a system can be simply constructed out of polarizing optical components.

It might be objected that the measurement could have been made with beam 1 alone, by observing features in the frequency spectrum of the output $I_1(t)$. But in that case, one would still be taking the difference between two light intensities, namely the intensities seen by the same phototube at different times.

Both types of intensity differencing are used by the human eye and by other natural optical systems. Sharp spots or edges in an image are immediately apparent to a person, and any motion of light patterns is noticed at once. On the other hand, the overall luminosity can change by orders of magnitude and the eye will adjust quite completely to keep the signal the same. Of course, one can make too much of any such comparison, but the results of the evolutionary process do seem to suggest that differences in light intensity are much more interesting than total light levels.

A comparison with a camera, and with the eye, is also useful because of what it shows about the concept of phase. One does not normally think of the human eye as making measurements of mutual coherence, but of course it does. An image is a diffraction maximum and any interference or diffraction effect depends upon the coherence of the light. Thus "phase" is a much broader category than one might have thought.

The term comes originally from the simple mathematical description of a nearly sinusoidal quantity:

$$a(t)\cdot\cos\left[\omega t + \phi(t)\right].$$

where

$$I_0 = \frac{c}{4\pi} 2|\underline{E}_1^{(+)}(\underline{r},t)|^2 = \frac{c}{4\pi} 2\left|\frac{\underline{E}_0}{2}\right|^2 = \frac{c}{8\pi}|\underline{E}_0|^2,$$

n_{e0} is the mean electron density,

$$\sigma_T = \left(\frac{e^2}{mc^2}\right)^2 \frac{|\underline{E}_0^{\perp}|^2}{|\underline{E}_0|^2}$$

is the differential Thompson scattering cross section, and

$$S(\underline{k}_\Delta,\omega_\Delta) = \frac{1}{2\pi n_{e0}}|n_e(\underline{k}_\Delta,\omega_\Delta;t)|^2$$

is called the "dynamic form factor."

In a scattering experiment, one records a spectrum of the light scattered into some direction $\hat{k}_s$. The relative variation in optical wavelength is usually negligible, so the scattering is all due to fluctuations of one wavelength, $2\pi|\underline{k}_\Delta|^{-1}$. This is customarily related to the plasma Debye length λ_D by a "scattering parameter",

$$\alpha \equiv \frac{1}{|\underline{k}_\Delta|\lambda_D}. \tag{I.13}$$

The spectrum of scattered light then provides a frequency spectrum of the $\underline{k}_\Delta$ component of n_e. By the Wiener-Khintchine theorem,[21]

$$\frac{1}{2\pi}|n_e(\underline{k}_\Delta,\omega)|^2 = \int d\tau e^{i\omega\tau}\,\overline{n_e^*(\underline{k}_\Delta,t)n_e(\underline{k}_\Delta,t+\tau)}, \tag{I.14}$$

this is equivalent to a measure of the time correlation function,

ACKNOWLEDGMENTS

It is a pleasure to acknowedge the help and encouragement which Prof. Wulf B. Kunkel and Dr. William S. Cooper have provided through the course of this work. Special thanks are due to Margaret R. Thomas for valuable advice on format and for her skill and patience in typing several versions of the manuscript. The author is indebted to Elliott B. Hewitt and to James E. Galvin for help with the apparatus, to Vincent J. Honey for aid with the electronics, and to the mechanical shop of Harlan A. Hughes for fabrication of several elements of the system. Thanks are also due Prof. Sumner P. Davis and Prof. Franklin A. Robben for several helpful discussions, and to Barton D. Billard for his assistance in conducting the experiments.

This work was performed under the auspices of the U. S. Atomic Energy Commission.

APPENDICES

A. Holography, Spectroscopy, and Scattering

In introducing the concept of multiple-beam spectroscopy, we first reviewed the standard technique of laser light scattering and then proposed its spectroscopic analogue, two-beam spectroscopy. What scattering and our two-beam system have in common is a dependence upon phase relations, a dependence which leads to results which are inexplicable in geometrical optics terms. Now there exists also another class of optical techniques of which the same thing is true. These are the various methods of holography,[24,25] which have been extensively investigated. There is an interesting connection between several of the different holographic methods and the scattering and spectroscopic systems which we have been considering. In the following appendix (which assumes some knowledge of holography) the relation between these different methods is examined briefly.

Holography can be explained in several ways. One explanation, which is particularly well suited for a comparison with scattering, is that presented by H. M. Smith in his book on holography.[24] Considering off-axis holograms (in which the reference wave and the object wave intersect the photographic plate at different angles) he describes the object wave as a superposition of plane wave components. When a hologram is made, each such component interferes with the light in the reference beam (which consists essentially of only one plane wave component) to produce a set of straight, evenly spaced interference fringes on the photographic plate. When

the resulting hologram is then reilluminated with the reference beam, each recorded set of fringes acts as a diffraction grating and diffracts the light into a reconstructed wave identical to that plane wave component which produced the fringes when the hologram was made. So the object wave is considered as a superposition of plane waves, or $\underline{k}$ components, and the hologram is then seen as a superposition of diffraction gratings, one for each $\underline{k}$ component of the object wave.

Seen from this point of view, the similarity to scattering is obvious. In a scattering experiment (see Sect. I.C) only a single $\underline{k}$ component of the scattered wave is observed. The intensity of this component gives the amplitude of one Fourier component of the distribution of scatterers.

In this respect, holography is more complete: The hologram is a record of both the amplitude and the phase of every $\underline{k}$ component of the object wave. It thus describes not one, but all of the Fourier components of the object under study. On the other hand, a scattering experiment gives information about the time or frequency dependence of the observed component of the scatterers. One can record a complete frequency spectrum of the scattered light which can be complicated and quite useful. In holography, one does not have such information, and the method will not work at all unless the object studied is precisely stationary or unless the light comes in a pulse so short that object motion is ignorable. Still, in spite of these differences, it is evident that the two methods share at least a substantial portion of a common theory.

This similarity suggests that two-beam spectroscopy, which was first introduced by a comparison with scattering, may also have a holographic analogue. This is, in fact, the case. The suggested similarity is to a very different type of holographic process, incoherent light holography, which can be used to make a hologram of a self luminous or incoherently illuminated object.

Incoherent light holography is usually discussed in terms of a somewhat different explanation of holography advanced by Rogers.[26] Rogers described a hologram not as a superposition of diffraction gratings, but as a superposition of Fresnel zone plates, one for each point of the object. When the hologram is illuminated, each zone plate acts as a lens to focus light towards the location of the corresponding object point. According to this explanation, when coherent light is used to make a hologram, light from each object point interferes with the light in the reference beam to make a fringe pattern which, when photographed, becomes the needed zone plate. But this technique is not the only way in which such patterns can be made. There are several other possibilities, some of which apply to incoherently illuminated objects.

One approach is just to use a mask cut as a zone plate. Placed between the object and the film, this mask will cast a set of shadows of the needed form--one for each object point. This technique was used by Mertz and Young[27] to make an x-ray star camera. In their device, each x-ray star produced a zone plate on a film. When the developed film was then illuminated with coherent visible light it acted as a hologram, focusing the light

into an image of the x-ray sky. Thus this technique resembled standard holographic methods in its reconstruction phase, but the formation of the "hologram" was due only to simple shadow casting. Mertz, however, then proposed[28] a purely optical arrangement which also used interference in the making of the hologram. His suggestion was to use a beam splitter to split light from an incoherently illuminated object into two components. These two waves could then be focused at two different points above a photographic plate. Assuming roughly equal lengths of path (which was assured in his suggested setup) the contributions to the two wavefronts from each single object point would interfere to make a set of fringes on the film. The system was arranged to make this pattern have the form of a Fresnel zone plate. For an incoherent source, the total illumination of the film would just be a sum of contributions from the separate source points, and the developed film would be a set of zone plates, just as in coherent light holography.

After Mertz' suggestion, several other people[29] proposed schemes for making holograms from light or other radiation from an incoherent source. The several methods outlined all involved the same idea of dividing the emitted radiation into two component waves, which can then be made to interfere, producing a pattern of fringes which, when photographed, becomes a hologram. Shortly thereafter, several authors[30] reported success in making holograms of some simple objects which were incoherently illuminated.

In practice, extension of the method to more complicated objects has proved difficult, because the superposition of many

intensity patterns tends to uniformly expose the film, giving a much lower contrast than is obtained in holograms made with coherent light. Several techniques have been employed to partially alleviate this problem,[31] but the art of making holograms with incoherent light apparently has not progressed beyond the stage of simple demonstrations. Nevertheless, experiments have clearly verified the theory of the technique: Light from an incoherent source contains sufficient information to construct a hologram.

It is evident from this work that incoherent light holography resembles multiple-beam spectroscopy in much the same way that coherent light holography resembles laser scattering. Like scattering, the spectroscopic system observes only one source density component, while a hologram, recording all the source components, permits reconstruction of a complete image of the object. But as in the coherent case, the holographic object must be strictly stationary, while the output of a spectroscopic system would follow the time variation of the observed component of the source.

Moreover, the need for contrast is also different in the two techniques. To obtain a photograph of a fringe pattern requires recording the intensity at many different points. A spectroscopic system, on the other hand, would measure only two intensities, I_1 and I_2, each containing roughly half of all the light accepted. Furthermore, a small difference between these two should also be more easily distinguished, since the two phototubes can be precisely balanced, as described in Sect. III.B. As explained there, a spectroscopic difference signal far below the level of the back-

ground light should still be readily observable--a situation very different from the need for contrast in a fringe pattern recorded for holography.

Nevertheless, the two techniques involve related theories, and thus the demonstrated possibility of making holograms with light from incoherent sources gives an added proof of the essential fact that measurements of phase made on such light can give a complete record of the spatial distribution of the source.

B. Some Mathematical Details

1. An Integration Needed in Section I.C

The expression,

$$\int d^3r\, e^{-i\underline{k}_s\cdot\underline{r}} \int d^3r'\, n_e\left(\underline{r}', t - \frac{|\underline{r} - \underline{r}'|}{c}\right)\left[\hat{n} \times (\hat{n} \times \underline{E}_0)\right] \cdot \frac{1}{|\underline{r} - \underline{r}'|} \cos\left[\underline{k}_i\cdot\underline{r}' - \omega_i\left(t - \frac{|\underline{r} - \underline{r}'|}{c}\right)\right], \qquad (B1)$$

occurs in Eq. (I.6). If one defines $\underline{r}'' \equiv \underline{r} - \underline{r}'$ (so $\hat{n} = \hat{r}''$), then (B1) becomes

$$\int d^3r'\, e^{-i\underline{k}_s\cdot\underline{r}'} \int d^3r''\, \frac{1}{|\underline{r}''|}\, n_e\left(\underline{r}', t - \frac{|\underline{r}''|}{c}\right)\left[\hat{r}'' \times (\hat{r}'' \times \underline{E}_0)\right] e^{-i\underline{k}_s\cdot\underline{r}''} \cdot \frac{1}{2}\left[e^{i\underline{k}_i\cdot\underline{r}'} e^{-i\omega_i(t-|\underline{r}''|/c)} + e^{-i\underline{k}_i\cdot\underline{r}'} e^{+i\omega_i(t-|\underline{r}''|/c)}\right]$$

$$= \frac{1}{2}\int d^3r''\, \frac{1}{|\underline{r}''|}\left[\hat{r}'' \times (\hat{r}'' \times \underline{E}_0)\right] e^{-i\underline{k}_s\cdot\underline{r}''} \cdot \left[e^{-i\omega_i(t-|\underline{r}''|/c)}\, n_e\left(\underline{k}_s - \underline{k}_i,\ t - \frac{|\underline{r}''|}{c}\right) + e^{+i\omega_i(t-|\underline{r}''|/c}\, n_e\left(\underline{k}_s + \underline{k}_i,\ t - \frac{|\underline{r}''|}{c}\right)\right]. \qquad (B2)$$

Here

$$n_e(\underline{k}, t) \equiv \int d^3r\, e^{-i\underline{k}\cdot\underline{r}}\, n_e(\underline{r}, t)$$

is the spatial Fourier transform of n_e. It is convenient to perform the $\underline{r}''$ integration in polar coordinates. Replacing $\int d^3r''$

by $\int d|\underline{r}''|\ |\underline{r}''|^2 d^2\hat{r}''$ gives

$$\frac{1}{2}\int_0^\infty d|\underline{r}''|\ |\underline{r}''| \left[e^{-i\omega_1(t-|\underline{r}''|/c)} n_e\left(\underline{k}_s - \underline{k}_1, t - \frac{|\underline{r}''|}{c} \right) \right.$$

$$\left. + e^{+i\omega_1(t-|\underline{r}''|/c)} n_e\left(\underline{k}_s + \underline{k}_1, t - \frac{|\underline{r}''|}{c} \right) \right]$$

$$\cdot \int d^2\hat{r}''\, e^{-i\underline{k}_s\cdot\underline{r}''} \left[\underline{r}'' \times (\underline{r}'' \times \underline{E}_0) \right] . \qquad (B3)$$

The integration over directions may be done separately. In a spherical coordinate system, $\underline{r}'' = (\rho,\theta,\phi)$, defined so that $\underline{k}_s = (|\underline{k}_s|,0,0)$ and $\underline{E}_0 = (|\underline{E}_0|,\eta,0)$

$$\underline{k}_s\cdot\underline{r}'' = |\underline{k}_s|\ |\underline{r}''|\ \cos\theta$$

and

$$\hat{r}''\cdot\underline{E}_0 = |\underline{E}_0|\ (\cos\theta\cos\eta + \sin\theta\sin\eta\cos\phi).$$

Using Cartesian components (unit vectors $\hat{e}_x$, $\hat{e}_y$, $\hat{e}_z$) to describe the vector integrand, (B3) may be expressed,

$$\int d^2\hat{r}''\, e^{-i\underline{k}_s\cdot\underline{r}''} \left[\hat{r}'' \times (\hat{r}'' \times \underline{E}_0) \right] = d^2\hat{r}''\, e^{-i\underline{k}_s\cdot\underline{r}''} \left[\hat{r}''(\hat{r}''\cdot\underline{E}_0) - \underline{E}_0 \right]$$

$$= \int\int d\theta\, d\phi\, \sin\theta\, e^{-i|\underline{k}_s||\underline{r}''|\cos\theta} \left[-\underline{E}_0 + |\underline{E}_0|\cos\theta\cos\eta \right.$$

$$\cdot (\hat{e}_z\cos\theta + \hat{e}_x\sin\theta\cos\phi + \hat{e}_y\sin\theta\sin\phi)$$

$$\left. + |\underline{E}_0|\sin\theta\sin\eta\cos\phi\,(\hat{e}_z\cos\theta + \hat{e}_x\sin\theta\cos\phi + \hat{e}_y\sin\theta\sin\phi) \right]$$

$$= \int_0^\pi d\theta\, \sin\theta\, e^{-i|\underline{k}_s||\underline{r}''|\cos\theta} \left[-2\pi\underline{E}_0 + 2\pi|\underline{E}_0| \right.$$

$$\cdot \left(\hat{e}_z \cos^2\theta \cos\eta + \hat{e}_x \frac{1}{2} \sin^2\theta \sin\eta\right) . \qquad (B4)$$

If $X \equiv - |\underline{k}_s|\,|\underline{r}''|\cos\theta = -\underline{r}''\cdot\underline{k}_s$,

$$\underline{E}_{0x} \equiv e_x|\underline{E}_0| \sin\eta$$
$$\underline{E}_{0z} \equiv e_z|\underline{E}_0| \cos\eta$$

then (B4) becomes

$$\int_{-|\underline{k}_s||\underline{r}''|}^{|\underline{k}_s||\underline{r}''|} dX \frac{1}{|\underline{k}_s||\underline{r}''|} e^{iX}\left\{-2\pi\underline{E}_0 + 2\pi\underline{E}_{0z}\frac{X^2}{(|\underline{k}_s||\underline{r}''|)^2} + \pi\underline{E}_{0x}\left[1 - \frac{X^2}{(|\underline{k}_s||\underline{r}''|)^2}\right]\right\}$$

$$= \int_{-|\underline{k}_s||\underline{r}''|}^{|\underline{k}_s||\underline{r}''|} dX \frac{1}{|\underline{k}_s||\underline{r}''|} e^{iX}\left[-2\pi\underline{E}_0 + \pi\underline{E}_{0x} + \frac{X^2}{(|\underline{k}_s||\underline{r}''|)^2}(2\pi\underline{E}_{0z} - \pi\underline{E}_{0x})\right]$$

$$= \left[\frac{1}{i|\underline{k}_s||\underline{r}''|} e^{iX}(-2\pi\underline{E}_0 + \pi\underline{E}_{0x}) + \frac{1}{(|\underline{k}_s||\underline{r}''|)^3} \cdot (2\pi\underline{E}_{0z} - \pi\underline{E}_{0x}) e^{iX}\left(\frac{X^2}{i} + 2X - \frac{2}{i}\right)\right]_{-|\underline{k}_s||\underline{r}''|}^{+|\underline{k}_s||\underline{r}''|}$$

$$= \left[\frac{1}{i|\underline{k}_s||\underline{r}''|} e^{iX}(-2\pi\underline{E}_{0x}) + \frac{1}{(|\underline{k}_s||\underline{r}''|)^3}(2\pi\underline{E}_{0z} - \pi\underline{E}_{0x}) \cdot e^{iX}\left(2X - \frac{2}{i}\right)\right]_{-|\underline{k}_s||\underline{r}''|}^{+|\underline{k}_s||\underline{r}''|} . \qquad (B5)$$

This expression is to be integrated over $|\underline{r}''|$. For this one may neglect all but the lowest order term in $1/|\underline{r}''|$. The higher order terms would make little contribution to the integral and would in any case vanish in a long time limit take later [see note below Eq. (B7)]. This leaves, from (B5)

$$-2\pi\underline{E}_{0x}\frac{1}{i|\underline{k}_s||\underline{r}''|}\left[e^{i|\underline{k}_s||\underline{r}''|} - e^{-i|\underline{k}_s||\underline{r}''|}\right] \qquad (B6)$$

$\underline{E}_{0x}$ is simply the component of $\underline{E}_0$ normal to $\underline{k}_s$. It is convenient to write this in the invariant form

$$\underline{E}_{0x} = \underline{E}_0{}^{\perp} \equiv (I - \hat{k}_s\hat{k}_s)\underline{E}_0.$$

Using the result (B6) for the integral over direction Ω leaves, for the entire expression (B3)

$$\frac{-\pi\underline{E}_0{}^{\perp}}{i|\underline{k}_s|}\int_0^{\infty} i|\underline{r}''|\left(e^{i|\underline{k}_s||\underline{r}''|} - e^{-i|\underline{k}_s||\underline{r}''|}\right)$$
$$\cdot\left[e^{-i\omega_i(t-|\underline{r}''|/c)}\cdot n_e\left(\underline{k}_s - \underline{k}_i,\ t - \frac{|\underline{r}''|}{c}\right)\right.$$
$$\left. + e^{+i\omega_i(t-|\underline{r}''|/c)}\cdot n_e\left(\underline{k}_s + \underline{k}_i,\ t - \frac{|\underline{r}''|}{c}\right)\right]$$

If $\tau \equiv t - \dfrac{|\underline{r}''|}{c}$

$\omega_s \equiv |\underline{k}_s|c$

then this becomes

$$\frac{-\pi \underline{E}_0^{\perp}}{i|\underline{k}_s|} \int_{-\infty}^{t} c d\tau \left[e^{i\omega_s(t-\tau)} - e^{-i\omega_s(t-\tau)} \right]$$

$$\cdot \left[e^{-i\omega t} n_e(\underline{k}_s - \underline{k}_1, \tau) + e^{+i\omega\tau} n_e(\underline{k}_s + \underline{k}_1, \tau) \right] . \qquad (B7)$$

For sufficiently large times, the expression

$$\int_{-\infty}^{t} d\tau \, e^{i\omega\tau} n_e(\underline{k}, \tau)$$

is equivalent to the usual Fourier transform if n_e vanishes for large τ. Furthermore, the terms in (B5) which were neglected would also vanish in this long time limit, because, for any given τ,

$$\frac{1}{|\underline{r}''|} = \frac{1}{c(t - \tau)} \to 0 \text{ as } t \to \infty .$$

Hence as $t \to \infty$, (B7) approaches

$$\frac{-\pi \underline{E}_0^{\perp} c}{i|\underline{k}_s|} \left\{ e^{i\omega_s t} \left[n_e(\underline{k}_s - \underline{k}_1, -\omega_s - \omega_1) + n_e(\underline{k}_s + \underline{k}_1, -\omega_s + \omega_1) \right] \right.$$

$$\left. - e^{-i\omega_s t} \left[n_e(\underline{k}_s - \underline{k}_1, \omega_s - \omega_1) + n_e(\underline{k}_s + \underline{k}_1, \omega_s + \omega_1) \right] \right\} \qquad (B8)$$

This is the desired integration of (B1).

2. An Integration Needed in Section II.A.3

A similar, but less complicated expression

$$\int d^3\rho_1 \int d^3\rho_2 \, \frac{1}{|\underline{\rho}_1|} \frac{1}{|\underline{\rho}_2|} e^{i\underline{k}_A \cdot \underline{\rho}_1} e^{-i\underline{k}_B \cdot \underline{\rho}_2}$$

$$\cdot s^{(+)*}(\underline{r}', t - |\underline{\rho}_1|/c) s^{(+)}(\underline{r}', t - |\underline{\rho}_2|/c) \qquad (B9)$$

appears in Eq. (II.14). It is again convenient to use polar coordinates. Replacing

$$\int d^3\rho \qquad \text{by} \qquad \int d|\underline{\rho}|\,|\underline{\rho}|^2 \int d^2\hat{\rho}$$

gives

$$\int d|\underline{\rho}_1| \int d|\underline{\rho}_2|\,|\underline{\rho}_1|\,|\underline{\rho}_2|\; s^{(+)*}\left(\underline{r}',\ t - \frac{|\underline{\rho}_1|}{c}\right) s^{(+)}\left(\underline{r}',\ t - \frac{|\underline{\rho}_2|}{c}\right)$$

$$\int d^2\hat{\rho}_1\, e^{+i\underline{k}_A\cdot\underline{\rho}_1} \int d^2\hat{\rho}_2\, e^{-i\underline{k}_B\cdot\underline{\rho}_2}. \qquad \text{(B10)}$$

The integration over directions can be done in spherical coordinates

$$\int d^2\rho_1\, e^{-i\underline{k}_A\cdot\underline{\rho}_1} = \int d\varphi \int \sin\theta\, d\theta\, e^{i|\underline{k}_A||\underline{\rho}_1|\cos\theta}$$

$$= \frac{2\pi}{|\underline{k}_A||\underline{\rho}_1|} \int_{-|\underline{k}_A||\underline{\rho}_1|}^{|\underline{k}_A||\underline{\rho}_1|} dX\, e^{-iX}$$

$$= \frac{2\pi}{i|\underline{k}_A||\underline{\rho}_1|}\left(e^{i|\underline{k}_A||\underline{\rho}_1|} - e^{-i|\underline{k}_A||\underline{\rho}_1|}\right). \qquad \text{(B11)}$$

The integration over $\hat{\rho}_2$ gives the same function of $|\underline{k}_B|$, $|\underline{\rho}_2|$ because this expression is invariant under complex conjugation. This leaves for (B10)

$$\frac{-4\pi^2}{|\underline{k}_A||\underline{k}_B|} \int_0^\infty d|\underline{\rho}_1| \left(e^{i|\underline{k}_A||\underline{\rho}_1|} - e^{-i|\underline{k}_A||\underline{\rho}_1|}\right) s^{(+)*}\left(\underline{r}',\ t - \frac{|\underline{\rho}_1|}{c}\right)$$

$$\cdot \int_0^\infty d|\underline{\rho}_2| \left(e^{i|\underline{k}_B||\underline{\rho}_2|} - e^{-i|\underline{k}_B||\underline{\rho}_2|}\right) s^{(+)}\left(\underline{r}',\ t - \frac{|\underline{\rho}_2|}{c}\right) =$$

$$= \frac{4\pi^2}{|\underline{k}|^2}\left| \int_0^\infty d|\underline{\rho}_1| \left(e^{i|\underline{k}||\underline{\rho}_1|} - e^{-i|\underline{k}||\underline{\rho}_1|} \right) \right.$$

$$\left. \cdot\, s^{(+)}\left(\underline{r}', t - \frac{|\underline{\rho}_1|}{c} \right) \right|^2 \qquad \text{(B12)}$$

since $|\underline{k}_A| = |\underline{k}_B| = |\underline{k}|$ (see Sect. II.A.3).

If $\tau \equiv t - |\underline{\rho}_1|/c$, then the $\underline{\rho}_1$ integration becomes

$$\int_{-\infty}^{t} c\,d\tau \left[e^{i|\underline{k}|c(t-\tau)} - e^{-i|\underline{k}|c(t-\tau)} \right] s^{(+)}(\underline{r}'\tau)$$

$$\xrightarrow{t \to \infty} c\left[e^{i|\underline{k}|ct} s^{(+)}(\underline{r}', -|\underline{k}|c - e^{-i|\underline{k}|ct} s^{(+)}(\underline{r}', |\underline{k}|c) \right],$$

where $s^{(+)}(\underline{r}', |\underline{k}|c)$ is the temporal Fourier transform of $s^{(+)}(\underline{r}', \tau)$. Since $(-|\underline{k}|c)$ is negative and $s^{(+)}(\underline{r}', -)$ by definition contains only positive frequency components, the first term in the above expression vanishes and the second term describes the integration in Eq. (B12). Hence, as $t \to \infty$, (B12) approaches

$$\frac{4\pi^2 c^2}{|\underline{k}|^2} \left| e^{-i|\underline{k}|ct} s^{(+)}(\underline{r}', |\underline{k}|c) \right|^2. \qquad \text{(B13)}$$

This is the desired integration of (B9)

C. The Design of a Multiple-Beam Spectroscopic Apparatus

1. Previous Conclusions

In Sect. II.A.1, the effect of an elementary two-beam spectrometer was described in fairly simple terms. In this appendix, that first discussion is extended to include analyses of several other spectroscopic systems.

Reviewing briefly, the two-beam system, which is shown in Fig. II-2, was designed to compare light emitted in different directions from the same volume of plasma. As explained in II.A.1, the screen at the end of the system would receive light from two types of (point) sources:

(a) Sources observed through one beam (A or B, but not both).

(b) Sources within the "common source volume" which are observed through both beams.

An (isotropic) source of the first type would produce on the screen a fairly broad smooth intensity distribution--one whose width would be determined by the diffraction of a single beam. The second type of source would produce a two-beam interference pattern on the screen.

The optical system was designed to use this difference to observe selectively a localized region within a distributed source. But there is a further complication: All the sources within the common source volume might not produce coincident interference patterns on the screen. The positions of the intensity maxima would depend upon the precise location of the source.

Some sources, however, would produce identical patterns. As

explained in Sect. II.A.1, a set of sources which lie in planes which are normal to $\underline{k}_\Delta \equiv \underline{k}_B - \underline{k}_A$ and spaced $2\pi/|\underline{k}_\Delta|$ apart (within the common source volume) would all produce the same interference pattern on the screen. ($\underline{k}_A$ and $\underline{k}_B$ are the wave vectors of the light in beams A and B.) Light from sources located halfway between these "source planes" would produce the opposite or complementary set of fringes on the screen. Hence any overall fringe pattern must represent not the total number of common sources, but rather the difference in numbers of two such groups of sources. The system observes not the total density, but rather the amplitude of one component of the fluctuations in the density of common sources.

It should be emphasized that these results do not involve any interference between light from different sources, as occurs, for example, in a scattering experiment. Here the light from the different source points is incoherent and the observed light intensity is just the sum of the intensities due to the various point sources--some of which produce sets of interference fringes.

Thus the apparatus must in some way separate a pair of complementary interference patterns which we have called "beams 1 and 2". The quantity of interest is the difference in intensity between beams 1 and 2. This difference is proportional to the amplitude of the $\underline{k}_\Delta$ spatial Fourier component of the distribution of light sources within the region observed through both beams A and B.

To use these results one must actually construct such a device. In planning for this, one is faced with several further questions: What is a practical way to separate "beams 1 and 2"? Are there

other equivalent but more convenient optical systems? Is it possible to make better use of the available light? And, finally, is this observation the only possibility, or is this system one of a larger class of devices with which one could make a variety of optical measurements?

We can note at once that beams A and B need not be restricted to narrow pencils of rays. To obtain more light, the apertures which define the beams may be enlarged to parallel slits. This increases the efficiency, but, as we shall see, the resulting system may be further improved.

2. A Modified Two-Beam System

To separate two complementary interference patterns, one might simply replace the screen with an array of light pipes and direct the light from the locations of the maxima of different patterns into different photomultiplier tubes. But for this to be feasible, the interference fringes would have to be rather widely spaced--which would probably require additional lenses to magnify the pattern. The resulting system would be fairly complicated. Furthermore, such an arrangement would only approximate the desired system because interference produces a sinusoidal intensity distribution, while a set of light pipes would separate two "square wave" patterns. Indeed, some light would go into each phototube, no matter what type of interference occurred.

To see what else one might do, consider again our reason for making these interference patterns. The object is to compare the phase of the light in beam A with that of the light in beam B.

The "interference patterns 1 and 2" are simply the result of two possible phase differences between the light in beams A and B. This technique, of course, could be used with any type of wave, but in an optical system one can also use the fact that light, a transverse wave, is characterized by its polarization, as well as by its intensity, frequency, and phase. This additional property provides an alternate method of making phase measurements, as is explained in Sect. II.B.1, and, more completely, in Ref. 39.

Consider the apparatus shown in Fig. C-1. Here we have again beams A and B. But now we wish to consider their polarization. A first polarizer transmits only one component of the light--the same for each beam. The two beams are then linearly polarized in orthogonal directions. They are then combined. If the two were in phase, their superposition would again be linearly polarized--in the intermediate direction "1" shown in Fig. C-1. If the two components were 180° out of phase, their superposition would also be linearly polarized, but in the orthogonal direction "2". Conveniently enough, these two intermediate polarizations are just beams 1 and 2, which we wish to separate.

So, to summarize, the conclusion is that if the light came from a source lying in one of a set of planes normal to $\underline{k}_{\Delta}$ and spaced $2\pi/|\underline{k}_{\Delta}|$ apart, within the common source volume, then the contributions to beams A and B would be separated in phase by an integral number of cycles and the light would (all) to into beam 1. Other sources within the c.s.v. would contribute to beam 2--or both 1 and 2. And sources outside the c.s.v. could at most

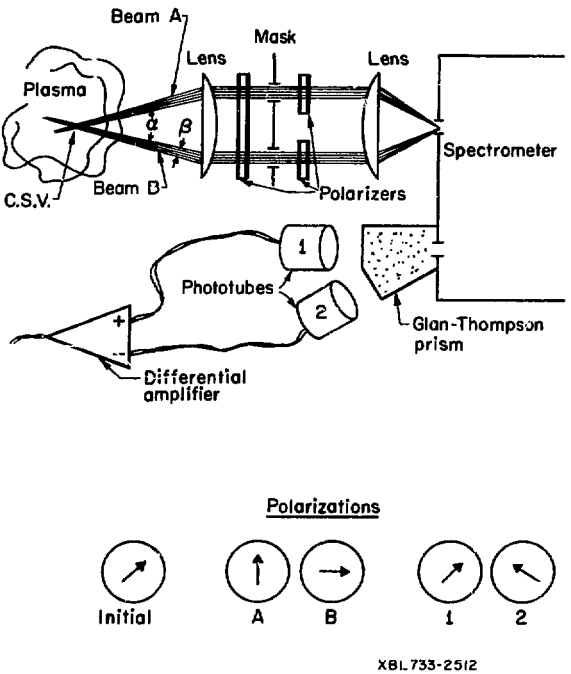

Fig. C-1. A system which uses polarization to measure relative phase.

contribute light only to beam A or only to beam B. This light would be divided equally between beams 1 and 2 and would contribute nothing to their intensity difference.

In the arrangement of Fig. C-1, the relative phase of beams A and B, and hence the resulting polarization, also depends upon the position of the point of observation (where the entrance slit to a spectrometer is indicated). Indeed, if there were coherence between A and B, then there would still be an interference pattern--and a set of fringes on the screen. But instead of a sinusoidal variation in intensity, there would be a variation of polarization. If a polarizer oriented to select beam 1 were placed before the screen, a set of fringes would appear, and if the polarizer were rotated to select beam 2, the complementary set of fringes would appear. The relative phase of beams A and B is shown not by which intensity pattern appears, but by which pattern corresponds to which polarization, making it possible to, in effect, observe both "patterns" while looking at only one fringe. The presence of spatial variation in the pattern also limits the size of the slit in the screen: Its width must be less than the width of one fringe.

Since, in a polarizing system, only a single slit is needed to observe the interference, the same slit can also serve as the entrance to a spectrometer, as shown in Fig. C-1. In such an arrangement, the frequency resolution would occur after the interferometry, and the filter shown in Fig. II-2 would not be needed.

This system, which uses polarization, has several convenient features. The separation into beams 1 and 2 is just what is

needed, and the possibility of simply mounting the interferometer before the entrance of an existing spectrometer is a big advantage. This not only simplifies construction of the system, it also minimizes the number of interferometer-quality optical components needed, because precise equality of path length is not important beyond the entrance to the spectrometer. Light of unwanted phase is blocked by the screen and the following part of the system simply measures the spectra of the accepted 1 and 2 components. As long as these remain distinct, the signal will be preserved.

Unfortunately, the new arrangement has a serious failing. It makes extremely poor use of the available light. The system is inefficient in two respects. First of all, because the angle β is small, beams A and B, as seen from the source, subtend only a small solid angle. Secondly, because less than one fringe of the pattern on the screen is used, most of the light which did go into beams A and B would be lost.

The second limitation is clearly removable in principle. One could, for example, construct a system which admitted light through several properly spaced slits. But there is a more convenient solution. In the arrangement of Fig. II-2, the interference fringes on the screen were needed for phase measurements. But the patterns on the screen in Fig. C-1 are simply an inconvenience, because the phase measurements are now made by comparing polarizations.

The small slit at the entrance to the spectrometer may be thought of as a device which combines beams A and B. It is

necessary, as noted above, that this slit be smaller than one fringe of the interference pattern made by beams A and B. But this is equivalent to a requirement that the maximum of a single slit diffraction pattern of the slit itself include beams A and B. In other words, within the spectrometer, beams A and B are superimposed. To permit use of a larger slit, another method of combining beams A and B is needed.

3. The Use of Birefringence

In constructing an optical system to define and focus beams of polarized light, it is often convenient to use optical elements made of birefringent materials. We have not yet discussed this possibility, but one can see at once a simple way to produce with such an element a pattern of varying polarization.

The optical system shown in Fig. C-2 includes a calcite rhomb, with the optic axis in the plane of the drawing, as indicated. If a beam of light is incident on the face of the rhomb, its path through the calcite depends upon its polarization. That component of the light which is linearly polarized with the electric field vector normal to the optic axis is propagated through the calcite as an "ordinary ray." At normal incidence, its direction is unchanged. The other linearly polarized component, however, becomes an "extraordinary ray" and a normally incident beam is deflected by $\sim 6.26^{\circ}$, a change in direction which is reversed at the opposite face of the rhomb. The two polarizations thus emerge as separate beams of light. The various rays are again parallel, but one component of the light has been laterally displaced by a

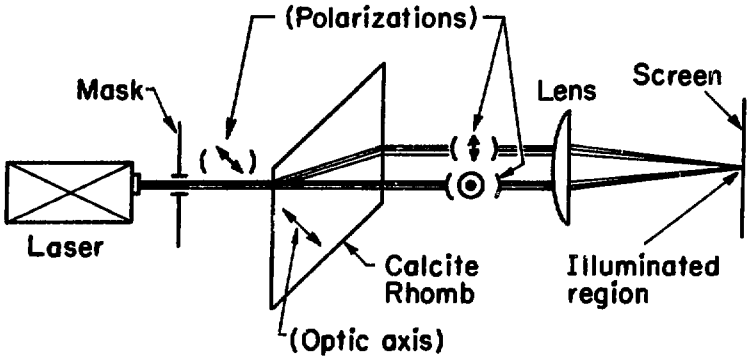

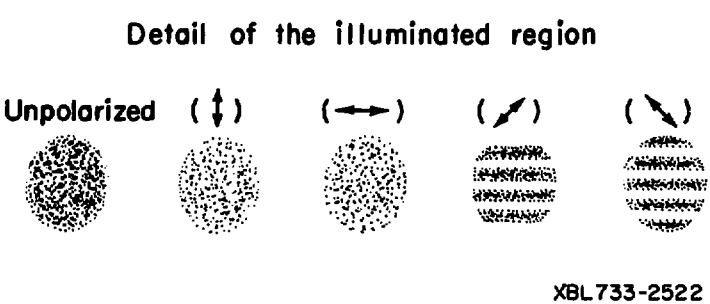

XBL733-2522

Fig. C-2. A demonstration: interference fringes produced with a calcite rhomb.

distance approximately 0.11 times the length of the rhomb.

On the arrangement of Fig. C-2, a small gas laser is used to produce the incident beam, which is linearly polarized in such a direction that it is divided by the calcite into two beams of equal intensity. The light is then focused onto a screen. (More simply, one could place the screen so far away that the divergence of the beams caused them to overlap.) The total illumination of the focal spot is then rather uniform, but the pattern of polarization contains more detail. If a linear polarizer aligned at 45° to the polarization of either beam--that is, parallel to the polarization of the original laser beam--is placed before the screen, a set of interference fringes appears. And if one selects the other, orthogonal, polarization, the complementary set of fringes appears on the screen.

This result is like that which was expected from the optical system of Fig. C-1. So, with the calcite rhomb, one can construct a simple demonstration of the "polarization fringes" which were described earlier. Moreover, this suggests that such an optical component could be useful in the type of spectroscopic system which we wish to design.

To explore this possibility, we need to consider more systematically our objective. If only two-beam optical arrangements are considered, then there are essentially, four requirements:

1. The apparatus must define a "common source volume"--the intersection of two beams.

2. It must define two directions beams A and B--from which

such sources are observed.

3. It must include some spectroscopic element--a filter or a spectrometer--to select a limited portion of the optical spectrum.

4. Finally, the apparatus must measure the correlation, or mutual coherence, of this spectral component of the light in the two beams.

Note that, in any one particular system, the size of the common source volume may be varied inversely with the range of directions included in the two beams. If beams A and B are separately focused at their intersection (Fig. C-3a), then the c.s.v. is relatively small, while the range of $\hat{k}_A$ and $\hat{k}_B$--and hence of $\underline{k}_\Delta$--is large. This spread in $\underline{k}_\Delta$ may be thought of as due to the small number of "source planes" in the c.s.v. If, on the other hand, the beams are not focused at their intersection (Fig. C-3b), then the resolution in space is less precise but the resolution in $\underline{k}_A$, $\underline{k}_B$, and $\underline{k}_\Delta$ is more precise. We shall consider only systems of the type of Fig. C-3a, but one could modify any arrangement to produce Fig. C-3b. Of course, good resolution in $\underline{k}_\Delta$ also requires good resolution in $|\underline{k}_A|$ and $|\underline{k}_B|$, that is, a spectrometer or a filter with sufficiently narrow pass band.

If the angle between them is small, it is convenient to observe beams A and B through different sections of a single lens, as shown in Figs. II-2 and C-1. If the remainder of the system accepts only light nearly parallel to the axis, then the observed beams will intersect in a common source volume around the focal point of the lens. For the interference measurement, the two beams

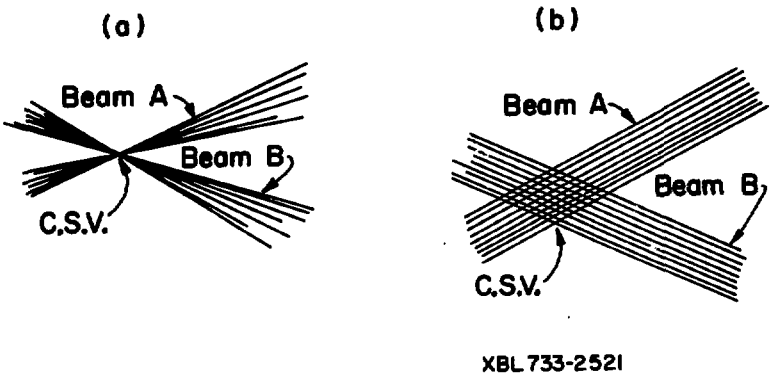

Fig. C-3. Forms of the observation region. (a) Good spatial resolution. (b) Good wavelength resolution.

must be recombined beyond the lens. So the rest of the optical system must define and then combine two parallel, adjacent beams of light.

The calcite rhomb in Fig. C-2 divides one beam of light into two separate parallel beams. If, however, the mask which defines the (single) beam is placed after the calcite element, then two, initially separate, incident beams are defined and superimposed. Conveniently enough, this is just what is needed.

The resulting system is shown in Fig. C-4. There a lens plus a rhomb not only define and combine beams A and B, but also determine their polarizations--something which required separate polarizers in the setup which we first discussed (Fig. C-1). The first polarizer, which insures that we start with a single component of the light is, however, still required.

This gain in simplicity is not, however, the principal difference between the two designs (Figs. C-1 and C-4). More important is the change in the distribution of light over the illuminated portion of the screen (before the spectrometer). In the new arrangement, the two-beam interference fringes are absent. Beams A and B are parallel at the screen and their phase difference is constant within the limitations of the collimation of each single beam.

An isotropic point source within the c.s.v. will here produce on the screen a single slit diffraction pattern due to either beam alone. (Since this is ahead of the spectrometer, consider also that the source is monochromatic.) We can distinguish these

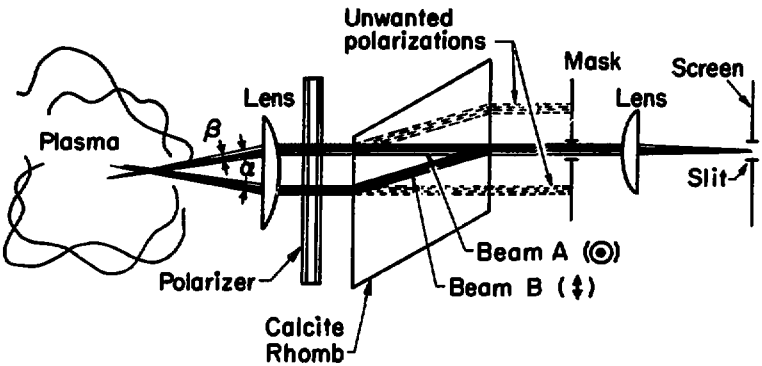

Fig. C-4. A two-beam spectroscopic system in which a calcite rhomb is used to combine the beams. The slit in the screen at the right is the entrance to a spectrometer. Beams 1 and 2 are separated at the spectrometer exit.

with a polarizer but, since the two components come from the same slit, the two patterns will be identical, provided that the two distributions of phase across the first slit are identical. (We assume, of course, that any polarization dependence of the effect of the slit is negligible.) If the two diffraction patterns are identical, than the variations in phase across the screen will also be the same for each component. Therefore the phase difference between the two--and hence the polarization of their superposition--will be constant across the screen. The entrance slit to the spectrometer may be made large enough to admit a substantial part of the light. The result is a more efficient system.

However, the second slit should probably still be narrower than the central maximum of a single-slit diffraction pattern of the first slit.[56] This would insure that the phases of the A and B components could not vary much across the second slit. Then their relative phase, and hence the polarization of their superposition would also be approximately uniform, and each point source within the plasma would contribute with a single polarization to the output light.

This is not to say that a larger second slit could not possibly be used. It could, but that would allow the polarization of the light from some point sources to vary across the width of the slit. The overall effect, given by an average over the slit area, could then include some cancellation between different contributions. Now the illumination of the second slit is just a sum of contributions (Huygens components) from the light which goes

through different portions of the first slit. If a source were near the edge of (or, for that matter, outside of) the common source volume, then the distributions in phase across the first slit, and hence the distributions in intensity and phase across the screen would be different for the light observed through the beams A and B,[57] and the polarizaton of the total light would vary with position. If the second slit were wider than the suggested limit, there could be some cancellation of effect. But this would not happen with all sources. A source near the center of the c.s.v., for example would produce uniform distributions of A and B across the first slit, making two identical patterns on the screen. The polarization of light from this source would not change, even over distances greater than the suggested slit width.

Thus, if a larger second slit were used, our simple statement that each common source contributes with one polarization to the output light would not be strictly valid. Some sources would, but the effect of others would be reduced or lost in averaging across the slit. Only some restricted portion of the c.s.v. would still make a definite contribution to the output signal. Other common sources would contribute only background light, as do the sources seen through just one beam.

Finally, the width of the second slit also limits the spatial resolution, since the c.s.v. is just an image of the second slit. Enlarging the slit would enlarge the c.s.v. but, on the other hand, reducing the slit to less than the limiting width would not further improv the resolution, since the image would then be

diffraction limited.

Even with this limitation on the second slit, the system shown in Fig. C-4 would still accept most of the light emitted in directions k_A and k_B by common sources. It thus overcomes the second of the two limitations--noted at the end of Sect. 2.3--of the apparatus shown in Fig. C-1. If we wish to study only light emitted into two narrow beams, the apparatus of Fig. C-4 satisfies our requirements.

4. Multiple-Beam Systems

The more efficient two-beam spectrometer which we have now designed has both the advantages and the limitations of the original concept. Any device which accepts only two narrow beams can use only a small part of the available light. To further improve the design we must consider a more general class of systems. On doing so, we can consider observation of various other aspects of the source distribution as well.

A simple two-beam apparatus responds, as we have seen, to a narrow portion of the spectrum of the spatial distribution of sources within a localized "common source volume." One has at once two types of spatial resolution: A coarse definition of an observation region and a fine definition of a wavelength--$2\pi|\underline{k}_\Delta|^{-1}$. One can make a local measurement, but only of fluctuations. Such an optical system is hardly the only possibility. We have yet to explore the range of possible observations. Could one, for example, select all the light emitted from within some localized volume and still reject that emitted from other regions?

Before considering other arrangements, it is convenient to summarize analytically the properties of the system already designed (Fig. C-5). This consists of a source region, a polarizer, a first optical system (I), a slit, and a second optical system (II). System II, beyond the entrance slit to the spectrometer, selects a narrow portion of the optical spectrum, separates two polarization components--1 and 2--and measures the difference between these two total intensities.

The preceding portion of the apparatus, System I, defines two beams, A and B, distinguished by their polarizations. A point source within the source region thus produces two illuminations (including zero amplitude as a possibility) of the entrance slit to the spectrometer. These vary in amplitude and phase along the slit. The effect of System I may thus be represented by two complex transfer functions, ϕ_A and ϕ_B (see Sect. II.B.2). If a point source of light of frequency ω is then represented by a (complex) source strength $p(\omega;t)$, that is, by a source density

$$s(\underline{r}',\omega;t) = p(\omega;t)\delta(\underline{r}' - \underline{r}_0)$$

then the resulting disturbances at the slit are determined by the products $(\phi_A p)$ and $(\phi_B p)$.

ϕ_A and ϕ_B depend upon the location of the source $(\underline{r}_0)$ and the location along the slit of the point of observation $(x")$. For completeness we include mention of a position across the width of the slit $(y")$. The intensities of light in beams A and B which passes the slit are

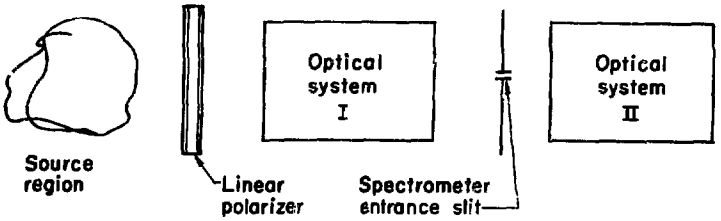

Fig. C-5a. Functional elements of the optical system.

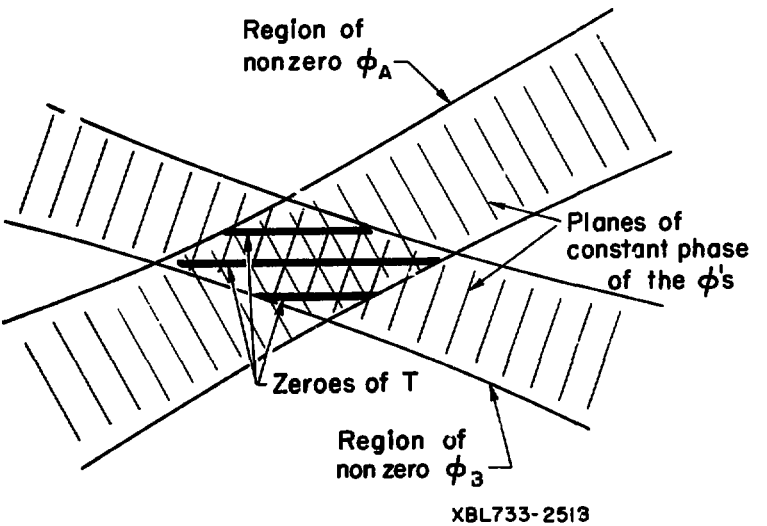

Fig. C-5b. The two transfer functions and the observed component of the source distribution for a simple two-beam system. T is everywhere zero except in the intersection of the two beams.

$$I_{A,B} = \int_{x_1''}^{x_2''} dx'' \int_{y_1''}^{y_2''} dy'' \left| \phi_{A,B}(x'',y'',\underline{r}_o,\omega) p(\omega;t) \right|^2$$

due to the point source. $(x_2'' - x_1'')$ and $(y_2'' - y_1'')$ are the dimensions of the slit.

A distributed source is described by a source density, $s(\underline{r}',\omega;t)$. We assume that the source is incoherent. That is, the total intensities are the sums of the intensities due to the separate elements of the source:

$$I_{A,B} = \frac{1}{\pi} \int d^3r' \int_{x_1''}^{x_2''} dx'' \int_{y_1''}^{y_2''} dy'' \left| \phi_{A,B}(x'',y'',\underline{r}',\omega) s(\underline{r}',\omega;t) \right|^2$$

Optical system II, however separates not these intensities, but those of the two intermediate polarization--1 and 2. The resulting signal, the difference in intensity, is

$$\begin{aligned} Y(\omega;t) &= I_2(\omega;t) - I_1(\omega;t) \\ &= \frac{1}{\pi} \int d^3r' \int_{x_1''}^{x_2''} dx'' \int_{y_1''}^{y_2''} dy'' \left[\left| \frac{1}{\sqrt{2}} (\phi_B s + \phi_A s) \right|^2 - \left| \frac{1}{\sqrt{2}} (\phi_B s - \phi_A s) \right|^2 \right]. \\ &= \frac{1}{\pi} \int d^3r' \; s^* s \int_{x_1''}^{x_2''} dx'' \int_{y_1''}^{y_2''} dy'' \\ &\quad \cdot \frac{1}{2} \left[(\phi_B^* + \phi_A^*)(\phi_B + \phi_A) - (\phi_B^* - \phi_A^*)(\phi_B - \phi_A) \right]. \end{aligned}$$

Defining an emitted spectrum as we did in Sect. II.A.3,

$$\mathcal{A}(\omega;\underline{r}',t) \equiv s^*(\underline{r}',\omega;t)s(\underline{r}',\omega;t)$$

and reducing the above result we have

$$Y(\omega;t) = \frac{1}{\pi}\int d^3r' \mathcal{A}\int_{x_1''}^{x_2''} dx'' \int_{y_1''}^{y_2''} dy'' \ (\phi_B^*\phi_A + \phi_A^*\phi_B).$$

The last factor can be written,

$$\phi_B^*\phi_A + \phi_A^*\phi_B = 2 \text{ Re } \phi_A^*\phi_B$$
$$= 2|\phi_A||\phi_B| \cos\theta$$

where θ is the difference in phase between the complex valued quantities ϕ_A and ϕ_B. Defining

$$T(\underline{r}',\omega) \equiv \frac{2}{\pi}\int_{x_1''}^{x_2''} dx'' \int_{y_1''}^{y_2''} dy'' \ |\phi_A(x'',y'',\underline{r}',\omega)||\phi_B(x'',y'',\underline{r}',\omega|$$
$$\times \cos\theta(x'',y'',\underline{r}',\omega)$$

we have

$$Y(\omega;t) = \int d^3r' \ T(\underline{r}',\omega)\mathcal{A}(\omega;\underline{r}',t).$$

In distinction to the ϕ's, T is a real (but not necessarily positive) quantity.

We have here a formal representation of the two types of optical interference which occur in the system: Diffraction due to the superposition of various Huygens components of each beam defines the beams and determines each of the two transfer functions ϕ.

Interference between the two beams is represented by the interference between the two functions ϕ. This determines the observed component of the source distribution--described by $T(\underline{r}',\omega)$.

For our two-beam apparatus, the general form of these three functions is shown in Fig. 5B. $|\phi_A|$ and $|\phi_B|$ are nonzero only within the respective beams. Therefore T is nonzero only within their intersection. This defines the c.s.v. The relative phase of the two (the $\cos\theta$ factor in T) varies within the c.s.v. as shown, defining a source wavelength, or $\underline{k}_\Delta$.

In this arrangement, the small size of the solid angle through which the system accepts light is due to each of the ϕ's separately, while the object of the measurement is defined by T. To use more of the available light, we need other "beams" ϕ_A and ϕ_B, ones which interfere to define either a $T(\underline{r}';\omega)$ like that we have already, or else some other T of particular interest.

If, in the system of Fig. C-4, one specifies an optical wavelength, and an arrangement of lenses and calcite, then both the location of the c.s.v. and the wavelength $2\pi|\underline{k}_\Delta|^{-1}$ are determined (the c.s.v. by the image of the entrance slit to the spectrometer, and $|\underline{k}_\Delta|$ by the angle α which is fixed by the distance by which the calcite element displaces an extraordinary ray). Finally, the direction $\hat{k}_\Delta$ is determined by the directions of the beams, that is, by the location of the aperture in the mask behind the calcite. Now, if α is small, the range of possible positions of this beam-defining aperture corresponds to only a small range of $\hat{k}_\Delta$. And the locations of the maxima of T (i.e., the "phase of T") are also

unchanged because the exact center of the c.s.v. is always a (zero order) maximum. So, over some range at least, $T(\underline{r}',\omega)$ is independent of the exact location of the aperture which defines the beams (at least near the center of the c.s.v.). The resulting existence of many equivalent sets of beams A and B suggests the possibility of obtaining more light by using several pairs of beams at once--in a multibeam system.

So far we have insured a localized measurement by defining separate interfering beams A and B with a well localized intersection. We shall for now retain this approach--which requires some sort of mask to define the separate beams.

To use a large solid angle while defining separate beams, one might employ a mask with many slits. Such an assembly is shown in Fig. C-6. The slit spacing (in the mask) has been set at twice the distance of the displacement due to birefrigence so that the beams are distinct. ϕ_A and ϕ_B now describe two sets of "beams A" and "beams B".

Beams 1 and 2 are again the intermediate polarizations--separated at the output of the spectrometer. So, again, only sources viewed through both A and B can contribute to the signal. And since the two only intersect near the focus of the first lens, a localized c.s.v. is again defined.

Within the c.s.v., however, the situation is different. The calculation of either ϕ_A or ϕ_B in the focal plane of the first lens reduces to the solution of a simple Fraunhofer diffraction problem for n identical, evenly spaced slits. Near the center of

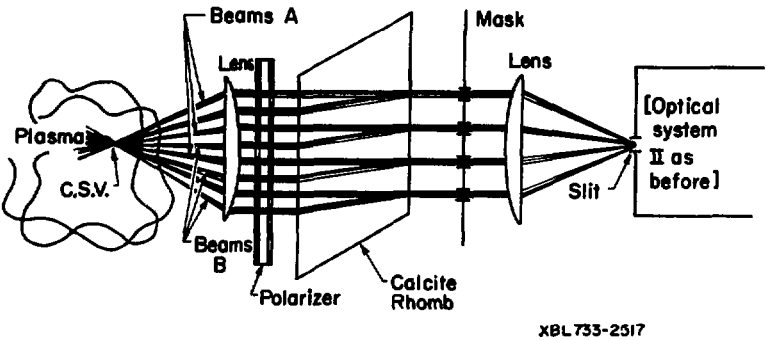

Fig. C-6a. A multiple-beam system.

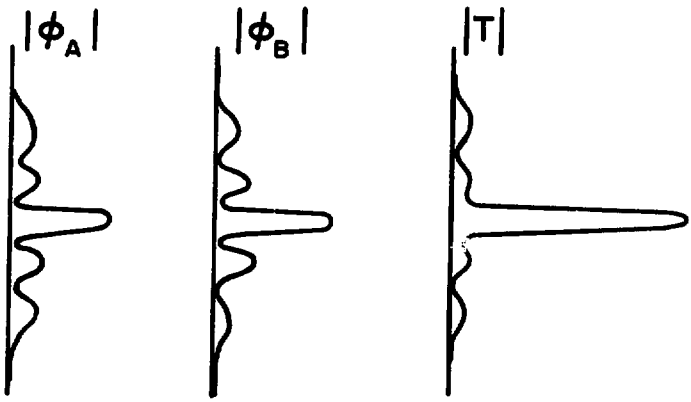

XBL733-2516

Fig. C-6b. The effect of sources in the focal plane of the first lens. A cross section of the central portion of the c.s.v.

the c.s.v. the various functions have the form shown in Fig. C-6b. The system thus achieves, at least in this region, a measurement of all the light from a small volume. This is something which could not be done with two beams because the angle α between the beams is, of course, larger than the angle β subtended by either. If β now denotes the range of directions included in either set of beams, then in Fig. C-6a, β is larger than α and the system permits a different kind of observation.

The situation is more complicated, however, because the effect of sources near the edge of the c.s.v.--particularly at other maxima of ϕ_A and ϕ_B--and the effect of sources before or behind the focal plane of the first lens remain to be considered. In any case, this arrangement is clearly not just a more efficient version of a two-beam spectrometer. The difference is due to the interference between the various "beams A" or "beams B". These interfere with each other as well as with the other polarized components to produce beams 1 and 2.

It is of interest to note that the nature of this interference depends upon the width of the entrance slit to the spectrometer. The narrow slit implicitly assumed above admits less than one fringe of the interference pattern. A wider slit would have a different effect. This is consistent with our earlier picture of the slit as an element which combines by diffraction light from different directions. A very narrow slit combines all incident light; a wider slit only combines nearly parallel beams. Clearly, this system should be discussed more completely and carefully--

probably with the help of numerical analysis. Such a discussion we defer for now to consider instead a different design.

In the device of Fig. C-6, the entrance slit to the spectrometer defines a c.s.v. by rejecting unwanted light. But if any light is rejected by a mask after the many beams are combined, then interference among them cannot be ignored. To obtain more light while making an observation such as one would obtain with a two-beam system, it is necessary to independently define the component beams. A system which does this is shown in Fig. C-7.

Here we have used the fact that in preceding systems the second lens is not really needed to define a c.s.v. The light from such sources is already focused--at infinity. One can define a c.s.v. and insure coherence by placing a defining aperture sufficiently far away. This can be done separately for each component pair of beams A and B. One must simply add a set of collimating slits to the apparatus. Beyond the collimator, a single lens may be used to focus the light onto the entrance slit to the spectrometer. This slit should now be large enough to admit all of the light transmitted by the collimator.[58]

The polarization components 1 and 2, and hence their intensity difference are simply the sum of contributions from various component beams. There is no interference here at all and the system is simply the sum of many two-beam assemblies--each with the same $T(\underline{r}',\omega)$.

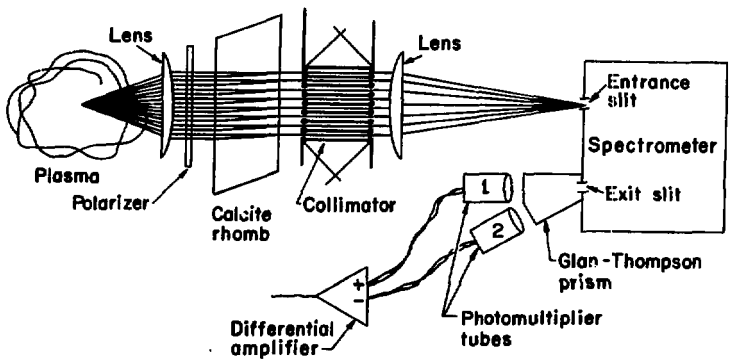

Fig. C-7. A system with several independently collimated pairs of beams.

5. Spectral Width, Beam Divergence, and the Quality of the Optical Components

Several idealizations have been used in this analysis. Are the conclusions realistic? To answer this, one must consider departures from the model system.

A calcite rhomb is to be used to combine two beams of nearly monochromatic light. Within the calcite, however, the two beams differ not only in path, but also in propagation velocity. This difference in velocity leads to a difference in optical path length--a difference which could, if necessary, be reduced with an additional birefringent optical element.[59]

Differences in path length are of great importance in any interferometric optical apparatus. If the difference in path exceeds the coherence length of the light, two beams with an initial partial coherence will almost certainly become incoherent and no net interference will be seen.

The ordinary ray is unchanged in direction within the calcite. Its velocity is just c/n_o, where n_o is the ordinary index of refraction, 1.658. Therefore the optical path is simply $s_o = 1.658D$, where D is the length of the calcite element.

The extraordinary ray is characterized by two velocities, a phase velocity and a group velocity, which differ both in magnitude and in direction. Conveniently, however, the projection of the group velocity onto the direction of the phase velocity is equal to the phase velocity. For normal incidence, this direction is the same as that of the ordinary ray--normal to the surface.

And because the light is focused at infinity and normal to the faces of the rhomb before and after, the optical path length within the calcite (the free space wavelength times the number of wavelengths along a ray) is found from just this normal component of the propagation. The magnitude of this phase velocity (which involves both n_0 and n_x, the extraordinary index of refraction) is approximately c/1.549, so the optical path length $s_x = 1.549D$.

The optical path length difference introduced by the birefringent element is

$$s_0 - s_x = 0.109D.$$

So, if the length of the calcite is one centimeter, the coherence length of the light must be considerably more than one millimeter, or corrections must be made to avoid loss of coherence. In practial terms, this means that the width of the spectral feature should be less than about two angstroms.

In our analysis of the effect of the calcite, we have considered only rays at normal incidence and used the conveniently simple result: One component of the light is laterally displaced by 0.109D. The effect of birefringence upon light incident other than normally is, of course, more complicated. Two orthogonal polarization components of the beam are then both displaced by the calcite and their resulting separation varies with the direction of incidence. Recall that, at normal incidence, the x-polarization is deflected by 6.26°. Clearly, our analysis is adequate only so long as any departures from normal incidence are much less

than this. We can hence consider only light from sources sufficiently close to the focal point of the first lens.

In optical interferometry, much care is often required to eliminate mechanical vibrations of the components of the system. But in a system designed to observe high-frequency phenomena, one can certainly ignore low-frequency virations. Mechanical vibrations are in general of much lower frequency than oscillations in a plasma and should therefore present no problems.

Even if one wishes to observe low-frequency phenomena, one needs to consider only relative changes in the length of the paths of the two components in the interference. Through most of our system the two paths are identical or at least adjacent and much mechanical vibration may still be ignored--a result which further illustrates the convenience of using polarization to define the interfering beams.

Finally, one must consider what optical quality is needed in the various components of the system. If the apertures were pinholes, such requirements would be minimal, but slits have been used to obtain more light and one must insure that the nature of the interference does not vary across the entrance to the spectrometer or across the apertures which define the beams.

Clearly, any imperfections in the system will distort the image of the plasma and reduce the accuracy of the measurement. That is, to a given point at the entrance to the spectrometer, there corresponds some observed source distribution $\left[T(x'',y'',\underline{r}',\omega)\right.$ with x'',y'' fixed$\left.\right]$. If the optical quality is poor, this will

differ from the desired distribution.

More serious than this, however, is the possibility that optical imperfections may destroy the interference altogether. This will occur if the various points across the entrance to the spectrometer observe different source distributions. That is, a given point source within the common source volume illuminates through each of the beams A and B a finite length of the entrance to the spectrometer. The two illumination patterns $\phi_A, (x'',y'',\underline{r}',\omega)$ with $\underline{r}'$ fixed must vary in the same manner along the length of the slit, or the polarization of their superposition will vary with x". That is, the function $T(x'',y'',\underline{r}',\omega) = \frac{2}{\tau} |\phi_A||\phi_B| \cos\theta$ may vary with x" because of the (same) change in $|\phi_A|$ and $|\phi_B|$, but must not vary in sign because of the charges in relative phase, θ.

To prevent such a loss of interference, the optical elements before the spectrometer (optical system I) must be of good quality. The two interfering beams go through different portions of the lenses and the calcite and any lens aberrations or curvature in the faces of the calcite will lead to a difference between ϕ_A and ϕ_B, the two interfering illuminations.

This sort of difficulty would also result from a wedge in the calcite rhomb. If the two faces are flat but not parallel, the beam cannot be normally incident at both faces. There will be a refraction at one or both surfaces. This is not in itself destructive of the interference. But because the indices of refraction are unequal, the two beams will be refracted differently. The resulting difference in direction can destroy the interference.

The refraction is described by Snell's law, which involves the phase velocities. These are approximately normal to both faces of the rhomb (inside the calcite as well as outside). If there is a small wedge angle ϕ to the rhomb, each beam will be defected by an angle $\theta = (n - 1)\phi$. This will cause a difference in direction

$$\Delta\theta = (n_A - 1)\phi - (n_B - 1)\phi = (n_A - n_P)\phi$$
$$= (1.658 - 1.549)\phi \cong \frac{1}{9}\phi$$

Therefore, the exposed portions of the faces of the rhomb must be parallel to within a few optical wavelengths. But they need not be parallel to within a fraction of one wavelength--because only differences in deflection are important.

Similarly, a small amount of wedge in the first polarizer (that before the rhomb) would not be detrimental, so long as the different beams were deflected equally.

The optical elements beyond the entrance slit to the spectrometer (optical system II) may be of lesser quality. All that is required is a measure of the intensities of polarization components 1 and 2 of one portion of the optical spectrum. The optical elements--such as the diffraction grating--must keep these two components distinct, but precise equality in path length is no longer important. It is for this reason that the interference is done before the spectrometer.

Finally, all of the optical elements must be of sufficient quality to avoid loss of light through partial reflection, absorp-

tion, or scattering. Any decrease in light intensity will, of course, degrade the final signal.

D. Studies of the Plasma with Langmuir Probes and with Conventional Spectroscopy

In preparation for the multiple-beam spectroscopic observations, the plasma produced in the beam-plasma device was observed with some standard diagnostic apparatus. The basic plasma paramters were already known from other work done with this plasma.[51] (for a description of the beam-plasma device, see Sect. IV.a and Ref. 51.) The plasma electron density had been found to be a few times 10^{13} cm^{-3} and the electron temperature had been estimated from spectroscopic observations to be greater than 4 eV, perhaps as high as 20 eV. The ion temperature was less than a few tenths of an eV.

To check the temperature measurement and to explore the possibility of using a probe to launch waves in the plasma, several Langmuir probes were made and used to obtain standard probe characteristics (current vs bias voltage). These curves had the expected form, showing an ion saturation region, where the trace was linear (with a non-zero slope) and an expontential increase in current as the voltage became less negative. The indicated electron temperature was about 4 eV, somewhat lower than had been found in the preceding work.[51] This is not surprising, since the earlier spectroscopic data showed mainly the central region, within the electron beam, while our probe data were taken outside of the beam, where the electron temperature would certainly be lower. (Probes could not be used within the beam, because a probe there would quickly have vaporized.)

In a helium plasma with $T_e \approx 4$ eV, ion waves should have a velocity of 10^6 cm/sec. This is only an estimate, however, since the plasma was strongly nonuniform, the electron temperature was higher in the center, and the effect of neutral atoms (and of doubly charged ions) may not be negligible. To observe ion waves directly, and to show that a probe could be used to launch such waves, a pair of Langmuir probes were inserted in the plasma. The probes were both biased to draw ion current and were placed a few centimeters apart, with one directly downstream (i.e., on the same magnetic field lines) from the other. The upstream probe was used as a transmitter and the downstream probe was used as a receiver. A series of one microsecond pulses (of a few volts, positive) were imposed on the transmitter, and the resulting fluctuations in receiver current were analyzed with a boxcar integrator. Figure D-1 shows the results obtained at three receiver positions. Each trace shows receiver current as a function of time--a 10 μsec sweep from left to right. Several propagating modes can be seen. There is a fast wave (the initial negative pulse) with a velocity exceeding 10^7 cm/sec, which is probably a potential fluctuation. There is a slow wave, only visible in the first trace (but seen at greater distances at later times in other traces not shown here) with a velocity of a few times 10^5 cm/sec, which probably involves the neutral gas. Finally, there is a pulse with intermediate velocity which is seen in all three traces. This disturbance moves with a velocity $\approx 1.3 \times 10^6$ cm/sec, acceptably close to the expected ion sound speed. (The velocity appears to increase slightly with probe

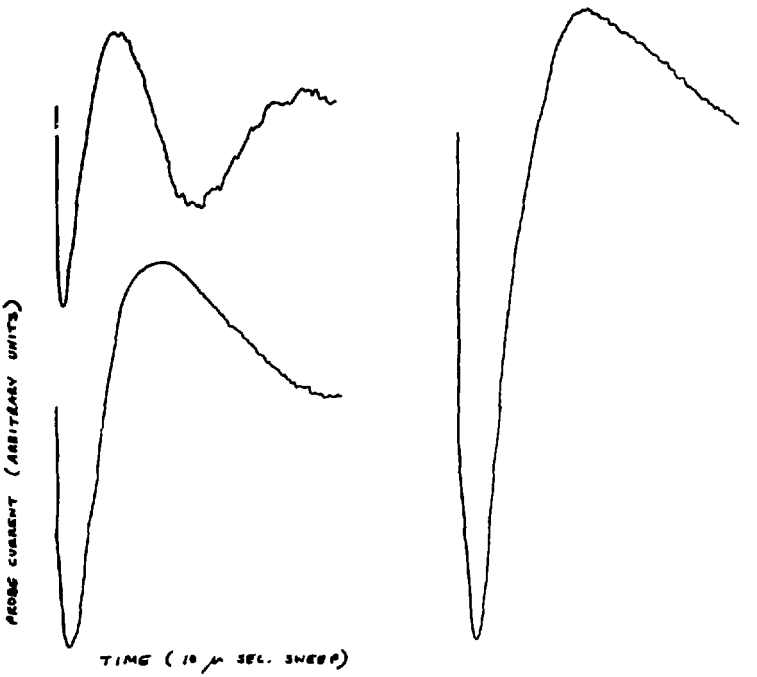

XBL 735-670

Fig. D-1. Langmuir probe observations of pulse propagation in the plasma. Top left: probe spacing 1-1/4 in.; bottom left: probe spacing 2-1/16 in.; right: probe spacing 2-7/8 in. (These are tracings of X-Y recorder plots of the output of the boxcar integrator.)

spacing. This is not surprising. The probes visibly perturbed the plasma and the perturbation was smaller when they were farther apart.) From these results it was concluded that our estimate of the ion sound speed in this plasma was correct, that plasma density disturbances would propagate at this speed for several centimeters along the magnetic field (without, in particular, being damped by collisions with the neutral gas) and that a negatively biased Langmuir probe could be used to launch such waves.

In order to select the spectral feature best suited for multiple-beam observations, a complete emission spectrum of the plasma was recorded, using a monochromator with automatic scan connected to a chart recorder. Virtually all the expected neutral helium lines were seen. The helium ion line at 4686 Å was also present. Most of the remaining lines were identified as due to a few impurities (oxygen, hydrogen, carbon).

The strongest line was the 4471 Å neutral helium line. The nearest line of any strength was one at 4437 Å and even that was far less intense than the 4471 Å line. Almost all the light within a hundred-Ångstrom band was found in the 4471 Å line. This was very convenient, since in a multiple-beam spectrometer the monochromator was to be used with a very large slit, giving poor spectral resolution, while the interference which was to be produced required light with a fairly narrow ($\sim$ 1 Å) spectrum. By tuning to the 4471 Å line the required coherence length could be obtained without precise spectral resolution.

To estimate the intensities of various spectral components,

a few photon counting measurements were also made. For this, the plasma was observed through a 2 x 2 cm aperture 50 cm away. The light was focused onto the entrance slit of a monochromator (25 μ x 23 mm, imaged to 68 μ x 8 mm within the plasma). Various spectral features were selected and the number of photocounts in 30 sec was recorded. The 4688 Å helium ion line gave, after subtraction of background, 11.7 million counts, or 3.9×10^5 counts/sec. The 4471 Å neutral helium line was not counted directly (in this setup it would have exceeded the counting speed of the equipment), but from integrated photocurrent measurements the 4686 Å line was found to be 0.8% as bright as the 4471 Å line. Thus the latter would have given a counting rate of 4.6×10^7/sec.

As a check on these measurements, it was assumed that the phototube was 10% efficient and that the 4471 Å line contained 10% of all the light emitted. Then an accounting of the total source volume and total solid angle gives an estimate of a few milliwatts of light emitted from the plasma. Judging by the apparent luminosity, this is a reasonable value.

E. Some Notes on the Definitions of Spectra

1. Direction-Dependent Spectra

In discussions of optical problems, the direction of emission or scattering of light is frequently defined (in $\underline{r}$-space) as the direction from a localized source to a distant observer. (See, for example, Ref.16.a.) In the present discussion, the directions of propagation of light waves have been defined (in $\underline{k}$-space) in terms of spatial Fourier transforms. The equivalence of the two descriptions should be noted.

In the $\underline{r}$-space formulation, one considers a source, $\underline{s}(\underline{r},t)$, which is non-zero only within a bounded region--say within a distance r_0 of an origin of coordinates. The emitted radiation is described by the usual retarded Green's function integral,

$$\underline{E}(\underline{r},t) = \int d^3r' \quad \frac{1}{|\underline{r} - \underline{r}'|} \underline{s}\left(\underline{r}', t - \frac{|\underline{r} - \underline{r}'|}{c}\right) . \qquad (E1)$$

One assumes that $\underline{E}(\underline{r},t)$ is observed at a distant point $\underline{r}(|\underline{r}| \gg r_0)$, where $|\underline{r} - \underline{r}'|$ may be expanded,

$$|\underline{r} - \underline{r}'| = (|\underline{r}|^2 - 2\underline{r}\cdot\underline{r}' + |\underline{r}'|)^{1/2} = |\underline{r}| - \hat{r}\cdot\underline{r}' + \cdots .$$

Keeping only leading terms in the magnitude, but including first order corrections in the phase, the radiation field is then approximated.

$$\underline{E}(\hat{r},|\underline{r}|,t) \equiv \underline{E}(\underline{r},t) \approx \frac{1}{|\underline{r}|}\int d^3r' \; \underline{s}\left[\underline{r}', t - \frac{1}{c}(|\underline{r}| - \hat{r}\cdot\underline{r}')\right] . \qquad (E2)$$

At large distances $|\underline{r}|$, the Poynting vector is nearly parallel

to r and the energy flux (per unit solid angle) is simply

$$I(\hat{r},t) = \frac{c}{4\pi} |\underline{r}|^2 |\underline{E}(\hat{r},|\underline{r}|,t)|^2. \tag{E3}$$

Except for retardation, this should be independent of $|\underline{r}|$.

The spectral density is then defined in terms of the temporal Fourier transform of $E(\hat{r},|\underline{r}|,t)$,

$$I(\hat{r},\omega) = \frac{c}{8\pi^2} |\underline{r}|^2 |\underline{E}(\hat{r},|\underline{r}|,\omega)|^2, \tag{E4}$$

where

$$\underline{E}(\hat{r},|\underline{r}|,\omega) \equiv \int dt\ e^{i\omega t} \underline{E}(\hat{r},|\underline{r}|,t). \tag{E5}$$

(We first consider only cases where this integral exists.) To compute the radiated energy, the intensity may be integrated in time or in frequency, since, according to Parseval's theorem,

$$\int dt\ |\underline{E}(\hat{r},|\underline{r}|,t)|^2 = \int \frac{d\omega}{2\pi} |\underline{E}(\hat{r},|\underline{r}|,\omega)|^2$$

and hence

$$\int dt\ I(\hat{r},t) = \int d\omega\ I(\hat{r},\omega), \tag{E6}$$

when $I(\hat{r},\omega)$ is normalized as in Eq. (E4).

Evaluating this spectral density,

$$I(\hat{r},\omega) = \frac{c}{8\pi^2} \int dt \int dt'\ e^{i\omega t} e^{-i\omega t'} \int d^3r' \int d^3r''$$
$$\cdot\ \underline{s}\left[\underline{r}', t' - \frac{1}{c}\left(|\underline{r}| - \hat{r}\cdot\underline{r}'\right)\right] \cdot \underline{s}\left[\underline{r}'', t' - \frac{1}{c}\left(|\underline{r}| - r\cdot\underline{r}''\right)\right].$$

Substituting

$$\alpha \equiv t + \frac{1}{c}\hat{r}\cdot\underline{r}' - \frac{|\underline{r}|}{c}$$

$$\alpha' \equiv t' + \frac{1}{c}\,\hat{r}\cdot\underline{r}'' - \frac{|\underline{r}|}{c}$$

gives

$$I(\hat{r},\omega) = \frac{c}{8\pi^2}\int d\alpha\; e^{i\omega\alpha}\int d\alpha'\; e^{-i\omega\alpha'}$$

$$\cdot\int d^3r'\; e^{i(\omega\hat{r}/c)\cdot\underline{r}'}\int d^3r''\; e^{-i(\omega\hat{r}/c)\cdot\underline{r}''}\,\underline{s}(\underline{r}',\alpha)\cdot\underline{s}(\underline{r}'',\alpha')$$

$$= \frac{c}{8\pi^2}\,\underline{s}\left(\frac{\omega\hat{r}}{c},\,\omega\right)\cdot\underline{s}\left(-\frac{\omega\hat{r}}{c},\,-\omega\right)$$

$$= \frac{c}{8\pi^2}\,\underline{s}\left(\frac{\omega\hat{r}}{c},\,\omega\right)\cdot\underline{s}^*\left(\frac{\omega\hat{r}}{c},\,\omega\right)$$

where

$$\underline{s}\left(\frac{\omega\hat{r}}{c}\right) = \int d^3r\int dt\; e^{-i\left(\frac{\omega\hat{r}}{c}\cdot\underline{r}' - \omega\alpha\right)}\,\underline{s}(\underline{r}',\alpha)$$

is the Fourier transform of $s(\underline{r}',\alpha)$. So, finally,

$$I(\hat{r},\omega) = \frac{c}{8\pi^2}\left|\underline{s}\left(\frac{\omega\hat{r}}{c},\omega\right)\right|^2 \qquad \text{(E7)}$$

independent of $|\underline{r}|$ [as anticipated in the notation, $I(\hat{r},\omega)$]. Hence, in the approximation of a localized source and a distant observer the definition in $\underline{r}$-space of the spectral density of the light emitted into a given direction $\hat{r}$ reduces to a simple expression involving the Fourier transform of the distribution of sources.

In the present discussion, however, both the direction of propagation and the spectral density of a light wave have been described by spatial Fourier transforms. This is convenient

because the transform of the field amplitude

$$\underline{E}(\hat{k},|\underline{k}|,t) \equiv \underline{E}(\underline{k},t)$$

$$\equiv \int d^3r\, e^{-i\underline{k}\cdot\underline{r}}\, \underline{E}(\underline{r},t)$$

defines in one step both a direction $\hat{k}$ and a wavelength $2\pi|\underline{k}|^{-1}$. [Here, as above, such expressions are considered well defined. If the simple Fourier integral does not converge, $\underline{E}(k,|\underline{k}|,t)$--and $\underline{E}(r,|\underline{r}|,\omega)$ discussed above--must be defined either as ensemble averages or as instantaneous spectra, as discussed in Sect. 3 below. We consider first the simple case in which the usual definition of a Fourier transform is sufficient.]

Using again the retarded Green's function [Eq. (E1)] to compute the field amplitude,

$$\underline{E}(\hat{k},|\underline{k}|,t) = \int d^3r\, e^{-i\underline{k}\cdot\underline{r}} \int d^3r' \, \frac{1}{|\underline{r}-\underline{r}'|}\, \underline{s}\left(\underline{r}', t - \frac{|\underline{r}-\underline{r}'|}{c}\right)$$

$$= \int d^3r'\, e^{-i\underline{k}\cdot\underline{r}'} \int d^3\rho\, e^{-i\underline{k}\cdot\underline{\rho}}\, \frac{1}{|\underline{\rho}|}\, \underline{s}\left(\underline{r}', t - \frac{|\underline{\rho}|}{c}\right)$$

where

$$\underline{\rho} \equiv \underline{r} - \underline{r}'.$$

If the $\underline{\rho}$ dependence is described in polar coordinates

$$(d^3\rho \to d|\underline{\rho}|\,|\underline{\rho}|^2 d^2\rho)$$

the integration over directions may be done at once [as in Eq. (B11)] leaving

$$\underline{E}(\hat{k},|\underline{k}|,t) = \frac{2\pi}{i|\underline{k}|}\int d^3r'\, e^{-i\underline{k}\cdot\underline{r}'} \int_0^\infty d|\underline{\rho}| \cdot \left(e^{i|\underline{k}||\underline{\rho}|} - e^{-i|\underline{k}||\underline{\rho}|}\right) \cdot \underline{s}\left(\underline{r}', t - \frac{|\underline{\rho}|}{c}\right)$$

$$= \frac{2\pi c}{i|\underline{k}|}\int_{-\infty}^{t} d\tau\, \underline{s}(\underline{k},\tau)\left[e^{i|\underline{k}|c(t-\tau)} - e^{-i|\underline{k}|c(t-\tau)}\right]$$

where $\tau \equiv t - \frac{|\underline{\rho}|}{c}$.

In the long time limit, which, of course, is also required in Eq. (E5), we have

$$\underline{E}(\hat{k},|\underline{k}|,t) \underset{t\to\infty}{\to} \frac{2\pi c}{i|\underline{k}|}\left[e^{i|\underline{k}|ct}\underline{s}(\underline{k},-|\underline{k}|c) - e^{-i|\underline{k}|ct}\underline{s}(\underline{k},|\underline{k}|c)\right] \quad \text{(E8)}$$

To use a $\underline{k}$-space formulation, the spectral density must be expressed in terms of $\underline{E}(\hat{k},|\underline{k}|,t)$. Yet $\underline{E}(\hat{k},|\underline{k}|,t)$ is here seen to involve two components of the source distribution, while $I(\hat{r},\omega)$, the spectral density discussed above, was found to depend upon only a single component of $\underline{s}$. Clearly, the simple expression

$$I(\hat{k},|\underline{k}|) \propto |\underline{k}|^2|\underline{E}(\hat{k},|\underline{k}|,t)|^2$$

is not equivalent to the usual frequency spectrum. The reason for the difference is evident in Eq. (E8): $\underline{E}(\hat{k},|\underline{k}|,t)$ contains negative as well as positive optical frequency components. The negative frequency components, which propagate in the $-\hat{k}$ direction, would not be observed with a detector on the $+\hat{k}$ side of the source.

On the other hand, negative frequency components of $\underline{E}(-\underline{k})$, which would be observed, have not been included.

This suggests the form,

$$I(\hat{k},|\underline{k}|) \propto |\underline{k}|^2 \left[|\underline{E}^{(+)}(\hat{k},|\underline{k}|,t)|^2 + |\underline{E}^{(-)}(-\hat{k},|\underline{k}|,t)|^2 \right] \qquad \text{(E9)}$$

where by $\underline{E}^{(+)}(\hat{k},|\underline{k}|,t)$ $\left[\underline{E}^{(-)}(\hat{k},|\underline{k}|,t)\right]$ is meant the positive (negative) frequency portion of $\underline{E}(\underline{k},t)$:

$$\underline{E}^{(+)}(\underline{k},t) \equiv \int_0^\infty \frac{d\omega}{2\pi} e^{-i\omega t} \int_{-\infty}^{\infty} dt' \, e^{i\omega t'} \underline{E}(\underline{k},t') \qquad \text{(E10a)}$$

$$\underline{E}^{(-)}(\underline{k},t) \equiv \int_{-\infty}^0 \frac{d\omega}{2\pi} e^{-i\omega t} \int_{-\infty}^{\infty} dt' \, e^{i\omega t'} \underline{E}(\underline{k},t') \qquad \text{(E10b)}$$

Equation (E9) can be further simplified, however, because the reality of $\underline{E}(\underline{r},t)$ implies that $\underline{E}(\underline{k},\omega) = \underline{E}^*(-\underline{k},-\omega)$. Hence the two terms in the above expression are identical and only one is needed.

This leaves

$$I(\hat{k},|\underline{k}|) \propto |\underline{k}|^2 |\underline{E}^{(+)}(\hat{k},|\underline{k}|,t)|^2.$$

Finally, according to Eq. (E8),

$$|\underline{k}|^2 |\underline{E}^{(+)}(\hat{k},|\underline{k}|,t)|^2 \underset{t \to \infty}{\to} 4\pi^2 c^2 |\underline{s}(\hat{k},|\underline{k}|c)|^2 \qquad \text{(E11)}$$

which is time independent. Comparing this result with that obtained for $I(r,\omega)$ $\left[\text{Eq. (E7)}\right]$, the $\underline{r}$- and $\underline{k}$-space formulations are seen to be equivalent provided that (1) the direction $\hat{k}$ is identified with the direction $\hat{r}$, (2) the wavelength $2\pi|\underline{k}|^{-1}$ is related to the frequency ω by the usual, $\omega = |\underline{k}|c$, (3) $I(\hat{k},|\underline{k}|)$ is cor-

rectly normalized, and (4) only positive frequency components of $\underline{E}(\hat{k},|\underline{k}|,t)$ are included.

The two expressions, $|\underline{s}(\omega\hat{r}/c,\omega)|^2$ and $|\underline{s}(\underline{k},|\underline{k}|c)|^2$, are still not quite equivalent, since the former includes negative frequency components, while the latter does not, but this is not an essential difference, because $\underline{s}(-\underline{k},-\omega) = \underline{s}^*(\underline{k},\omega)$. Indeed, since ω appears in both the wave vector and the frequency of $\underline{s}(\omega\hat{r}/c,\omega)$, the two halves of the spectrum in Eq. (E7) simply correspond to the two terms in Eq. (E9).

The normalization of $I(\hat{k},|\underline{k}|)$ should be chosen to equate the integrated spectrum to the total radiated energy [as in Eq. (E6)]. The proper value is

$$I(\hat{k},|\underline{k}|) \equiv \lim_{t\to\infty}\left(\frac{|\underline{k}|}{4\pi^2}\right)^2 |\underline{E}^{(+)}(\hat{k},|\underline{k}|,t)|^2, \qquad \text{(E12)}$$

for then,

$$\int_{-\infty}^{\infty} d\omega\, I(\hat{r},\omega) \quad \int_{-\infty}^{\infty} d\omega \frac{c}{8\pi^2} |\underline{s}\left(\frac{\omega r}{c},\omega\right)|^2$$

$$= \int_0^{\infty} d\omega \frac{c}{4\pi^2} |\underline{s}\left(\frac{\omega r}{c},\omega\right)|^2$$

$$= \int_0^{\infty} cd|\underline{k}| \frac{c}{4\pi^2} |\underline{s}(\underline{k},|\underline{k}|c)|^2$$

$$= \int_0^{\infty} d|\underline{k}| \frac{1}{(4\pi^2)^2}\left[\lim_{t\to\infty} |\underline{E}^{(+)}(\hat{k},|\underline{k}|,t)|^2\right]$$

$$= \int_0^\infty d|\underline{k}|\ I(\hat{k},|\underline{k}|)$$

as required. The normalization of the two intensities is most transparent from a comparison of differentials,

$$I(\hat{r},\omega)d\omega\, d^2\hat{r} = \frac{c}{4\pi}\left(\frac{d\omega}{2\pi}\right)|\underline{r}|^2 d^2\hat{r}\,|\underline{E}(\hat{r},|\underline{r}|,\omega)|^2 \qquad \text{(E13a)}$$

$$I(\hat{k},|\underline{k}|)d|\underline{k}|d^2\hat{k} = (2)\left(\frac{1}{4\pi}\right)\left(\frac{d|\underline{k}|}{2\pi}\right)\left[|\underline{k}|^2\,\frac{d^2\hat{k}}{(2\pi)^2}\right]\lim_{t\to\infty} |\underline{E}^{(+)}(\hat{k},|\underline{k}|,t)|^2 \qquad \text{(E13b)}$$

[Again, the factor of two in $I(\hat{k},|\underline{k}|)$ reflects the fact that this spectral density is non-zero only for positive frequencies, $|\underline{k}|c > 0$.]

This definition is in accord with standard practice. In analyses of optical problems, the light intensities and correlation functions are often defined in terms of the positive frequency portion of the radiation field.[2c] In an $\underline{r}$-space formulation, $\underline{E}(\underline{r},t)$ is real and $\underline{E}^{(+)}(\underline{r},t)$, which is called the associated analytic signal, is a complex valued quantity which completely describes the field $\underline{E}(\underline{r},t)$. The use of an analytic signal is a generalization of the familiar device of replacing a cosine by a complex exponential. If $\underline{E}(\underline{r},t)$ is nearly monochromatic, the magnitude of the analytic signal $|\underline{E}^{(+)}(\underline{r},t)|$ is a slowly varying quantity.

The magnitude of the positive frequency portion of the spatial Fourier transform $|\underline{E}^{(+)}(\underline{k},t)|$ which was used above also contains no

rapid oscillation. [See Eq. (E8). There either term alone has constant magnitude, but their sum does not.] This elimination of the rapid optical frequency variation is convenient because it permits one to define a slowly varying or constant light intensity without resort to a time averaging procedure.

However, $\underline{E}^{(+)}(\underline{k},t)$ was introduced above for a different reason: to define a direction of propagation of the wave. The definition of an optical spectrum $I(\hat{k},|\underline{k}|)$ in terms of the spatial Fourier transform of the field requires the use of only the positive frequency portion of $\underline{E}(\underline{k},t)$. If negative frequencies were included, the results would not be equivalent to the frequency spectrum $I(\hat{r},\omega)$ of the light emitted in the $\hat{k} = \hat{r}$ direction. Yet the quantity $\underline{E}^{(+)}(\underline{k},t)$, which was seen to be needed for this, is just the transform of the usual analytic signal $\underline{E}^{(+)}(\underline{r},t)$ since, at least for well behaved functions, the two operations commute:

$$\left[\underline{E}(\underline{k},t)\right]^{(+)} = \int_0^\infty \frac{d\omega}{2\pi} e^{-i\omega t} \int_{-\infty}^{\infty} dt' \, e^{i\omega t'} \int d^3r \, e^{-i\underline{k}\cdot\underline{r}} \underline{E}(\underline{r},t')$$

$$= \int d^3r \, e^{-i\underline{k}\cdot\underline{r}} \int_0^\infty \frac{d\omega}{2\pi} e^{-i\omega t} \int_{-\infty}^{\infty} dt' \, e^{i\omega t'} \underline{E}(\underline{r},t)$$

$$= \int d^3r \, e^{-i\underline{k}\cdot\underline{r}} \, \underline{E}^{(+)}(\underline{r},t)$$

It should be noted also that different definitions of the analytic signal are in use. Some authors[2c] consider $E^{(+)}(\underline{r},t)$, while others[1a,36] define an analytic signal equal to twice this quantity [to eliminate the factor of two in Eq. (E14) below]. A

superscript r--for "real"--is sometimes used to identify the original signal, but this is inappropriate when spatial Fourier transforms are employed, since $\underline{E}(\underline{k},t)$ is not necessarily a real quantity. Throughout the present discussion, a superscript (+) is used to identify the analytic signal, as defined by Eq. (E10) [and similarly for other quantities, $s^{(+)}$, $\underline{\xi}^{(+)}$, $\underline{E}^{(+)}(\underline{r},t)$, etc.]. Since $\underline{E}(\underline{r},t)$ is real, Eq. (E10) implies that

$$\underline{E}(\underline{r},t) = 2 \text{ Re } \underline{E}^{(+)}(\underline{r},t). \tag{E14}$$

In k-space, however, both $\underline{E}(\underline{k},t)$ and $\underline{E}^{(+)}(\underline{k},t)$ are, in general, complex valued functions. For such functions, Parseval's theorem implies that

$$\int_{-\infty}^{\infty} dt|\underline{E}(\underline{k},t)|^2 = \int_{-\infty}^{\infty} dt|\underline{E}^{(-)}(\underline{k},t)|^2 + \int_{-\infty}^{\infty} dt|\underline{E}^{(+)}(\underline{k},t)|^2.$$

For a real valued function such as $\underline{E}(\underline{r},t)$, this reduces to

$$\int_{-\infty}^{\infty} dt|\underline{E}(\underline{r},t)|^2 = 2\int_{-\infty}^{\infty} dt|\underline{E}^{(+)}(\underline{r},t)|^2. \tag{E15}$$

Using this relation, the time-averaged intensity of polychromatic as well as monochromatic light can be expressed in terms of the associated analytic signal.

The analysis of optical interference, however, requires an expression for the rapidly varying amplitude, as well as the mean intensity, of the interfering waves. Both the amplitude and the intensity of the light transmitted by a spectrometer may be expressed in terms of the Fourier transform of the input, as can be

seen from an analysis of the actual effect of such an instrument. A brief review of this discussion is included here.

In a grating spectrometer, the length of the path from the entrance slit to the exit slit is different for light reflected from different lines of the grating. Components of the light are delayed by different amounts and the output of the instrument is a superposition of many preceding inputs.

$$\underline{E}^{(out)}(t) = \sum_{\substack{\text{(lines of} \\ \text{grating)}}} \left[\begin{matrix}\text{amount of} \\ \text{light reflected}\end{matrix}\right] \underline{E}^{(in)}(t\text{-delay})$$

$$= \int_{0_{\text{(delay time)}}}^{\infty} d\tau\, f(\tau)\underline{E}^{(in)}(t - \tau).$$

$f(\tau)$ is a real valued quantity which, according to Eq. (E14) may be expressed in terms of an associated analytic signal. Making this replacement,

$$\underline{E}^{(out)}(t) = 2\,\mathrm{Re}\int_0^{\infty} d\tau\, f^{(+)}(\tau)\underline{E}^{(in)}(t - \tau)$$

$$= 2\,\mathrm{Re}\int_{-\infty}^{t} d(t - \tau)\int_0^{\infty} \frac{d\omega}{2\pi} e^{i\omega(t-\tau)}e^{-i\omega t}f(\omega)E^{(in)}(t - \tau)$$

$$\underset{t \to \infty}{\to} 2\,\mathrm{Re}\int_0^{\infty} \frac{d\omega}{2\pi} e^{-i\omega t}f(\omega)\underline{E}^{(in)}(\omega) \qquad \text{(E16)}$$

which just describes the effect of the spectrometer in terms of a transfer function $f(\omega)$.

In the limit of perfect resolution, that is, of an infinite

sinusoidal grating, $f(\tau) = \cos\omega_0\tau$, $f(\omega) = \pi\,\delta(\omega - \omega_0) + \delta(\omega + \omega_0)$, and Eq. (E16) reduces to

$$\underline{E}^{(out)}(t) \underset{t \to \infty}{\to} \mathrm{Re}\; e^{-i\omega_0 t}\,\underline{E}^{(in)}(\omega_0).$$

To calculate the mean intensity of this, only the magnitude $|\underline{E}(\omega_0)|$ is needed, since, after time averaging,

$$I = \frac{c}{4\pi}\,\overline{|\mathrm{Re}\; e^{-i\omega_0 t}\,\underline{E}(\omega_0)|^2} = \frac{c}{8\pi}\,|\underline{E}(\omega_0)|^2.$$

To describe interference, however, the rapid oscillation of the field must also be considered. It is again useful to express the result both in terms of wave vector $\underline{k}$ and in terms of direction $\hat{r}$ and frequency ω. Considering once more a localized source, a distant observer, and a temporal Fourier transform, $\underline{E}(\hat{r},|\underline{r}|,\omega)$, we have from Eq. (E16) an expression for the amplitude,

$$\underline{E}^{(out)}(t) \propto \mathrm{Re}\left[|\underline{r}|e^{-i\omega t}\underline{E}(\hat{r},|\underline{r}|,\omega)\right].$$

The factor of $|\underline{r}|$ permits normalization of the intensity to solid angle as was done with $I(\hat{r},\omega)$ in Eq. (E4).

The same amplitude can also be expressed in terms of the spatial Fourier transform of the field and the two forms can be related to the source density as was done with $I(\hat{k},|\underline{k}|)$ and $I(\hat{r},\omega)$. In exactly the same manner as in that discussion, one obtains the two equations

$$\mathrm{Re}\left[|\underline{r}|e^{-i\omega t}\underline{E}(\hat{r},|\underline{r}|\omega)\right]_{|\underline{r}| \to \infty} \to \mathrm{Re}\left[e^{i(\omega|\underline{r}|/c-\omega t)}\,\underline{s}\left(\frac{\omega\hat{r}}{c},\omega\right)\right] \qquad \text{(E17a)}$$

$$\mathrm{Re}\left[|\underline{k}|\,\frac{1}{2\pi i c}\,e^{i\underline{k}\cdot\underline{r}}\underline{E}^{(+)}(\hat{k},|\underline{k}|,t)\right]_{t\to\infty} \to \mathrm{Re}\left[e^{i(\underline{k}\cdot\underline{r}-|\underline{k}|ct)}\cdot\underline{s}(\underline{k},|\underline{k}|c)\right]. \qquad (E17b)$$

Either of these forms can be used to describe the field amplitude. The normalization, if needed, can be obtained from the corresponding expression for the spectral density, Eq. (E13a) or (E13b). If the form of (E17b) is used, it should be noted that the order of the operations is important, since (+) and (Re) do not commute.

2. A Property of the Analytic Signal

Equation (E14) implies that

$$\left[\mathrm{Re}\,\underline{E}^{(+)}(\underline{r},t)\right]^{(+)} = \frac{1}{2}\,\underline{E}^{(+)}(\underline{r},t). \qquad (E18)$$

Equation (E14) applies only to real valued functions, $\underline{E}(\underline{r},t)$, but the relation (E18) is in fact more generally valid. Because this result is used in Chapter II, a simple derivation is included here.

Consider a complex valued quantity, $\underline{E}(\underline{k},t)$. The positive frequency portion, $\underline{E}^{(+)}(\underline{k},t)$, may be written

$$\underline{E}^{(+)}(\underline{k},t) = \left[\mathrm{Re}\,\underline{E}(\underline{k},t)\right]^{(+)} + i\left[\mathrm{Im}\,\underline{E}(\underline{k},t)\right]^{(+)}. \qquad (E19)$$

Re $\underline{E}(\underline{k},t)$ and Im $\underline{E}(\underline{k},t)$ are both real valued quantities, and hence a relation like (E14) must hold for either term alone. This suggests that even though $\underline{E}(\underline{k},t)$ is clearly not equal to the real part of $2\underline{E}^{(+)}(\underline{k},t)$, the imaginary part of $\underline{E}^{(+)}(\underline{k},t)$ may still be redundant.

Taking the real part,

$$\text{Re } \underline{E}^{(+)}(\underline{k},t) = \text{Re} \int_0^\infty \frac{d\omega}{2\pi} e^{-i\omega t} \int_{-\infty}^{\infty} dt' \, e^{i\omega t'} \underline{E}(\underline{k},t')$$

$$= \int_0^\infty \frac{d\omega}{2\pi} \int_{-\infty}^{\infty} dt' \, \frac{1}{2} \Big[\underline{E}(\underline{k},t') e^{-i\omega(t-t')} + \underline{E}^*(\underline{k},t') e^{+i\omega(t-t')} \Big] .$$

The positive frequency portion of this,

$$\text{Re } \underline{E}^{(+)}(\underline{k},t)^{(+)} = \int_0^\infty \frac{d\omega}{2\pi} e^{i\omega t} \int_{-\infty}^{\infty} dt' \, e^{i\omega t'} \int_0^\infty \frac{d\omega'}{2\pi} \int_{-\infty}^{\infty} dt''$$

$$\cdot \frac{1}{2} \Big[\underline{E}(\underline{k},t'') e^{-i\omega'(t'-t'')} + \underline{E}^*(\underline{k},t'') e^{+i\omega'(t'-t'')} \Big]$$

$$= \int_0^\infty \frac{d\omega}{2\pi} e^{-i\omega t} \int_0^\infty \frac{d\omega'}{2\pi} \int_{-\infty}^{\infty} d\tau \int_{-\infty}^{\infty} dt'' \, \frac{1}{2} e^{i\omega t''}$$

$$\cdot \Big[\underline{E}(\underline{k},t'') e^{i(\omega-\omega')\tau} + \underline{E}^*(\underline{k},t'') e^{i(\omega+\omega')\tau} \Big]$$

$$= \int_0^\infty \frac{d\omega}{2\pi} e^{-i\omega t} \int_0^\infty \frac{d\omega'}{2\pi} \int_{-\infty}^{\infty} d\tau \, \frac{1}{2}$$

$$\cdot \Big[\underline{E}(\underline{k},\omega) e^{i(\omega-\omega')\tau} + \underline{E}(\underline{k},-\omega) e^{i(\omega+\omega')\tau} \Big],$$

where $\tau \equiv t' - t''$. The τ integration gives

$$\int_0^\infty \frac{d\omega}{2\pi} e^{-i\omega t} \int_0^\infty \frac{d\omega'}{2\pi} \, \frac{1}{2} \Big[\underline{E}(\underline{k},\omega) 2\pi\delta(\omega - \omega') + \underline{E}(\underline{k},-\omega) 2\pi\delta(\omega + \omega') \Big] .$$

Since the ω and ω' integrations include only positive frequencies, the second term contributes nothing $\Big[\underline{E}(\underline{k},\omega) = 0 \text{ at } \omega = 0 \Big]$, and

the first gives

$$\int_0^\infty \frac{d\omega'}{2\pi} 2\pi\delta(\omega - \omega')\underline{E}(\underline{k},\omega) = \begin{cases} \underline{E}(\underline{k},\omega), & \omega > 0. \\ 0, & \omega < 0. \end{cases}$$

Using this, we have

$$\left[\text{Re } \underline{E}^{(+)}(\underline{k},t)\right]^{(+)} = \int_0^\infty \frac{d\omega}{2\pi} e^{-i\omega t} \frac{1}{2} \underline{E}(\underline{k}\omega)$$

$$= \frac{1}{2} \underline{E}^{(+)}(\underline{k},\omega). \qquad \text{(E20)}$$

This result, identical in form to Eq. (E18), applies to complex valued functions $\underline{E}(\underline{k},t)$, [i.e., to any well behaved complex valued function of time. We have assumed only that simple algebraic steps are valid, the the integrals used exist, and that there is no contribution from $\omega = 0$.]

The same result can be obtained by evaluating separately the contributions of the two terms in Eq. (E19).

3. Time Dependent Spectra

The use of Fourier transforms to describe a spectroscopic measurement is convenient for analysis, but such a description is highly idealized. Literally, the measurement of any wave vector component, $\underline{E}(\underline{k},t)$, of a field, $\underline{E}(\underline{r},t)$, requires observation of $\underline{E}(\underline{r},t)$ at every point in space. A description in terms of frequency components requires knowledge of the field throughout all time. A long time limit is also needed in the $\underline{k}$-space analysis [c.f., Eq. (I.7) or Eq. (II.15)].

The output of a real spectrometer is not a single spectral

amplitude; it is a time-varying signal which depends upon the past, but not the future input to the instrument. This situation is not unique to optics. Any actual spectral measurement is related only in a long time limit to a simple Fourier transform. To improve upon this description, other mathematical techniques have been developed (primarily for studies of electrical signals in communication systems) which better represent the effect of a spectrometer.

Most simply, the usual Fourier transform $f(\omega)$ of a signal $f(t)$ is sometimes replaced by an integral over past, but not future times. The result is a time dependent quantity which is called a running spectrum:[60]

$$f(\omega;t) \equiv \int_{-\infty}^{t} dt' \, e^{i\omega t'} f(t'). \qquad (E21)$$

This definition can be further modified to reduce or eliminate the effect of events in the distant past. By integrating over only a finite interval or by including an appropriate weighting factor in the integrand, one obtains a time localized expression which is called an instantaneous spectrum.[60] An instantaneous spectrum not only better represents the effect of a real spectral instrument, it has the added advantage of being well defined for many functions whose Fourier transform does not exist at all.

The analyses in this report have all been done with reference only to a simple Fourier transform, but much the same discussion could be done in terms of time-dependent spectra. Indeed, expressions for running spectra and for instantaneous spectra emerge in

a simple and straightforward way from calculations done in Chapters I and II. For this reason it seems appropriate at least to mention how these concepts could be introduced in this discussion.

Expressions of the form of Eq. (E21) appeared both in the analysis of scattering in Chapter I [see Eqs. (I.7) and (B7), from which it comes] and in the analysis of a two-beam spectrometer in Chapter II [see Eq. (II.15) and the discussion after Eq. (B11)]. In each case a long time limit was invoked to change the result into a standard Fourier integral. But one could instead consider the expression as a running spectrum. So one need not introduce this concept--it is already present in the calculations as they stand.

Both of the same calculations started with a spatial Fourier transform, which involves an integral of the field over all space. Since this represents the effect of the diffraction grating in the spectrometer, it would be more realistic to replace the Fourier integral by one over a finite volume comparable to the dimensions of the grating. If this were done, the final expressions just discussed [Eq. (B7), etc.] would have a finite lower limit too. (The integrals over the retarded times came from integrals over $|\underline{\rho}| = |\underline{r} - \underline{r}'|$, which cameoriginally from the spatial Fourier transforms.) Thus a more realistic model of the spectrometer would give at once an instantaneous spectrum as the output.

In Chapters I and II, the time dependence of the measured spectra, $I_{1,2}(\omega;t)$, and of the corresponding sources $\mathcal{A}(\omega;\underline{r}',t)$ was reintroduced after the Fourier transformation, essentially be treating the two time scales separately. If instantaneous spectra

were explicitly employed, this separation of time scales would not be necessary. The difficulty with such an approach is, of course, that it would not permit use of the standard theory of Fourier transformation. In particular, the light intensity, which was defined by integration over the complete time axis would then have to be restated locally. (Recall that the intensity was written in terms of an analytic signal, which was in turn defined in terms of the whole Fourier transformation.) Also, the treatment of the total intensity as just an integral over $|\underline{k}|$ components [in Eqs. (II.8) and after] would have to be rewritten for a local definition of intensity. Thus a conversion to an instantaneous spectral formulation would require a new definition of intensity, and probably also of analytic signals.

Finally, it should be noted also that the concept of a time-dependent spectrum is closely related to the concept of a time-dependent correlation function. (Here "time" means the instant of observation, not the length of a delay.) Both a scattering experiment and a simple two-beam spectroscopic apparatus would give a measurement of one Fourier component of the fluctuations in the source or electron density within a plasma. According to the Wiener Khintchine theorem[19] [see Eq. (I.14)], this gives information about the two-point correlation function of the source or electron distribution. This correlation function is customarily defined in terms of a stationary ensemble of systems. But any real observation is made on a single system, and most experiments involve pulsed plasmas which are far from stationary. These

differences are just as basic as--and, in fact, related to--the difference between a *Fourier transform* and a *measured spectrum*. It is possible, however, to define a correlation function which does not assume a stationary situation. The correlation function, like the spectrum, can also be defined in terms of a time-localized expression. Several authors[61] have used definitions of this sort to generalize the Wiener-Khintchine theorem--obtaining a relation between this type of correlation function and a corresponding instantaneous power spectrum. Thus a more realistic treatment of the correlation function leads again to the idea of a time-dependent spectrum. Conversely, a description of the radiation from a plasma in terms of instantaneous spectra--a description which emerges naturally from a more realistic model of the optical devices used--would lead to a description of the plasma in terms of time-localized expressions for the correlations between particles.

F. Notation

The Fourier transform is used repeatedly in this discussion. For any function, such as $\xi(\underline{r},t)$, the spatial Fourier transform is denoted by $\xi(\underline{k},t)$, while $\xi(\underline{r},\omega)$ denotes the temporal Fourier transform. [For the definition used, see Eq. (1.8).] For any function of time, such as $\xi(\underline{r},t)$ or $\underline{E}(\underline{r},t)$, a superscript (+) is used to denote the positive frequency (or analytic signal) portion, $\xi^{(+)}(\underline{r},t)$, $\underline{E}^{(+)}(\underline{r},t)$, etc. [This is defined by Eq. (E10a) in Appendix E.]

A wave amplitude which is linear in the source may be divided into separate contributions from the different source points. This is occasionally indicated by a second spatial variable, as in $\xi(\underline{r},t;\underline{r}')$ which means the contribution to $\xi(\underline{r},t)$ from sources near the point $\underline{r}'$.

A vector quantity is denoted by an underscore, as $\underline{r}$, its magnitude by the addition of an absolute value sign, as $|\underline{r}|$, and its direction by the same symbol with circumflex, as $\hat{r}$. Thus $\underline{r} = |\underline{r}|\hat{r}$, $\underline{E} = |\underline{E}|\hat{E}$, etc.

Strictly speaking temporal Fourier transformed quantities are functions of frequency and do not depend on time. But in practice, measured spectra are time varying, a fact which cannot always be ignored. In our notation, a time dependence is explicitly indicated in such quantities as $\mathcal{A}(\omega;\underline{r}',t)$ in those equations where it is important. (The mathematical basis of this procedure is discussed in Appendix E.3.)

The principal symbols used in the discussion are:

a	angular spread of a beam (in Sect. I.B)
$a(\underline{r}'t)$	amplitude of a nearly monochromatic source [see Eq. (II.36)]
$\underline{a}$	acceleration
$\underline{a}'$	acceleration of a particle at time t' (in Sect. I.C)
$\underline{A}$	magnetic vector potential
b	apparent angular size of a focus (in Sect. I.B)
$\underline{B}$	magnetic field strength
c	speed of light
c_A, c_B, c_0, $\tilde{c}$, c_0'	(used in Sect. II.B.3) various time delays in multiple-beam spectrometers
$C_{n_e}(\tau)$	electron density time correlation function
d	lateral displacement of the extraordinary ray in a calcite rhomb
d	a difference in optical path of one wavelength (in Fig. I-4b)
D	the length of a calcite rhomb
e	electronic charge
$\hat{e}_x$, $\hat{e}_y$, $\hat{e}_z$	unit vectors of a Cartesian coordinate system
$\underline{E}$	electric field strength
$\underline{E}_i$	electric field of an incident light wave (in a scattering experiment)
$\underline{E}_0$	amplitude of an incident light wave, $\underline{E}_i$
$\underline{E}_0^{\perp}$	$= (\underline{I} - \hat{k}_s\hat{k}_s)\underline{E}_0$, the component of $\underline{E}_0$ normal to $\underline{k}_s$

$\underline{E}_s$	electric field of a scattered wave
f_1, f_2	focal lengths of the input and output lenses of a multiple-beam spectrometer (see Fig. II-6)
$f(\omega)$	the (complex valued) transfer function of a spectrometer or spectral filter
$F(y')$	a function which defines the region observed by a multiple-beam spectrometer [see Eq. (II.28)]
g_A, g_B	Green's functions which describe the central section of a multiple-beam spectrometer [see Eq. (II.21)]
$\underline{\underline{I}}$	the unit tensor of the second rank
$I(\hat{k}, \lvert\underline{k}\rvert)$	the spectral density of a light wave defined in terms of spatial Fourier transforms
$I(\hat{r}, \omega)$	the spectral density of light emitted in direction $\hat{r}$ [see Eq. (E4)]
I_0	the intensity of an incident light wave
$I_1(t)$, $I_2(t)$	the two light intensities which are measured in a multiple-beam spectrometer
$\underline{j}$	electric current density
$\underline{k}_A$, $\underline{k}_B$	wave vectors of light in beams A and B
$\underline{k}_i$	wave vector of an incident light wave
$\underline{k}_s$	wave vector of an observed scattered wave
$\underline{k}_\Delta$	a difference wave vector ($= \underline{k}_s - \underline{k}_i$ or $\underline{k}_B - \underline{k}_A$)
L	the length of a collimator
m	mass of a particle

n	index of refraction
n	the number of pairs of beams in a multiple-beam spectrometer (i.e., the number of slits in the mask which defines the beams)
$\hat{n}$	a unit vector = $(\underline{r} - \underline{r}')/(\lvert\underline{r} - \underline{r}'\rvert)$
n	number of photocounts (in Sect. III.C)
n_e	electron density
n_{e_0}	mean electron density
n_s	density of light sources (in Sect. II.C)
N	noise level in a spectrum of the output of a multiple-beam spectrometer
$p(\omega;t)$	a complex-valued source strength (in Appendix C)
P	the photocount rate due to signal light
$P_Y(n)$	the photocount probability distribution associated with the signal Y(t); similarly for $P_{Y'}(n)$, etc. (in Sect. III.C)
Q	the mean photocount rate due to background light received by each of the photomultiplier tubes 1 and 2 (in Sect. III.C)
$\underline{r}$	position vector
$\underline{r}'$	position of a particle at time t'
$\underline{r}_A$, $\underline{r}_B$	points of observation of the selected $\underline{k}$ components of ξ_A and ξ_B [see Eq. (II.5)]
$\underline{r}'$, $\underline{r}''$	points in a multiple-beam spectroscopic system
$\underline{r}^{(in)}$, $\underline{r}^{(out)}$	(see Fig. II-6)
$\underline{r}_j(t)$	the position of one of a set of point sources (in Chapter V)

$\underline{r}^{\sim}$	points immediately behind a calcite rhomb (in Sect. II.B.3)
$\underline{r}^{\approx}$	points immediately behind a collimator (in Sect. II.B.3)
s	a scalar wave source [from Eq. (I.3)]
S	the signal level in a spectrum of the output of a multiple-beam spectrometer (in Sect. III.C)
$S(\underline{k}_\Delta, \omega_\Delta)$	dynamic form factor in scattering (Sect. I.C)
$\mathcal{A}(\omega, \underline{r}')$	the spectrum of the light emitted by sources near $\underline{r}'$ [see Eq. (II.15b)]
t	time
t'	retarded time
T	the total time of an observation (Sect. III.C)
$T(\underline{r}', \omega)$	the transmission function of a multiple-beam spectrometer [see Eq. (II.24)]
$\underline{v}_0$	the velocity of a moving frame of reference (in Sect. V.A)
$\underline{v}_s$	the velocity of a moving source (in Sect. V.A)
x	distance from a focus (in Sect. I.B)
x', x'' $x^{(in)}, x^{(out)}$	components of $\underline{r}'$, $\underline{r}^{(in)}$, etc.
X	$= (\omega/c)\left[x'/f_1 + x''/f_2\right]$ a quantity used in Sect. II.B.3
y', y'' $y^{(in)}, y^{(out)}$	components of $\underline{r}'$, $\underline{r}^{(in)}$, etc.

$Y(t)$	the output signal from a multiple-beam spectrometer
$Y'(t)$	the result of frequency mixing and then time averaging the signal $Y(t)$ (in Sect. III.C)
$Y_1(t)$, $Y_2(t)$	the positive and negative portions of $Y'(t)$ (in Sect. III.C)
Y	$= (\omega/c)\left[y'/f_1 + y''/f_2\right]$
z', z'' $z^{(in)}$, $z^{(out)}$	components of $\underline{r}'$, $\underline{r}^{(in)}$, etc.
$Z(t)$	$= \left[Y'(t)\right]^2$ (in Sect. III.C)
α	scattering parameter $= 1/(\lvert\underline{k}_\Delta\rvert\lambda_T)$
α	the angle at which two observed beams intersect at a source
β	the angle subtended at the source by a single observed beam
$\tilde{\Gamma}_{BA}(\tau,\lvert\underline{k}\rvert)$	the mutual coherence between the $\lvert\underline{k}\rvert c$ frequency components of the light in beams A and B [see Eq. (II.12)]
$\Gamma_{BA}(\tau,\lvert\underline{k}\rvert,\underline{r}')$	the contribution to $\Gamma_{BA}(\tau,\lvert\underline{k}\rvert)$ from sources near $\underline{r}'$; this is only meaningful for an incoherent source
$\Gamma^{(m,n)}$	a complex correlation function [see Eq. (II.34)]
$\Gamma_{BA}(\tau,\lvert\underline{k}\rvert)$	the mutual coherence between beams A and B observed after beam B is Doppler shifted in frequency [see Eq. (V.4)]
$\Gamma_{BA}(\tau,\lvert\underline{k}_A\rvert,\lvert\underline{k}_B\rvert)$	a mutual coherence between light of different wavelengths [see Eq. (V.7a)]

δ	focal spot size (in Sect. I.B)
$\underline{\delta}$	a small displacement of a source within a common source volume (in Sect. II.A.1)
$\delta^2\Omega$	the small solid angle subtended at the source by an observed beam
Δ	the distance between adjacent beam-defining slits in a multiple-beam spectrometer
Δk	the width of a spectrometer instrument function
$\Delta\omega$	a spectrometer bandwidth, or the width of an observed spectral line, whichever is narrower
θ	the angle at which two interfering beams intersect at a screen
$\theta(x'',y'',\underline{r}',\omega)$	the difference in phase between the transfer functions ϕ_A and ϕ_B
λ_D	plasma Debye length
$\xi(\underline{r},t)$	scalar wave amplitude [from Eq. (I.3)]
$\xi_0(\underline{r},t)$	the amplitude of the light accepted by a multiple-beam spectrometer
$\xi_A(\underline{r},t)$, $\xi_B(\underline{r},t)$	amplitudes of the light in beams A and B, or of the A and B polarization components of the light
$\tilde{\xi}_B(\underline{r},t)$	the light in beam B observed from a moving frame of reference [see Eq. (7.3b)]
ρ	charge density
σ_T	differential Thompson scattering cross section
τ	the inverse bandwidth of the spectrum analyzer used to obtain a signal spectrum (in Sect. III.C)

τ_0	$= 1/\omega_0$, a time interval characteristic of the $\underline{k}_\Delta$ component of a light source distribution
τ_A, τ_B	time required for beams A and B to travel through the calcite rhomb
ϕ	electromagnetic scalar potential
ϕ	angle subtended at a screen by one of a pair of interfering beams
ϕ	$= \underline{k}_B \cdot \underline{r}_B - \underline{k}_A \cdot \underline{r}_A$, a phase factor in the measured mutual coherence
$\phi(\underline{r}', t)$	the phase of a nearly monochromatic source [see Eq. (II.36)]
$\phi_A(\underline{r}'', \underline{r}', \omega)$, $\phi_B(\underline{r}'', \underline{r}', \omega)$	the two complex-valued transfer functions of a multiple beam spectrometer
$\phi_j(t)$	the phase of one of a set of point sources (in Chapter V)
$\phi_1(\underline{r}^{(in)})$, $\phi_2(\underline{r}^{(out)})$	optical path lengths added by the input and output lenses of a multiple-beam spectrometer
ϕ_{10}, ϕ_{20}	constant contributions to ϕ_1 and ϕ_2
Φ	a mean path length for rays in a multiple-beam spectrometer [see Eq. (II.30)]
ω	angular frequency
ω_0	a characteristic frequency of the $\underline{k}$ component of a light source distribution
ω_0	a frequency of a nearly monochromatic source [see Eq. (II.36)]
ω_A, ω_B	the frequencies of light in beams A and B (in Chapter V)

ω_i	frequency of incident light
ω_j	the frequency of one of a set of point sources (in Chapter V)
ω_s	frequency of scattered light
ω_Δ	a difference frequency (= $\omega_s - \omega_i$ or $\omega_B - \omega_A$)

FOOTNOTES AND REFERENCES

Chapter I

1. Of particular importance here is progress made in the understanding and use of partially coherent light. This work is summarized in several recent books:
   a. M. J. Beran and G. B. Parrent, Jr., Theory of Partial Coherence (Prentice-Hall, Englewood Cliffs, N. J., 1964).
   b. E. L. O'Neill, Introduction to Statistical Optics (Addison-Wesley, Reading, Mass., 1963).
   c. L. Mandel and E. Wolf, Eds., Selected Papers on Coherence and Fluctuations in Light (Dover, New York, 1970).

   Several articles in the series Progress in Optics, E. Wolf, Ed. (North-Holland Publishing Co., Amsterdam), also pertain to this subject.
2. Discussions of related quantum problems are available in several recent books on quantum optics:
   a. R. J. Glauber, Ed., Quantum Optics, Proceedings of the International School of Physics "Enrico Fermi" Course XLII, Summer 1967 (Academic Press, New York, 1969).
   b. S. M. Kay and A. Maitland, Eds., Quantum Optics, Proceedings of the Tenth Scottish Summer School, 1969 (Academic Press, New York, 1970).
   c. J. R. Klauder and E. C. G. Sudarshan, Fundamentals of Quantum Optics (Benjamin, New York, 1968).

3. The general subject of plasma diagnostics is discussed in several books, including

   a. R. H. Huddlestone and S. L. Leonard, Eds., Plasma Diagnostic Techniques (Academic Press, New York, 1965).

   b. H. R. Griem and R. H. Lovberg, Eds., Plasma Physics, Vol. 9 of Methods in Experimental Physics, L. Marton, Ed.-in-Chief (Academic Press, New York, 1970).

   c. W. Lochte-Holtgreven, Ed., Plasma Diagnostics (North-Holland Publishing Co., Amsterdam, 1968).

4. P. S. Rostler, W. S. Cooper, and W. B. Kunkel, Multiple-Beam Spectroscopy, Bull. Am. Phys. Soc. 17, 986 (1972).

5. J. D. Jackson, Classical Electrodynamics (Wiley and Sons, New York, 1962), p. 180.

6. See, for example, S. L. Leonard, Basic Macroscopic Measurements, in Plasma Diagnostic Techniques, R. H. Huddlestone and S. L. Leonard, Eds. (Academic Press, New York, 1965).

7. See References 3 and also

   a. H. R. Griem, Plasma Spectroscopy (McGraw-Hill Book Co., New York, 1964).

   b. G. V. Marr, Plasma Spectroscopy (Elsevier, Amsterdam, 1968).

8. The mechanisms of bremsstrahlung and cyclotron emission are discussed in Chapter 15 of J. D. Jackson, Classical Electrodynamics (Wiley and Sons, New York, 1962), and in Chapter 3 of P. C. Clemmow and J. P. Dougherty, Electrodynamics of Particles and Plasmas (Addison-Wesley, Reading, Mass., 1969).

9. Here and throughout, the term "observed beam" is used to denote a bundle of rays accepted by an optical system. This does not mean incident light, the light is all emitted by the plasma.

10. J. Richter, Radiation of Hot Gases, (Sect. 2.1) in Plasma Diagnostics, W. Lochte-Holtgreven, Ed. (North-Holland Publishing Co., Amsterdam, 1968).

11. H. R. Griem, Plasma Spectroscopy (McGraw-Hill Book Co., New York, 1964), Ch. 7.

12. F. C. Jahoda and G. W. Sawyer, Optical Refractivity of Plasmas, in Plasma Physics, H. R. Griem and R. H. Lovberg, Eds., Vol. 9 of Methods in Experimental Physics, L. Marton, Ed.-in-Chief (Academic Press, New York, 1970).

13. a. R. A. Adler and D. R. White, Optical Interferometry, in Plasma Diagnostic Techniques, R. H. Huddlestone and S. L. Leonard, Eds. (Academic Press, New York, 1965).

b. U. Ascoli-Bartoli, Plasma Diagnostics Based on Refractivity, in Physics of Hot Plasmas, B. J. Rye and J. C. Taylor, Eds. (Proceedings of the Ninth Scottish Summer School, 1968) (Oliver and Boyd, Edinburgh, 1970).

14. K. L. Bowles, Observation of Vertical Incidence Scatter from the Ionisphere at 41 Mc/sec, Phys. Rev. Letters 1, 454 (1958).

15. a. M. N. Rosenbluth and N. Rostoker, Scattering of Electromagnetic Waves by a Nonequilibrium Plasma, Phys. Fluids 5, 776 (1962).

b. J. P. Dougherty and D. T. Farley, A Theory of Incoherent Scattering of Radio Waves by a Plasma, Proc. Royal Soc. (London) A259, 79 (1960); and D. T. Farley, J. P. Dougherty, and D. W. Barron, A Theory of Incoherent Scattering of Radio Waves by a Plasma II. Scattering in a Magnetic Field, Proc. Royal Soc. (London) A263, 238 (1961).

c. E. E. Salpeter, Electron Density Fluctuations in a Plasma, Phys. Rev. 120, 1528 (1960); and Effect of the Magnetic Field in Ionispheric Backscatter, J. Geophys. Res. 66, 982 (1961).

d. J. A. Fejer, Scattering of Radio Waves by an Ionized Gas in Thermal Equilibrium, Can.J. Phys. 38, 1114 (1960).

16. The literature of this type of experiment is quite extensive. The general state of the subject and the available reference material are summarized in several recent reviews:

a. D. E. Evans and J. Katzenstein, Laser Light Scattering in Laboratory Plasmas, Reports on Progress in Physics 32, 207 (1969).

b. S. A. Ramsden, Light Scattering Experiments in Physics of Hot Plasmas, B. J. Rye and J. L. Taylor, Eds., (Proceedings of the Ninth Scottish Summer School, 1968) (Oliver and Boyd, Edinburgh, 1970).

c. A. W. DeSilva and G. C. Goldenbaum, Plasma Diagnstoics by Light Scattering, in Plasma Physics, H. F Griem and R. H. Lovberg, Eds., Vol. 9 of Methods in Experimental

Physics, L. Marton, Ed.-in-Chief (Academic Press, New York, 1970).

17. That is, the coherence length of the incident light exceeds the dimensions of the scattering volume and the width of the laser spectrum is much less than that of features in the spectrum of the scattered light.

18. In the limit discussed here (the "Born approximation") the electric field of the scattered light is neglected in calculating the particle accelerations. The index of refraction is assumed equal to unity and the small effects of plasma particles are calculated separately. An alternate approach is to consider the scattering as due to variation in the index of refraction. See, for example, H. G. Booker, A Theory of Radio Scattering in the Troposphere, Proc. IRE 38, 401 (1950).

19. See J. D. Jackson, Classical Electrodynamics (Wiley and Sons, New York, 1962), Sect. 14.1; or W. K. H. Panofsky and M. Phillips, Classical Electricity and Magnetism (Addison-Wesley, Reading, Mass., 1955).

20. a. R. C. Davidson, Methods in Nonlinear Plasma Theory (Academic Press, New York, 1972).

    b. V. N. Tsytovich, Nonlinear Effects in Plasma (Plenum Press, New York, 1970).

21. See F. Reif, Fundamentals of Statistical and Thermal Physics (McGraw-Hill Book Co., New York, 1965), p. 585; or C. Kittel, Elementary Statistical Physics (Wiley and Sons, New York,

1958), p. 133.

22. See, for example, S. E. Schwarz, Plasma Diagnosis by Means of Optical Scattering, J. Appl. Phys. 36, 1836 (1965).

23. See, for example, O. A. Anderson, Laser Light Scattering Measurement of Plasma Density, Temperature, and Correlation Spectrum (Ph.D. Thesis), Lawrence Livermore Laboratory Report UCRL-50699; or D. A. Reilly, Light Scattering by Ion Thermal Fluctuations in a Dense Plasma (Ph.D. Thesis), Lawrence Berkeley Laboratory Report UCRL-20815.

24. H. M. Smith, Principles of Holography (Wiley and Sons, New York, 1969).

25. a. Dennis Gabor, Holography, 1948-1971, Science 177, 299 (July 1972).

    b. G. W. Stroke, An Introduction to Coherent Optics and Holography (Academic Press, New York, 1969).

    c. R. J. Collier, C. B. Burkhardt, and C. W. Lin, Optical Holography (Academic Press, New York, 1971).

26. G. L. Rogers, Experiments in Diffraction Microscopy, Proc. Roy. Soc. (Edinburgh) 63, 193 (1952).

27. a. L. Mertz and N. O. Young, Fresnel Transformations of Images, in Optical Instruments and Techniques, K. J. Habell, Ed. (Chapman and Hall, London, 1962), pp. 305-12.

    b. Neils O. Young, Photography without Lenses or Mirrors, Sky and Telescope, Jan. 1963, p. 8.

28. L. Mertz, Another Optical Fresnel Transformer, (advertisement) in J. Opt. Soc. Am. 54, iv (1964).

29. a. Gary Cochran, New Method of Making Fresnel Transforms with Incoherent Light, J. Opt. Soc. Am. 55, 615 (1965).

b. A. W. Lohmann, Wavefront Reconstruction for Incoherent Objects, J. Opt. Soc. Am. 55, 755 (1965).

c. J. T. Winthrop and C. R. Worthington, X-Ray Microscopy by Successive Fourier Transformation, Phys. Letters 15, 124 (1965).

30. a. George W. Stroke and Robert C. Restrick III, Holography with Spatially Noncoherent Light, Appl. Phys. Letters 7, 229 (1965). This work is described also by G. W. Stroke in An Introduction to Coherent Optics and Holography (Academic Press, New York, 1969), Sect. VI 9.

b. Gary Cochran, New Method of Making Fresnel Transforms with Incoherent Light, J. Opt. Soc. Am. 56, 1513 (1966).

c. P. J. Peters, Incoherent Holograms with Mercury Light Source, Appl. Phys. Letters 8, 209 (1966).

d. H. R. Worthington, Jr., Production of Holograms with Incoherent Illumination, J. Opt. Soc. Am. 56, 1397 (1966).

31. a. Adam Kozma and Norman Massey, Bias Level Reduction of Incoherent Holograms, Appl. Opt. 8, 393 (1969).

b. O. Bryngdahl and A. Lohmann, One Dimensional Holography with Spatially Incoherent Light, J. Opt. Soc. Am. 58, 625 (1968).

Chapter II

32. For a slightly different statement of the same comparison, one can note that scattered light is described by a complex

valued amplitude and that the total scattered wave is found by adding a set of complex numbers, one for each scattering center. In the two-beam spectroscopic observation, the mutual coherence between the light in beams A and B is also a complex valued quantity, and, if the source is incoherent, this coherence just consists of contributions from the different source points. It is this superposition of complex valued contributions to the mutual coherence which corresponds to summing up the complex amplitudes of scattered wavelets in a scattering experiment.

33. B. D. Cullity, Elements of X-Ray Diffraction (Addison Wesley, Reading, Mass., 1956).

34. G. B. Benedek, J. B. Lastovka, K. Fritsch, and T. Greytak, Brillouin Scattering in Liquids and Solids Using Low Power Lasers, J. Opt. Soc. Am. 54, 1284 (1964).

35. See, for example, L. J. Cutrona, E. N. Leith, L. J. Porcello, and W. E. Vivian, On the Application of Coherent Optical Processing Techniques to Synthetic-Aperture Radar, Proc. IEEE 54, 1026 (1966).

36. See Max Born and Emil Wolf, Principles of Optics (Pergamon Press, Oxford, 1970), p. 275.

37. a. F. Durst, A. Melling, and J. H. Whitelaw, Laser Anemometry: A Report on EUROMECH 36, J. Fluid Mech. 56, pt. 1, 143 (1972).

b. Hartmut H. Bossel, W. J. Hiller, and G. E. A. Meier, Noise-Cancelling Signal Difference Method for Optical

Velocity Measurements, J. Phys., E (London) 5, 893 (1972).

38. See Ref. 5, p. 186.

39. M. Francon and S. Mallick, Polarization Interferometers (Wiley and Sons, New York, 1971).

40. See Ref. 5, p. 188.

41. See H. B. Dwight, Tables of Integrals and Other Mathematical Data (Macmillan, New York, 1961), p. 223 (integral 858.713).

42. E. Wolf, Light Fluctuations as a New Spectroscopic Tool, Japan J. Appl. Phys. 4, Suppl. 1, 1 (1965).

43. Also, an additional factor of $2^{(m+n)}$ has been included in Eq. (II.34). This is to compensate for a difference of a factor of two in the definition of the analytic signal. See the discussion preceding Eq. (E.14) in Appendix E.

Chapter III

44. R. Hanbury Brown and R. Q. Twiss, Correlation Between Photons in Two Coherent Beams of Light, Nature 177, 27 (1956) and A Test of a New Type of Stellar Interferometer on Sirius, Nature 178, 1046 (1956), both reprinted in Selected Papers on Coherence and Fluctuations of Light, L. Mandel and E. Wolf, Eds. (Dover, New York, 1970), pp. 250-255.

45. R. Hanbury Brown and R. Q. Twiss, Interferometry of the Intensity Fluctuations in Light, I. Basic Theory: The Correlation Between Photons in Coherent Beams of Radiation, Proc. Roy. Soc. (London) A242, 300 (1957), reprinted in Selected Papers on Coherence and Fluctuations of Light,

L. Mandel and E. Wolf, Eds. (Dover, New York, 1970), pp. 272-324.

46. E. M. Purcell, The Question of Correlation Between Photons in Coherent Light Rays, Nature 178, 1449 (1956), reprinted in Selected Papers on Coherence and Fluctuations of Light, L. Mandel and E. Wolf, Eds. (Dover, New York, 1970), pp. 270-271.

47. In observations of high-frequency phenomena, however, some variation in n could be tolerated. If the signal frequency were greater than the frequency of the variations in the line integrals of n, the effect of interference could be seen but the apparent frequency of the phenomenon would be affected by the time dependence of the optical path lengths.

48. R. J. Glauber, Photon Counting and Field Correlations, in Physics of Quantum Electronics (conference proceedings), P. L. Kelley, B. Lax, and P. E. Tannenwald, Eds. (McGraw-Hill Book Co., New York, 1966), pp. 788-811.

49. L. Mandel, Fluctuations of Light Beams, in Progress in Optics, E. Wolf, Ed. (North-Holland Publishing Company, Amsterdam, (1963), Vol. II, pp. 181-248.

50. F. Robben, Noise in the Measurement of Light with Photomultipliers, Appl. Optics 10, 776 (1971).

Chapter IV

51. R. A. Hess, Study of a Beam-Plasma Instability by Spectroscopic Methods (Ph.D. Thesis), Lawrence Berkeley Laboratory Report LBL-1531, December 1972.

Chapter V

52. H. Z. Cummins and H. L. Swinney, Light Beating Spectroscopy in Progress in Optics, E. Wolf, Ed. (North-Holland Publishing Co., Amsterdam, 1970), Vol. VIII, pp. 133-200.

53. To shift the frequency light one can use a Bragg cell in which light is reflected from a sound wave in a liquid. See H. Z. Cummins and N. Knable, Single Sideband Modulation of Coherent Light by Bragg Reflection from Acoustical Waves, Proc. IEEE 51, 1246 (1963). There are also electro-optic methods for frequency shifting of light waves. See C. F. Buhrer, V. J. Fowler, and L. R. Bloom, Single Sideband Suppressed-Carrier Modulation of Coherent Light Beams, Proc. IRE 50, 1827 (1962); and C. F. Buhrer, D. Baird, and E. M. Conwell, Optical Frequency Shifting by Electro-Optic Effect. Appl. Phys. Letters 1, 46 (1962).

54. See M. A. Pugay and J. W. Hansen, An Ultrafast Light Gate, Appl. Phys. Letters 15, 192 (1969).

55. a. Arthur Ruark, Fast Modulation Effects in the Optical Region, Phys. Rev. 73, 181 (1948).

b. A. Theodore Forrester, Richard A. Gudmundsen, and Philip O. Johnson, Photoelectric Mixing of Incoherent Light, Phys. Rev. 99, 1691 (1955), reprinted in Selected Papers on Coherence and Fluctuations of Light, L. Mandel and E. Wolf, Eds. (Dover, New York, 1970), pp. 220-229.

Appendix C

56. This is equivalent to a requirement that the first slit be smaller than the maximum of a single slit diffraction pattern of the second slit. That is, the path length from any point across the width of one to any point across the width of the other must vary by less than half a wavelength.

57. Indeed, it is this which defines the beams: If the source is outside a beam, then the resulting distribution of phase across the first slit will be such as to destructively interfere at the second slit; the light which passes through the first slit is going in another direction. The first slit is many wavelengths wide. The light retains "memory" of direction to an accuracy slightly less than needed to distinguish the small angle subtended by the second slit. This is, of course, just the connection between geometrical optics ("beams A and B") and the physical optics which determines the forms of the interference fringes and the associated polarization patterns.

58. In using such a system, the optics would have to be rather carefully aligned, so that all of the light transmitted by the collimator would then enter the spectrometer. One might even want to remove the spectrometer entrance slit, and just let the second lens focus the collimated light into an image of a slit at the same place.

59. One solution is to use a series of two rhombs, the second rotated 90° with respect to the first about the axis of the

system. Then each polarization is extraordinary in one rhomb or the other and the differences in optical path length introduced will cancel, but the lateral displacements, which are perpendicular, will not. This combination of elements is called a Savart plate, or "polariscope". (See Ref. 39.)

Appendix E

60. A. A. Kharkevich, Spectra and Analysis (Consultants Bureau, N. Y., 1966).

61. a. R. M. Fano, Short-Time Autocorrelation Functions and Power Spectra, J. Acoust. Soc. Am. 22, 546 (1950).

b. C. H. Page, Instaneous Power Spectra, J. Appl. Phys. 23, 103 (1952).

c. D. G. Lampard, Generalization of the Wiener-Khintchine Theorem to Nonstationary Processes, J. Appl. Phys. 25, 802 (1954).